

Alma Mater Studiorum – Università di Bologna

DOTTORATO DI RICERCA IN
**Biologia Funzionale dei Sistemi Cellulari e
Molecolari**

Ciclo XXIII

Settore scientifico-disciplinare di afferenza: BIO/11

**Identification and characterization of the sRNA network
in *Neisseria meningitidis***

Presentata da: **Laura Fantappiè**

Coordinatore Dottorato

Chiar.mo Prof.
Vincenzo Scarlato

Relatori

Chiar.mo Prof.
Vincenzo Scarlato

Dott.ssa
Isabel Delany

Esame finale anno 2011

Durante il Dottorato di ricerca mi sono occupata dello studio della regolazione dell'espressione genica in *Neisseria meningitidis*. In particolare la mia attenzione si è focalizzata sulla regolazione mediata da piccoli RNA non codificanti (sRNAs). Ho studiato il fenotipo di un mutante knock-out del gene dell'RNA chaperone *hfq* e ho identificato e caratterizzato 2 nuovi sRNAs in meningococco e i loro rispettivi circuiti di regolazione. Ho inoltre identificato altri possibili nuovi sRNAs attraverso l'analisi del trascrittoma di *N. meningitidis* tramite la tecnologia "Illumina sequencing". Infine, ho anche caratterizzato il circuito di regolazione di un regolatore trascrizionale della famiglia AraC.

Nel periodo di Dottorato sono stata co-autrice dei seguenti lavori scientifici:

Metruccio M.M., **Fantappiè L.**, Serruto D., Muzzi A., Roncarati D., Donati C., Scarlato V., Delany I. "The Hfq-dependent small non-coding (s) RNA NrrF directly mediates Fur-dependent positive regulation of succinate dehydrogenase in *Neisseria meningitidis*." *J. Bacteriol.* 2009 Feb; 191(4):1330-42. Epub 2008 Dec 5.

Fantappiè L., Metruccio M.M., Seib K., Oriente F., Cartocci E., Ferlicca F., Giuliani M., Scarlato V., Delany I. "The RNA chaperone Hfq is involved in the stress response and virulence in *Neisseria meningitidis* and is a pleiotropic regulator of protein expression". *Infect. Immun.* 2009 May; 77(5):1842-53. Epub 2009 Feb 17

Fantappiè L., Oriente F., Muzzi A., Serruto D., Scarlato V., Delany I. "A novel Hfq-dependent sRNA that is under Fnr control and is synthesized in oxygen limitation in *Neisseria meningitidis*". *Mol Microbiol.* 2011 Feb 21. doi: 10.1111/j.1365-2958.2011.07592.x. [Epub ahead of print]

Fantappiè L., Scarlato V., Delany I. "Identification of the target of an iron-responsive AraC like protein from meningococcus that is in a regulatory cascade with Fur". (Submitted to Microbiology, 2011)

Table of Contents

Riassunto	7
Abstract	9
Introduction	12
1.1 Meningococcal disease	12
1.2 The pathogen	13
1.3 Colonization and invasion	14
1.4 Virulence factors.....	16
1.5 Adaption to the host environment.....	19
1.6 Small regulatory RNAs.....	21
1.7 The pleiotropic regulator Hfq	26
1.8 How to identify new sRNAs.....	31
Results	37
I Characterization of a <i>hfq</i> knock out in <i>Neisseria meningitidis</i>	37
1.9 The <i>hfq</i> locus of <i>N. meningitidis</i>	37
1.10 Expression of the Hfq protein and generation of an Hfq null mutant	39
1.11 Complementation of the Hfq mutant.....	42
1.12 Hfq plays a major role in stress tolerance in <i>N. meningitidis</i> ...	44
1.13 Hfq contributes to the survival in <i>ex vivo</i> and <i>in vivo</i> models .	45
1.14 Identification of proteins differentially expressed in <i>Δhfq</i> mutant.....	49
1.15 Global analysis of gene expression in the Hfq null mutant	55
II Identification of AniS, a novel sRNA synthesied under oxygen limitation	59
1.16 NMB1205 is a small transcript deregulated in the Hfq mutant	59
1.17 The synthesis of the novel sRNA is regulated by FNR.	63
1.18 AniS negatively regulates NMB1468 and NMB0214 genes ...	66
1.19 Validation of the direct targeting of NMB1468 by AniS.....	71
1.20 AniS is a small RNA bound by Hfq.....	73
III Molecular mechanism of action of the sRNA NrrF	76
1.21 A bioinformatic approach identified a Fur-regulated sRNA in . the <i>N. meningitidis</i> MC58 genome.....	76
1.22 A base pairing mechanism mediated by Hfq is the molecular mechanism of action of NrrF	77
1.23 Fumarate hydratase and superoxide dismutase are regulated by at least a novel Hfq-dependent sRNA.....	83
IV Global investigation of sRNAs	85
1.24 Solexa RNA sequence revealed 19 putative novel sRNAs in meningococcus	86
Discussion	92
1.25 Characterization of a <i>hfq</i> knock out in <i>Neisseria meningitidis</i>	92
1.26 Identification of AniS, a novel sRNA synthesied under oxygen limitation	96
1.27 Molecular mechanism of action of the sRNA NrrF	101
1.28 Concluding remarks	104
Materials and methods	105
1.29 Bacterial strains and culture conditions	105
1.30 DNA techniques.	106

1.31	Construction of plasmids and recombinant strains	106
1.32	Expression and purification of the Hfq protein	109
1.33	<i>In vitro</i> cross-linking	110
1.34	Generation of anti-Hfq antiserum	111
1.35	Western blot analysis	111
1.36	Fractionation of proteins of <i>N. meningitidis</i>	112
1.37	Separation of total proteins by 2D gel electrophoresis	113
1.38	In-gel protein digestion and MALDI-TOF mass spectrometry analysis.	113
1.39	<i>In vitro</i> antimicrobial stress assays	114
1.40	<i>Ex vivo</i> human serum assay and <i>ex vivo</i> whole-blood model of meningococcal bacteremia.	115
1.41	<i>In vivo</i> animal model.	116
1.42	RNA extraction	116
1.43	Microarray procedures: design, cDNA labelling, hybridization, and data analysis.	117
1.44	Primer extension, S1 nuclease mapping, Northern blot and real time PCR.	119
1.45	cDNA library construction and Illumina sequencing.....	121
1.46	Read mapping and visualization	122
1.47	DNase I footprinting	123
1.48	Generation of <i>in vitro</i> transcripts	123
1.49	Electrophoretic mobility shift assays of <i>in vitro</i> transcription products.	125
Tables		127
References		140

RIASSUNTO

I piccoli RNA batterici (sRNAs) sono regolatori post-trascrizionali coinvolti nelle risposte a diversi stress. Questi piccoli trascritti non codificanti sono sintetizzati in risposta a un certo segnale e controllano l'espressione genica dei loro regoloni modulando la traduzione o la stabilità di mRNA targets, spesso insieme all' RNA chaperone Hfq. In questa tesi si è caratterizzato in *Neisseria meningitidis* un mutante knock out per il gene *hfq*, dimostrando che ha un fenotipo pleiotropico. Questo suggerisce un importante ruolo della proteina Hfq nell'adattamento agli stress e nella virulenza del batterio, nonché la presenza di sRNAs dipendenti da Hfq. Inoltre, un'analisi globale dell'espressione genica, per identificare trascritti regolati nel mutante di Hfq, ha rivelato l'esistenza di uno sRNA, impropriamente annotato come una open reading frame (ORF), che abbiamo chiamato AniS. Si è dimostrato che la sintesi di questo nuovo sRNA è indotta in condizioni di anaerobiosi, grazie all'azione del regolatore trascrizionale FNR che ne attiva la trascrizione. Abbiamo inoltre identificato 2 possibili targets di AniS attraverso analisi dell'espressione genica globale.

In questa tesi si è anche effettuata una dettagliata analisi molecolare dell'azione dello sRNA NrrF, il primo ad essere stato identificato in *N. meningitidis*. Si dimostra che NrrF regola la succinato deidrogenasi formando un duplex con una zona di complementarietà all'interno della regione *sdhDA* del trascritto della succinato deidrogenasi. Hfq aumenta

l'efficienza del legame tra i 2 RNA e questo probabilmente determina una rapida degradazione del trascritto *in vivo*. Inoltre, allo scopo di identificare altri possibili sRNAs in *N. meningitidis* abbiamo sequenziato il trascrittoma del batterio in condizioni standard di crescita *in vitro* e in condizioni di carenza di ferro. Questa analisi ha rivelato geni che sono attivamente trascritti nelle 2 condizioni. La nostra attenzione si è rivolta in particolare alle regioni non codificanti attivamente trascritte nel genoma. Questo ha permesso di identificare 19 possibili nuovi sRNAs e regioni 5' e 3' UTRs (regioni non tradotte). Ulteriori studi saranno focalizzati sull'identificazione dei circuiti regolatori di questi sRNAs e sui loro targets.

ABSTRACT

Bacterial small regulatory RNAs (sRNAs) are posttranscriptional regulators involved in stress responses. These short non-coding transcripts are synthesised in response to a signal, and control gene expression of their regulons by modulating the translation or stability of the target mRNAs, often in concert with the RNA chaperone Hfq. Characterization of a Hfq knock out mutant in *Neisseria meningitidis* revealed that it has a pleiotropic phenotype, suggesting a major role for Hfq in adaptation to stresses and virulence and the presence of Hfq-dependent sRNA activity. Furthermore, global gene expression analysis of regulated transcripts in the Hfq mutant revealed the presence of a regulated sRNA, incorrectly annotated as an open reading frame, which we renamed AniS. We demonstrated that the synthesis of this novel sRNA is anaerobically induced through activation of its promoter by the FNR global regulator and through global gene expression analyses we identified at least two predicted mRNA targets of AniS.

In this thesis we also performed a detailed molecular analysis of the action of the sRNA NrrF, the first one identified in *N. meningitidis*. We demonstrated that NrrF regulates succinate dehydrogenase by forming a duplex with a region of complementarity within the *sdhDA* region of the succinate dehydrogenase transcript, and Hfq enhances the binding of this sRNA to the identified target in the *sdhCDAB* mRNA; this is likely to result in rapid turnover of the transcript *in vivo*.

In addition, in order to globally investigate other possible sRNAs of *N. meningitidis* we Deep-sequenced the transcriptome of this bacterium under

both standard *in vitro* and iron-depleted conditions. This analysis revealed genes that were actively transcribed under the two conditions. We focused our attention on the transcribed non-coding regions of the genome and, along with 5' and 3' untranslated regions, 19 novel candidate sRNAs were identified. Further studies will be focused on the identification of the regulatory networks of these sRNAs, and their targets.

INTRODUCTION

1.1 Meningococcal disease

N. meningitidis is a strictly human pathogen responsible for meningitis and sepsis, two devastating diseases that can kill children and young adults within hours, despite the availability of effective antibiotics.

Studies performed in Europe (Caugant *et al.*, 2007) have demonstrated that carriage rates are very low in the first few years of life, but sharply rise during adolescence, peaking at 10–35% in 20–24-year olds, before decreasing to less than 10% in older age groups (Caugant *et al.*, 2007; Claus *et al.*, 2005). Compared with the carriage rate, meningococcal disease is rare, and disease rates vary in different geographic regions of the world (Hill *et al.*, 2010). What changes the colonization state of the organism into a disease state is not entirely clear. It appears that a combination of bacterial virulence factors and host susceptibility, including age, prior viral infection, smoking (Cartwright & Ala'Aldeen, 1997) and genetic polymorphisms (reviewed in Emonts *et al.*, 2003) may ultimately lead to meningococcal disease. The human nasopharyngeal mucosa, in fact, is the only natural reservoir of *N. meningitidis*, however meningococcus can invade the pharyngeal mucosal epithelium and, in the absence of bactericidal serum activity, disseminate into the bloodstream, causing septicaemia. In a subset of cases, the bacteria can also cross the blood-brain barrier and infect the cerebrospinal fluid, causing meningitis.

In general, mortality occurs in up to 10% of patients with invasive meningococcal disease (Stephens, 2007). Mortality rates are dependent on the type and severity of invasive disease, and are greatest for fulminant

septicaemia (up to 55%) followed by meningitis with associated septicaemia (up to 25%), and lowest for meningitis without sepsis (generally <5%) (Brandtzaeg & van Deuren, 2005). However, patients who survive invasive meningococcal disease often live with a number of physical and mental sequelae, including amputation of limbs and digits, scarring of skin, speech impairment and seizures (Borg *et al.*, 2009).

1.2 The pathogen

N. meningitidis is a Gram-negative diplococcus (Fig. 1). It is aerobic, non-motile, non-sporulating, usually encapsulated and piliated. Traditionally different *N. meningitidis* strains are classified into serogroups according to the immunological reactivity of their capsule polysaccharides. With this method 13 different serogroups have been identified, but only A, B, C, Y, X and W135 commonly cause invasive infections. Meningococci are further classified into serotype and serosubtype, based on antigenic differences in their major outer membrane proteins (OMPs), PorA and PorB. The serological classification system, however, is limited due to high frequency of phase and antigenic variation of outer-membrane structures, which has led to the development of DNA-based approaches to characterize meningococcal strains. The most important of these methods is multilocus sequence typing (MLST), which characterizes isolates on the basis of the nucleotide sequences of internal fragments of seven housekeeping genes defining their sequence type (ST) (Maiden *et al.*, 1998). Meningococci can in this way be classified into lineages, termed clonal complexes (cc). A clonal complex is a group of STs that share at least four of the seven loci in common with a central ancestral genotype. Despite huge diversity in

meningococcal population, only a minority of these clonal complexes are associated with invasive disease, known as hyperinvasive lineages (Maiden, 2008). Why hyperinvasive meningococcal lineages are more pathogenic than others remain still unknown.

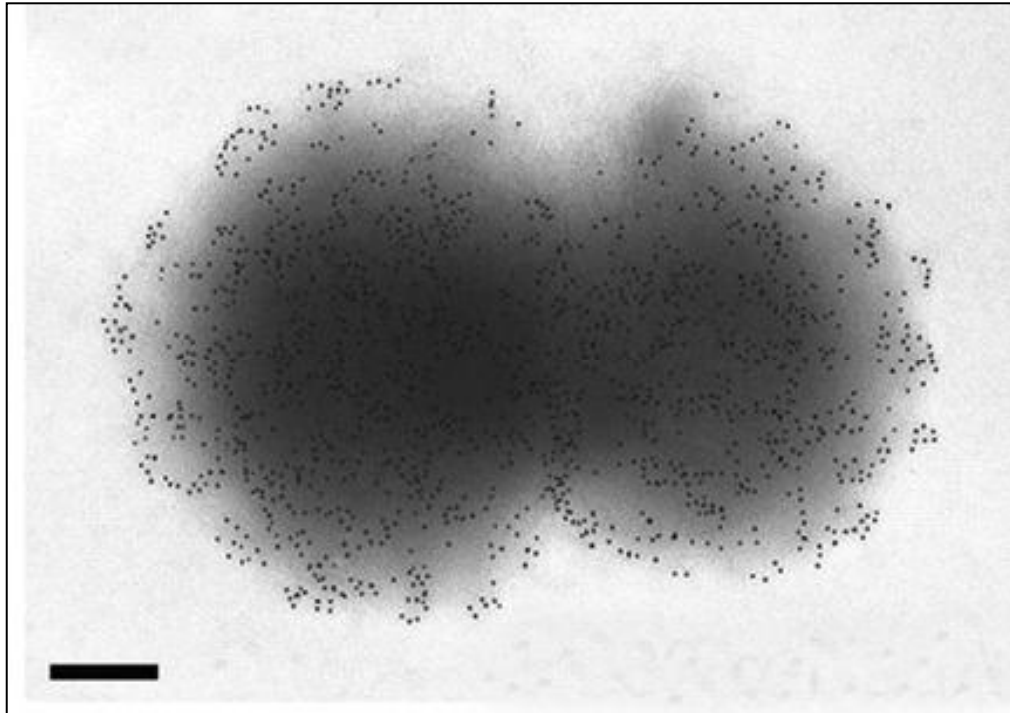
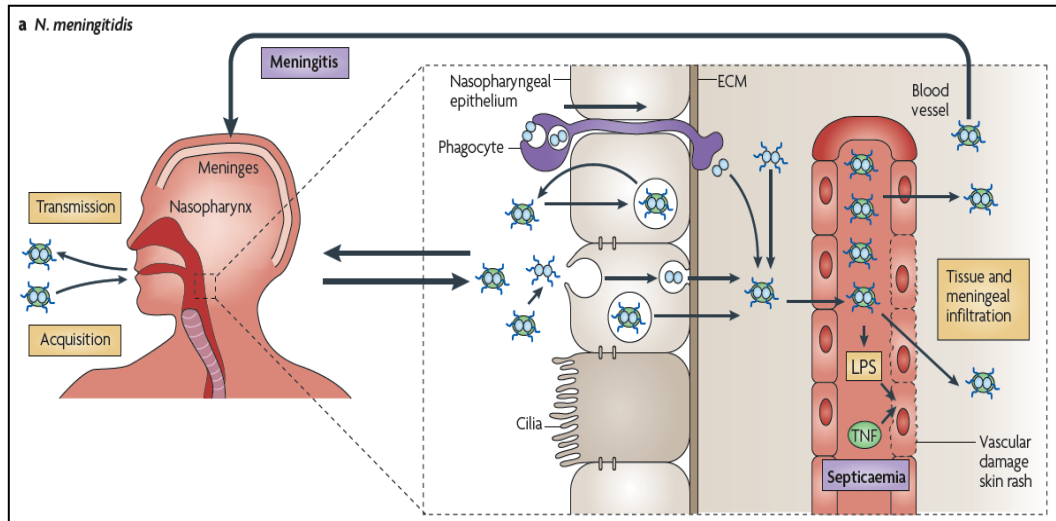


Figure 1: ImmunoGold labelling and transmission electron microscopy of *N. meningitidis*. Analysis of the strain was performed with antisera raised against NadA adhesin (Scale bars: 200 nm.) (Pizza *et al.*, 2000)

1.3 Colonization and invasion

Colonization of the upper respiratory mucosal surfaces by *N. meningitidis* is the first step in the establishment of a human carrier state and invasive meningococcal disease (Stephens, 2009). Initial contact with nasopharyngeal epithelial cells is mediated by Type IV pili. Then, meningococci proceed to proliferate on the surface of human non-ciliated epithelial cells, forming small microcolonies at the site of initial attachment

(Stephens, 2009). After the initial colonization, there is a loss or down regulation of the capsule, which sterically masks the outer membrane proteins. This event is thought to occur both via cell contact induced repression (Deghmane *et al.*, 2002), and by selection of low or no-capsule expressing bacteria due to phase variation (Hammerschmidt *et al.*, 1996). Close adherence of meningococci to the host epithelial cells is mediated by a variety of possible redundant adhesins, previously masked by the capsule. This results in the appearance of cortical plaques and the recruitment of factors leading to the formation and extension of epithelial cell pseudopodia that internalize the bacteria (Stephens, 2009). Once internalized in the epithelial cells meningococcus can evade the host immune response, find more available nutrients and can also cross the epithelium and enter the bloodstream (Stephens, 2009). Intracellular survival is determined by factors including IgA1 protease, which degrades lysosome-associated membrane proteins, and upregulation of expression of capsule, which is anti-opsonic and anti-phagocytic and therefore aids survival in blood (Stephens, 2009; Virji, 2009)). (Fig 2). The next steps of meningococcal invasion of the bloodstream and the passage across the brain vascular endothelium, which results in infection of the meninges and the cerebrospinal fluid, are still poorly understood.



Virji, 2009

Figure 2: Stages in the pathogenesis of *N. meningitidis*. *N. meningitidis* may be acquired through the inhalation of respiratory droplets. The organism establishes intimate contact with non-ciliated mucosal epithelial cells of the upper respiratory tract, where it may enter the cells briefly before migrating back to the apical surfaces of the cells for transmission to a new host. Asymptomatic carriage is common in healthy adults in which bacteria that enter the body by crossing the epithelial barrier are eliminated. Besides transcytosis, *N. meningitidis* can cross the epithelium either directly following damage to the monolayer integrity or through phagocytes in a ‘Trojan horse’ manner. In susceptible individuals, once inside the blood, *N. meningitidis* may survive, multiply rapidly and disseminate throughout the body and the brain. Meningococcal passage across the brain vascular endothelium (or the epithelium of the choroid plexus) may then occur, resulting in infection of the meninges and the cerebrospinal fluid (Nassif, 1999).

1.4 Virulence factors

The major virulence factor (Fig 3) of meningococcus is the polysaccharide capsule that protects the bacterium during airborne transmission between hosts (Romero & Outschoorn, 1997), confers protection from effectors of the innate immunity (Vogel *et al.*, 1997), allows survival in blood, as mentioned before, and may shield bacterial surface from the host immune

effectors mechanisms (Virji, 2009). The second principle virulence factor, mainly involved in the interface between the host and the bacterium, are the pili, long surface proteins that protrude from the capsule.

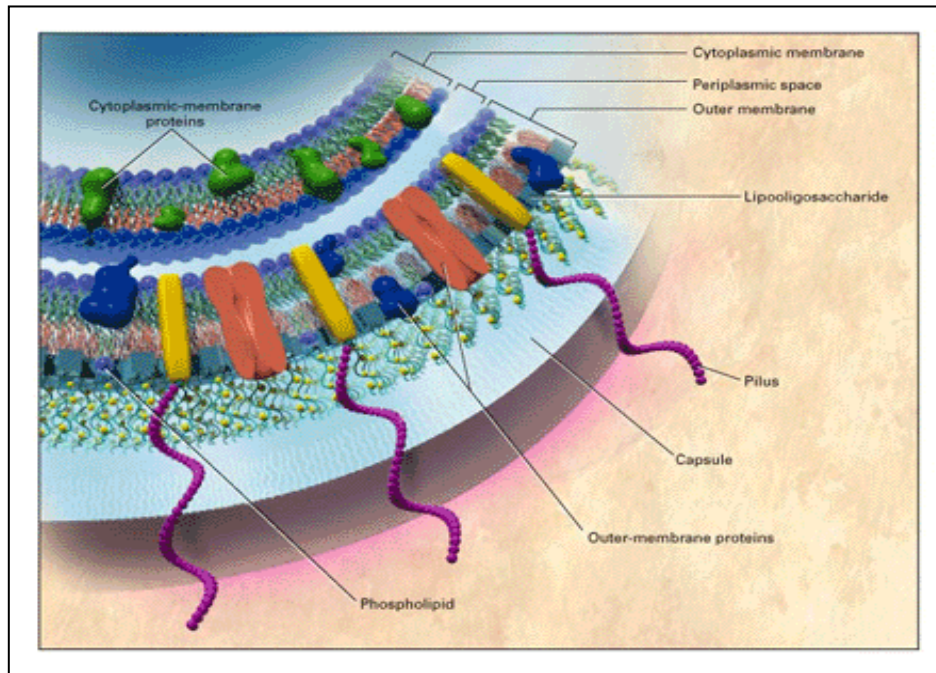


Figure 3: Virulence factors in meningococcal cell membranes (from Rosenstein *et al.*, 2001)

Together with the outer membrane adhesins, pili facilitate adhesion to host tissues having a crucial role in the initial establishment of encapsulated bacteria on mucosal surfaces, helping the penetration of the negatively charged barrier at the host-pathogen interface (Heckels *et al.*, 1976). In addition to adhesion, pili, are involved in several other functions, for example facilitating uptake of foreign DNA from the extracellular environment, increasing transformation frequency of bacteria and maintaining the genetic diversity that supports the success of *Neisseria* in the human host (Helaine *et al.*, 2007). The pilus of meningococcus is expressed from the *pilE* locus, but homologous recombination between the

pilE gene and a number of non-expressed 'silent' *pilS* genes results in a change in the *pilE* sequence. These variants differ in their transformability, adherence and immunogenicity (Virji *et al.*, 1992). Additionally, *N. meningitidis* spp. possess host specific iron acquisition systems and numerous immune evasion mechanisms such as factor H binding protein that is able to down-regulate complement deposition (Virji, 2009). Close adhesion and invasion is mainly mediated by an array of proteins such as opacity proteins (Opc, Opa) and other adhesins. These proteins are believed to be responsible for the host specificity as well as for tissues within the host (Virji, 2009). Numerous additional apparently minor adhesins (several of which were identified by homology searching of the available genomes) are generally expressed at low levels during *in vitro* growth but may be important in *in vivo* infections. Their expression can in fact be regulated at different levels in the different environment the bacterium encounter during its infection. It has been reported, for example that in conditions that mimic the host infection such as iron (Delany *et al.*, 2006) and oxygen limitation (Bartolini *et al.*, 2006) or interaction with epithelial cells (Dietrich *et al.*, 2003) and blood (Echenique *et al.*, in press) the transcriptome of *N. meningitidis* is considerably altered and, as a result, some virulence factors may be over-expressed. Furthermore, several adhesins are subject to antigenic variation and/or phase variation, which allow bacteria to generate a broad and variable repertoire of surface structure that facilitates evasion of immune effectors mechanisms and adaptation to different niche (Virji, 2009).

1.5 Adaptation to the host environment

N. meningitidis, during its infection, is subjected to constant selective pressures and its ability to adapt rapidly to environmental changes is essential for its survival (Hill *et al.*, 2010). Phase and antigenic variation of a number of surface components permits immune evasion during infection, but since the bacterium can infect diverse sites within the human host, which represent a unique niche with respect to nutrients, environmental factors and competing microorganisms, it has to rapidly change its metabolism and cellular composition to adapt to different environments. Much of this adaptation is carried out at the transcriptional level. Different transcriptional regulators, activated by different stresses encountered during infection, regulate the transcription of many genes important for survival and virulence. However, only few transcriptional regulators are found in the pathogenic *Neisseria* (*meningitidis* and *gonorrhoeae*): 35 putative regulators in *N. meningitidis* MC58 strain, compared to *Escherichia coli*, which harbours more than 200 transcriptional regulators. This reveals a striking limitation for transcriptional regulation, which is possibly related to the restricted ecological niche of the Neisseriaceae (Schielke *et al.*, 2010). The mechanisms of adaptation of *N. meningitidis* to two different conditions it encounters during infection are described below.

Iron limitation

It has been very well established that bacterial pathogenesis and survival are dependent on the ability to acquire iron within the host (Andrews *et al.*, 2003; DeVoe, 1982). Cell growth and multiplication, in fact, require essential nutrients such as iron, which is limiting in the human host being sequestered by human iron proteins. Although *N. meningitidis* does not

produce siderophores for iron acquisition, it possesses outer membrane receptors that have been postulated to scavenge the iron-loaded siderophores secreted by other bacteria colonizing the nasopharyngeal tract (Carson *et al.*, 1999). Once inside the host, the organism must compete for iron with host iron proteins, and meningococcus possesses receptors for transferrin, lactoferrin, and hemoglobin (Perkins-Balding *et al.*, 2004). However, iron overload results in toxicity for the bacterium; therefore, iron uptake is tightly regulated and in meningococcus, as in many bacteria, this regulation is mediated by the ferric uptake regulator (Fur) protein (Delany *et al.*, 2003; Escolar *et al.*, 1999). Fur senses internal iron concentration and binds to and represses iron uptake genes using ferrous iron as a co-repressor (Delany *et al.*, 2003). Fur has been also reported to act positively in the expression of certain genes, both with a direct mechanism (binding upstream promoter sequences (Delany *et al.*, 2004) and an indirect mechanism which involves a posttranscriptional regulation mediated by a Fur repressed small regulatory RNA named NrrF (Mellin *et al.*, 2007; Metruccio *et al.*, 2009). The regulatory circuit of NrrF is a part of this thesis work.

Oxygen limitation

During its infection *N. meningitidis* encounters numerous complex extracellular and intracellular environments, since it moves from the upper respiratory tract, to mucous membranes, blood and CSF (Archibald & Duong, 1986), being exposed to highly divergent partial pressures of oxygen (high in the upper respiratory tract and low in the mucus membranes and in the blood (Archibald & Duong, 1986). It has been shown that although *N. meningitidis* fails to grow under strictly anaerobic

conditions, under oxygen limitation the bacterium expresses a denitrification pathway system that supplement growth (Anjum *et al.*, 2002; Rock & Moir, 2005). Pathogenic *Neisseria* use FNR as a global transcription factor, to control these responses under oxygen limitation, in particular to induce the denitrification and sugar fermentation pathways (Bartolini *et al.*, 2006) as an alternative to aerobic respiration. FNR is only active as a dimer containing [4Fe-4S] cluster. The cluster dissociates in the presence of oxygen, destabilizing the dimer, with loss of FNR activity (Kiley & Beinert, 2003). Only a total of 9 transcriptional units have been identified as being responsive to the FNR regulator in *N. meningitidis* (Bartolini *et al.*, 2006). Interestingly factor H binding protein (fHBP,) which enables the bacterium to evade complement-mediated killing by binding factor H (Madico *et al.*, 2006; Schneider *et al.*, 2006), and which is a component of the MenB vaccine currently in development, has been shown to be positively regulated by oxygen limitation through a FNR dedicated promoter (Oriente *et al.*, 2010). This result, together with the observation that a knock-out of FNR in *N. meningitidis* is attenuated in the mouse and infant rat animal models (Bartolini *et al.*, 2006), indicate the importance of these responses for the pathogenesis and the survival of meningococcus in the human host. The identification and analysis of a novel sRNA induced under oxygen limitation by FNR is a part of this thesis work.

1.6 Small regulatory RNAs

Small regulatory RNAs (sRNAs) are crucial regulatory elements in bacterial stress responses and virulence (reviewed in: (Gottesman, 2004), (Waters & Storz, 2009), (Papenfert & Vogel, 2010). These regulators

mostly function as coordinators of adaptation processes in response to environmental changes, integrating environmental signals and controlling target gene expression, primarily at posttranscriptional levels (Wassarman, 2002), Gottesman, 2004). Regulatory RNAs can modulate transcription, translation, mRNA stability and DNA maintenance or silencing (Waters & Storz, 2009). They can act using diverse mechanisms, including changes in RNA conformation, protein binding, base pairing with others RNAs and interaction with DNA. There are different classes of sRNAs classified according to their mechanism of action in bacterial cells. One class of sRNA comprises riboswitches. They are sequences at the 5' end of mRNAs they regulate that can adopt different conformations in response to environmental changes, (Grundy & Henkin, 2006) regulating in this way the expression of the coding sequence. Another class of sRNAs can bind to proteins, including global regulators, and antagonize their function (Pichon & Felden, 2007). A recently discovered group of RNA regulators, named CRISPR (clustered regulatory interspaced short palindromic repeats) provide resistance to bacteriophage (Sorek *et al.*, 2008) and prevent plasmid conjugation (Marraffini & Sontheimer, 2008) . CRISPR RNAs contain short regions of homology to bacteriophage and plasmid sequences and can interfere with bacteriophage infection and plasmid conjugation, most likely by targeting the homologous foreign DNA. But the largest and most studied group of sRNA, which is also analyzed in this thesis, acts through base pairing with mRNAs, modulating their translation and stability. This class of regulatory RNAs has two distinct broad classes: the *cis* encoded sRNAs (Fig 4A), that have a perfect complementarity with their targets and the *trans* encoded (Fig 4B) ones, which undergo base-pairing through regions

of partial complementarity and may have many distinct mRNA targets. The binding of sRNAs to target mRNAs is very specific: a single base substitution in the sRNA or target mRNA can be sufficient to disrupt duplex formation. Although sRNAs binding is very specific, each sRNAs can act on more than one target mRNA and each target mRNA can be regulated by multiple sRNAs (reviewed in (Repoila & Darfeuille, 2009). RNA base-pairing interactions are usually in the 5' UTR of the target mRNA and have been shown to alter mRNA structure ultimately leading to changes in translation efficiency and, as a consequence, mRNA stability (Wassarman, 2002, Waters & Storz, 2009). It has recently been shown that sRNAs can also interact with coding regions, regulating their targets not by translational control, but by accelerating RNase E-dependent mRNA targets decay (Pfeiffer *et al.*, 2009). The majority of the regulation by the known trans-encoded sRNAs is negative (Aiba, 2007; Gottesman, 2004); base pairing with the target mRNA usually leads to repression of protein levels through translational inhibition, mRNA degradation or both (Sharma *et al.*, 2007; Vecerek *et al.*, 2007; Morita *et al.*, 2006). However sRNAs can also activate expression of their target mRNAs. Base pairing of the sRNA disrupt an inhibitory secondary structure, which sequesters the ribosome binding site (Hammer & Bassler, 2007; Urban & Vogel, 2008; Prevost *et al.*, 2007); Soper *et al.*, 2010).

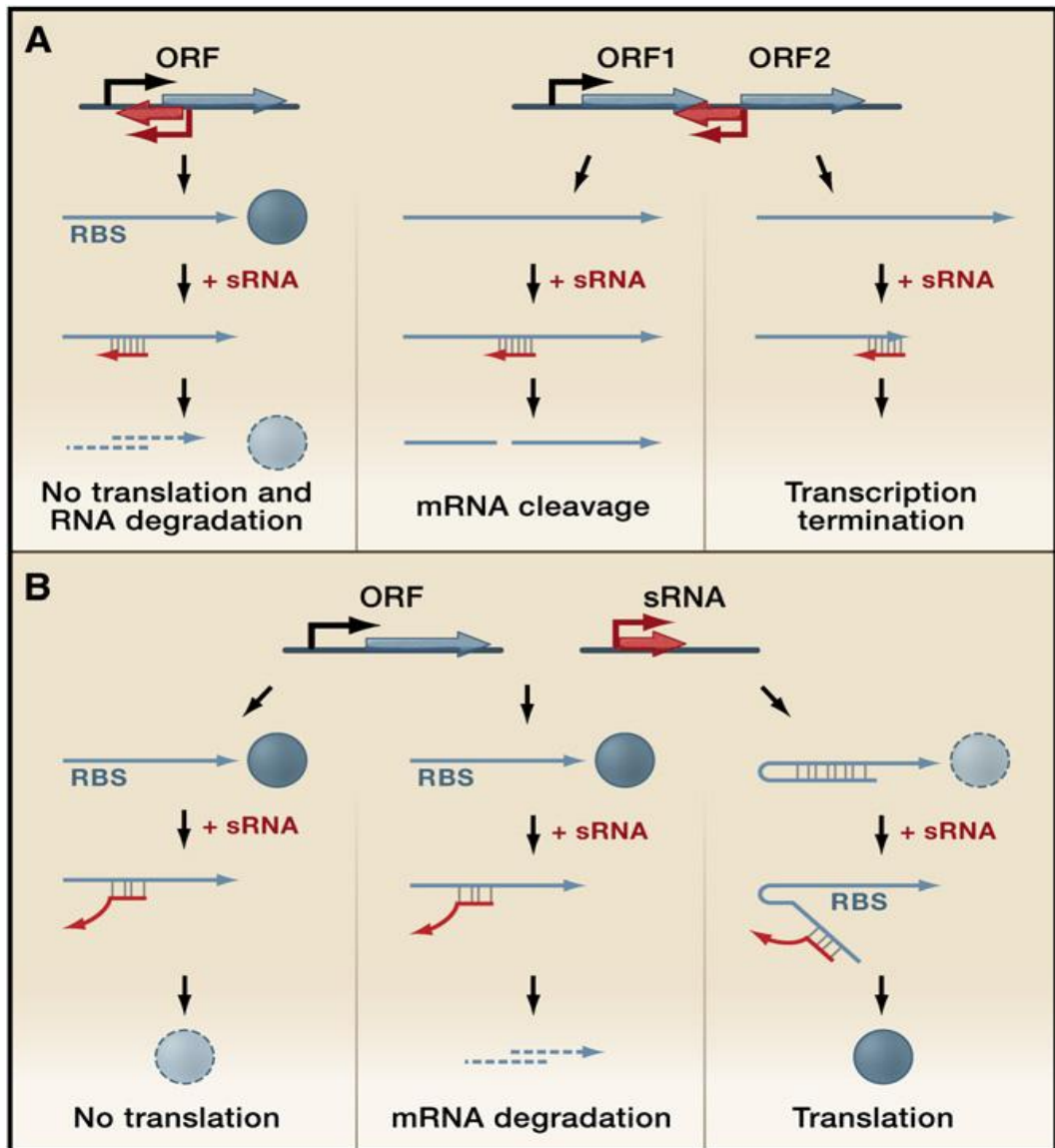


Figure 4 Gene regulation mediated by regulatory RNAs which act by base-pairing (Waters & Storz, 2009)

(A) Two possible configurations of cis-encoded antisense sRNAs (red) and their target RNAs (blue), which share extensive complementarity. (Left panel). A sRNA encoded opposite to the 5'UTR of its target mRNA. Base pairing inhibits ribosome binding and often leads to target mRNA degradation. (Right panels) A sRNA encoded opposite to the sequence separating two genes in an operon. Base pairing of the sRNA can target RNases to the region and cause mRNA cleavage, with various regulatory effects, or the sRNA can cause transcriptional termination, leading to reduced levels of downstream genes.

(B) Genes encoding trans-encoded antisense sRNAs (red) are located separately from the genes encoding their target RNAs (blue) and only have limited complementarity. Trans-encoded sRNA can act negatively by base pairing with the 5'UTR and blocking ribosome binding (left panel) and/or targeting the sRNA-mRNA duplex for degradation by RNases (middle panel). Trans-encoded sRNA can act positively by preventing the formation of an inhibitory structure, which sequesters the ribosome-binding site (RBS) (right panel).

However two recent papers suggest that in *Clostridium* and *Streptococcus* the VR-RNA and FasX sRNAs, exert positive regulation of virulence genes primarily at the level of mRNA stabilization (Obana *et al.*, 2010; Ramirez-Pena *et al.*, 2010) and reviewed in (Podkaminski & Vogel, 2010). Those sRNAs for which a function has been elucidated are involved in many different cellular processes including, adaptation and resistance to stresses (Repoila *et al.*, 2003), metabolism and homeostasis (Bejerano-Sagie & Xavier, 2007; Masse *et al.*, 2007), control of the expression of outer membrane proteins (Vogel & Papenfort, 2006), virulence and pathogenesis (Johansson & Cossart, 2003; Romby *et al.*, 2006; Toledo-Arana *et al.*, 2007). The trans-acting antisense class of sRNAs often require the RNA chaperone Hfq as a cofactor, which facilitates the interaction between sRNAs and target mRNAs (Valentin-Hansen *et al.*, 2004; Aiba, 2007; Chao & Vogel, 2010) (Fig 5). The binding of Hfq can affect the structure of sRNA and target mRNAs (Moller *et al.*, 2002; Zhang *et al.*, 2002; (Geissmann & Touati, 2004) and Hfq has been demonstrated to accelerate strand exchange to facilitate dynamic RNA-RNA interactions (Arluison *et al.*, 2007); furthermore Hfq protects many sRNAs from degradation, most likely by binding to RNase E cleavage sites within these sRNAs (Moll *et al.*, 2003).

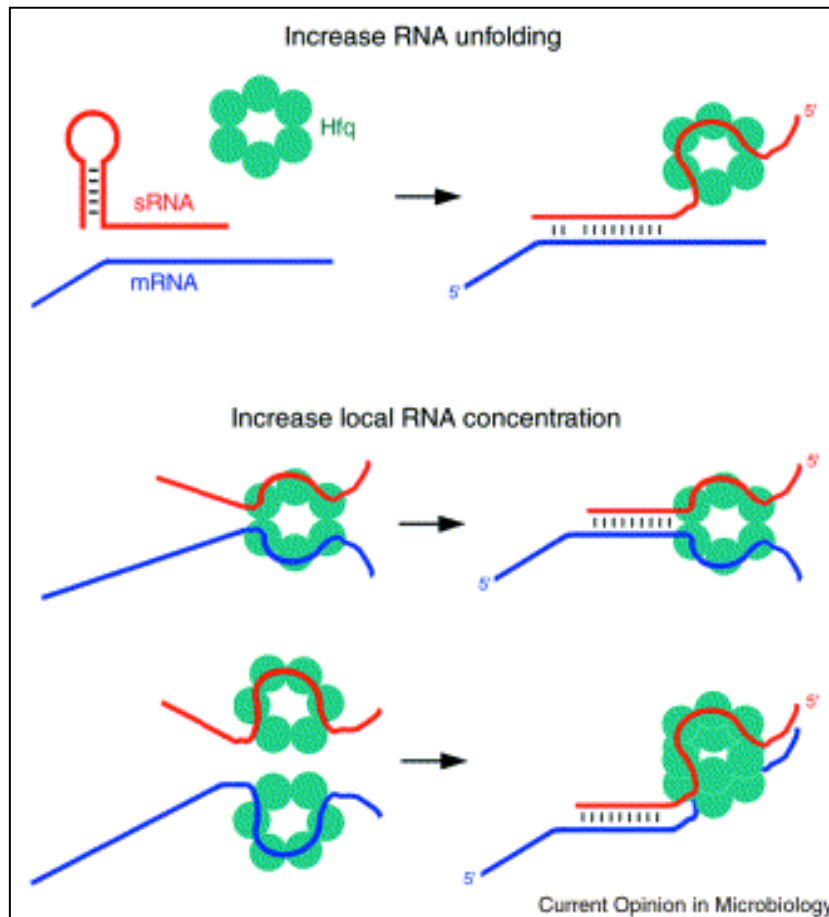


Figure 5: Mechanisms by which Hfq might facilitate sRNA-mRNA basepairing. (Storz *et al.*, 2004)

Hfq (aqua ring) may promote RNA unfolding or may increase the local concentrations of the sRNA (red) and its mRNA target (blue).

1.7 The pleiotropic regulator Hfq

Hfq is a hexameric RNA binding protein which was originally identified in *E. coli* as a host factor required for the replication of Q β bacteriophage (Kajitani & Ishihama, 1991). It shares structural and functional homology with the Sm proteins in eukaryotes, which have central roles in RNA metabolism (Pannone & Wolin, 2000). It has more recently been described as a pleiotropic regulator that modulates the stability or translation of an

increasing number of mRNAs (Valentin-Hansen *et al.*, 2004; Aiba, 2007; (Brennan & Link, 2007) and facilitates pairing of sRNAs with their target mRNAs (Moller *et al.*, 2002; Kawamoto *et al.*, 2006); Zhang *et al.*, 2002). Available structural data, the latest showing *E. coli* Hfq bound to polyriboadenilate RNA (Link *et al.*, 2009), suggest that Hfq acts as an RNA chaperone by binding sRNAs and mRNAs (Fig 6).

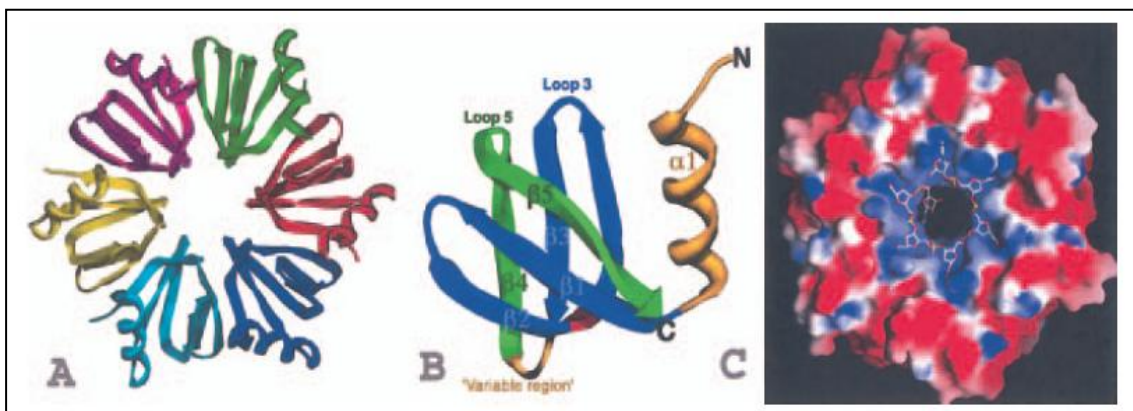


Figure 6. Structures of the *S. aureus* Hfq and an Hfq–RNA complex. (Valentin-Hansen *et al.*, 2004)

(A) Structure of the Hfq hexamer with each subunit coloured differently.

(B) Ribbon diagram of an Hfq subunit. The Sm1 motif is coloured blue and the Sm2 motif is green. Regions outside the two motifs, i.e. the N-terminal α -helix and the variable region, are colored yellow.

(C) Electrostatic surface representation of the RNA binding site of the Hfq hexamer. Blue is electropositive and red is electronegative. The RNA is shown as a stick model, with oxygen, nitrogen, carbon and phosphorus atoms colored red, blue, white and yellow respectively.

It has been shown that Hfq binds with greater avidity to RNA sites containing a short-single stranded stretch of uridines and adenosines (Brennan & Link, 2007; Brescia *et al.*, 2003; Mikulecky *et al.*, 2004; Sun &

Wartell, 2006). The Hfq protein is conserved in a wide range of bacteria and varies in length from 70 to 100 amino acids (Valentin-Hansen *et al.*, 2004) (Fig 7). In all cases, the Sm motif is located in the N-terminal region of the molecule. The C-terminal domain seems not to play a significant role in the major functions of Hfq. In fact, a C-terminal truncated form of the *E. coli* Hfq lacking the last 27 amino acids can replace all tested functions of the intact *E. coli* Hfq (102 amino acid residues) (Sonnleitner *et al.*, 2002). To date, Hfq candidates have been identified in about half the completed or nearly completed bacterial genomes. Two distinct copies are found in few species, including *Bacillus anthracis* and *Ralstonia* sp., and tandem Hfq sequences are present within a single 193-residue protein from *Novosphingobium aromaticivorans* (Sun *et al.*, 2002). Hfq can also modulate the decay of some mRNAs (e.g. rpsO, which encodes for ribosomal protein S15) by binding to their poly(A) tails, stimulating poly(A) adenylation by poly(A) polymerase I (PAP I) and protecting this message from polynucleotide phosphorylase (PNP), RNase II and RNase E, enzymes involved in mRNA degradation (Hajnsdorf & Regnier, 2000); (Mohanty *et al.*, 2004; Folichon *et al.*, 2005, Folichon *et al.*, 2003). It has been shown that Hfq can also protect many sRNAs from degradation, most likely by binding to RNase E cleavage sites within these sRNAs (Moll *et al.*, 2003). However, recently it has been demonstrated that in *Rhodobacter sphaeroides* the sRNA RSs0019 is stabilized in the absence of Hfq (Berghoff *et al.*, 2009) and also in this thesis we provide evidences for a sRNA being more stable in Δhfq of meningococcus. Based on the literature the contribution of Hfq to sRNA stability is controversial. While it has been shown that the binding of this chaperone, in the absence of basepairing,

stabilizes sRNAs protecting them from RNaseE cleavage (Moll *et al.*, 2003, Masse *et al.*, 2003); it has also been shown that Hfq-mediated pairing of sRNAs to their targets promotes coupled degradation of the interacting RNAs (Masse *et al.*, 2003). So it could be possible that binding of Hfq to a particular sRNA can accelerate its turnover.

Considering the role of Hfq as a pleiotropic regulator in bacteria it is not surprising that the inactivation of the *hfq* gene results in sensitivity to a wide number of environmental stresses and alters the synthesis of many proteins, including outer membrane porins (Muffler *et al.*, 1997; Sittka *et al.*, 2007; Tsui *et al.*, 1994; Valentin-Hansen *et al.*, 2007). Hfq also influences the fitness and virulence of many pathogenic bacteria. Mutants lacking Hfq are often sensitive to host defence mechanisms and highly attenuated in animal models (Ding *et al.*, 2004; Kulesus *et al.*, 2008; McNealy *et al.*, 2005; Sittka *et al.*, 2007; Pichon & Felden, 2005; Sonnleitner *et al.*, 2003). Interestingly, in *N. meningitidis* by signature-tagged mutagenesis *hfq* was identified as one of 73 genomic loci that attenuated *N. meningitidis* virulence in rats (Sun *et al.*, 2000). In this thesis we show that in *N. meningitidis* Hfq plays a major role in adaptation to stresses and virulence and by a transcriptome study we identified 152 Hfq-regulated genes which suggest the presence of Hfq-dependent sRNAs circuits in this bacterium. Indeed the meningococcal Hfq protein was shown to interact specifically with many sRNAs when expressed in the heterologous system *Salmonella typhimurium* (Sittka *et al.*, 2009) suggesting that the meningococcal protein has a conserved major function as a sRNA-binding protein. To date, virulence phenotypes of *hfq* mutants are most dramatic in Gram-negative pathogens. The role of Hfq in Gram-

positive species is still under investigation. It has been reported, in fact, that *Hfq* strains of *L. monocytogens* and *S. aureus* have wild type sRNA profiles (Christiansen *et al.*, 2004; Bohn *et al.*, 2007), but the conservation of key aminoacids (Valentin-Hansen *et al.*, 2004) and the proven role in antisense regulation (Nielsen *et al.*, 2010) suggest the functional conservation of Hfq in such species. We can speculate that transcriptional regulation by sRNAs can occur by both Hfq-dependent and independent mechanisms. It is not still understood if Hfq-independent trans-acting sRNAs can act on their own (depending on the free energy for sRNA-mRNA pairing interaction (Jousselin *et al.*, 2009), or if they depend on other factors that substitute the Hfq protein.

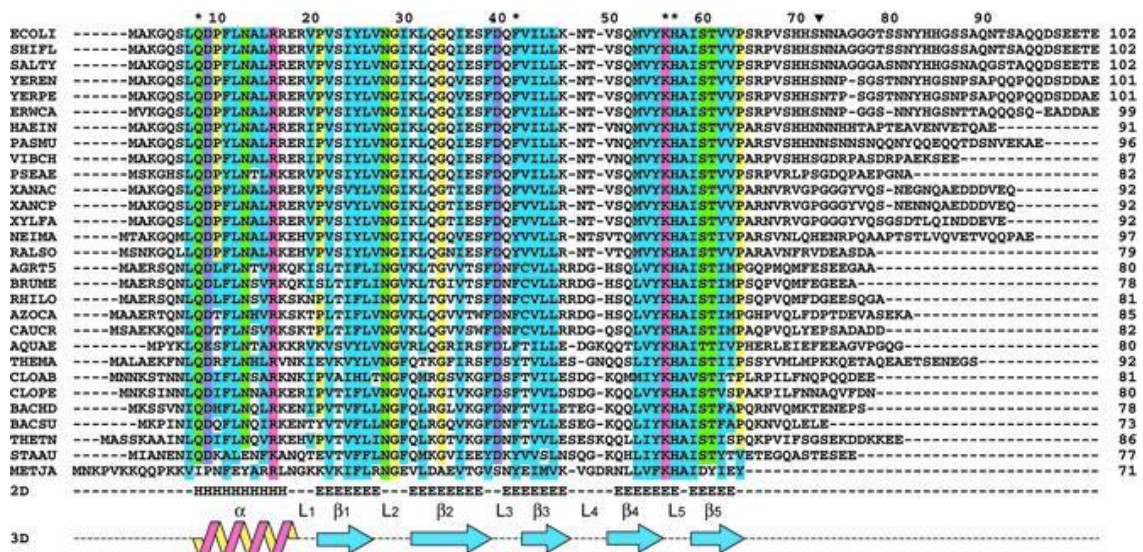


Figure 7: The Hfq family (Sauter *et al.*, 2003)

The organisms corresponding to the sequences are indicated on the left. Conserved polar, basic and acidic residues appear in green, pink and violet, respectively, Gly and Pro in yellow, and a star indicates those involved in RNA binding in *S.aureus* (Schumacher *et al.*, 2002). Blue boxes are conserved patches of hydrophobic residues. The 2D structure prediction from Jpred is indicated at the bottom as well as the 2D features seen in 3D structures.

1.8 How to identify new sRNAs

It is very well established that sRNAs play critical regulatory roles in many bacterial processes (reviewed in (Zhou & Xie, 2011; Beisel & Storz, 2010; Liu & Camilli, 2010; Toledo-Arana *et al.*, 2007; Repoila *et al.*, 2003). However, unlike regulatory proteins, non-coding regulatory sRNAs have not been readily identified and annotated in the bacterial genome sequences that are available in the databases, and in many systems, including *Neisseria* spp., their existence is still largely unexplored. For this reason experimental strategies have become increasingly important for sRNAs discovery. The first sRNAs were discovered about four decades ago fortuitously using genetic screens, or through radiolabeling of total RNA and subsequent isolation from gels (Wassarman *et al.*, 1999). But it was only very recently that many new sRNAs have been identified and characterized in a wide range of bacterial species. This was mainly possible thanks to the increased availability of novel technologies such as computational predictions of sRNAs, tiling arrays and high-throughput cDNA sequencing (RNA-seq) that are used to study sRNAs at the genome-wide level (Sharma & Vogel, 2009). The last two techniques not only allow the identification of novel sRNAs, but also the analysis of the whole transcriptome of bacteria in different growth conditions. The high density (tiling) arrays carry up to hundreds of thousands of DNA oligonucleotides systematically covering the sense and antisense strand of a genome, including the intergenic regions (IGRs) from which most known sRNAs are expressed. An important issue in this kind of technique, as well as the RNA-seq, is choosing physiological conditions in which sRNAs are

expressed. Genomic tiling arrays have been successfully used to study the transcriptome of *Listeria monocytogenes* (Toledo-Arana *et al.*, 2009), *Bacillus subtilis* (Rasmussen *et al.*, 2009) and *Mycoplasma pneumoniae* (Guell *et al.*, 2009), as well as specific genomic features in *E. coli* (Selinger *et al.*, 2000) and *Caulobacter crescentus* (McGrath *et al.*, 2007). However, the array-based approach requires hundreds of thousands probes and is limited by background noise and cross hybridization, and therefore requires extensive normalization (Sorek & Cossart, 2010). In contrast to microarray methods, RNA-seq directly determine the cDNA sequence. This technique uses recently developed deep-sequencing technologies. In general, a population of RNA is converted to a library of cDNA fragments with adaptors attached to one or both ends. Each molecule, with or without amplification, is then sequenced in a high-throughput manner to obtain short sequences. The reads are typically 30–400 bp, depending on the DNasequencing technology used. To generate a transcriptome map, these reads are computationally mapped to the reference genome (Fig 8).

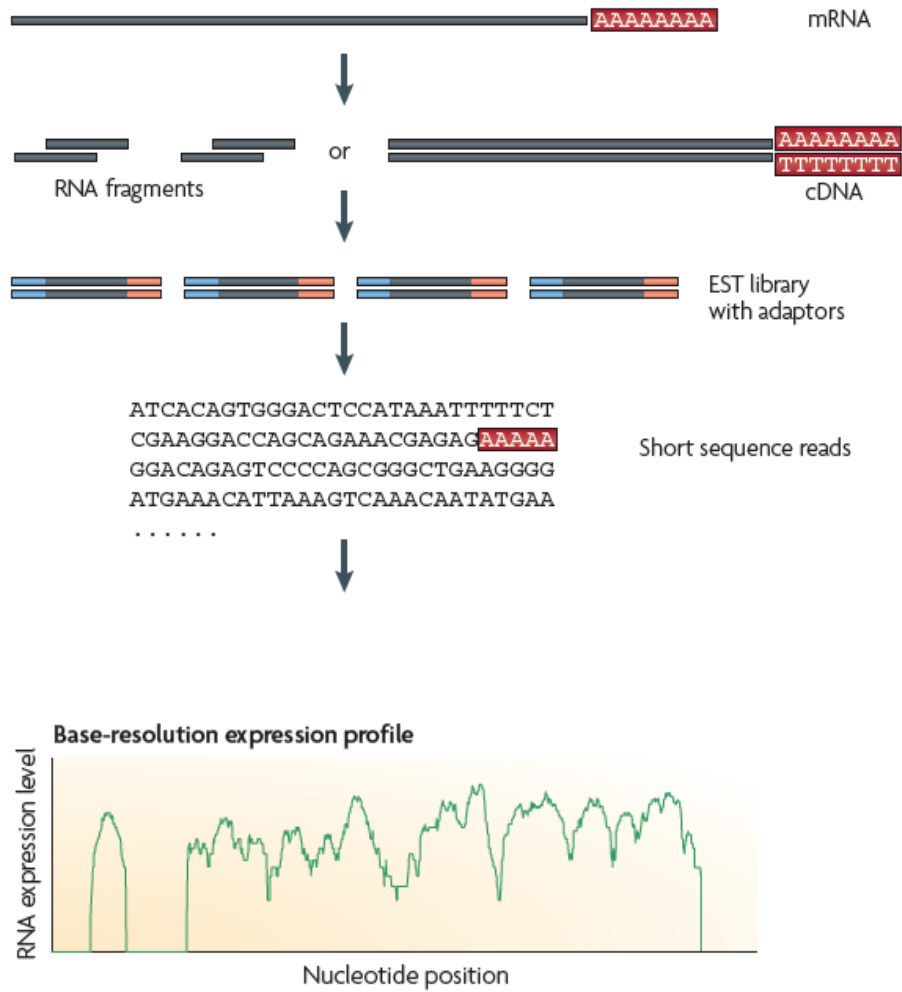


Figure 8: A typical RNA-seq experiment. (Wang *et al.*, 2009)

Briefly, long RNAs are first converted into a library of cDNA fragments through either RNA fragmentation or DNA fragmentation. Sequencing adaptors (blue) are subsequently added to each cDNA fragment and a short sequence is obtained from each cDNA using high-throughput sequencing technology. The resulting sequence reads are aligned with the reference genome or transcriptome and used to generate a base-resolution expression profile. In principle, any high-throughput sequencing technology can be used for RNA-Seq (Wang *et al.*, 2009), and the Illumina, Applied Biosystems SOLiD and Roche 454 Life Science systems have already been applied for this purpose in bacteria (Passalacqua *et al.*, 2009; Perkins *et al.*, 2009; Sittka *et al.*, 2008; Yoder-Himes *et al.*, 2009; Wurtzel *et al.*, 2010). An important

advantage of RNA-Seq is that it has very low, if any, background signal because DNA sequences can be unambiguously mapped to unique regions of the genome. A transcriptome analysis can be used to improve genome annotation by enabling: the discovery of new genes, the correction of gene annotation; the detection of UTRs and transcription start sites and the determination of operon relationship (Sorek and Cossart, 2009 and Fig 9). Furthermore, whole-transcriptome analysis now allows the global interrogation of sRNA abundance and antisense RNAs in any species primarily by detecting expression from non-protein-coding regions. In this way, for example, 13 sRNAs that were induced during niche switching in the opportunistic pathogen *B. cenocepacia* were recently discovered (Yoder-Himes *et al.*, 2009). Similarly, Perkins *et al.* detected 55 intergenic regions that are likely to encode new sRNAs in *Salmonella* Typhi Ty2 (Perkins *et al.*, 2009), and the number of known sRNAs in *L. monocytogenes* has been more than doubled to 50 sRNAs by a tiling arraybased study (Toledo-Arana *et al.*, 2009). Interestingly, sRNAs can also be enriched by co-immunoprecipitation with the Hfq protein (Zhang *et al.*, 2003; Stikka *et al.*, 2008) and subsequently sequenced. In conclusion, with whole-transcriptome analysis it is now possible to study the involvement of elements such as sRNAs, riboswitches and cis-antisense regulators in the physiology and pathogenicity of any prokaryote.

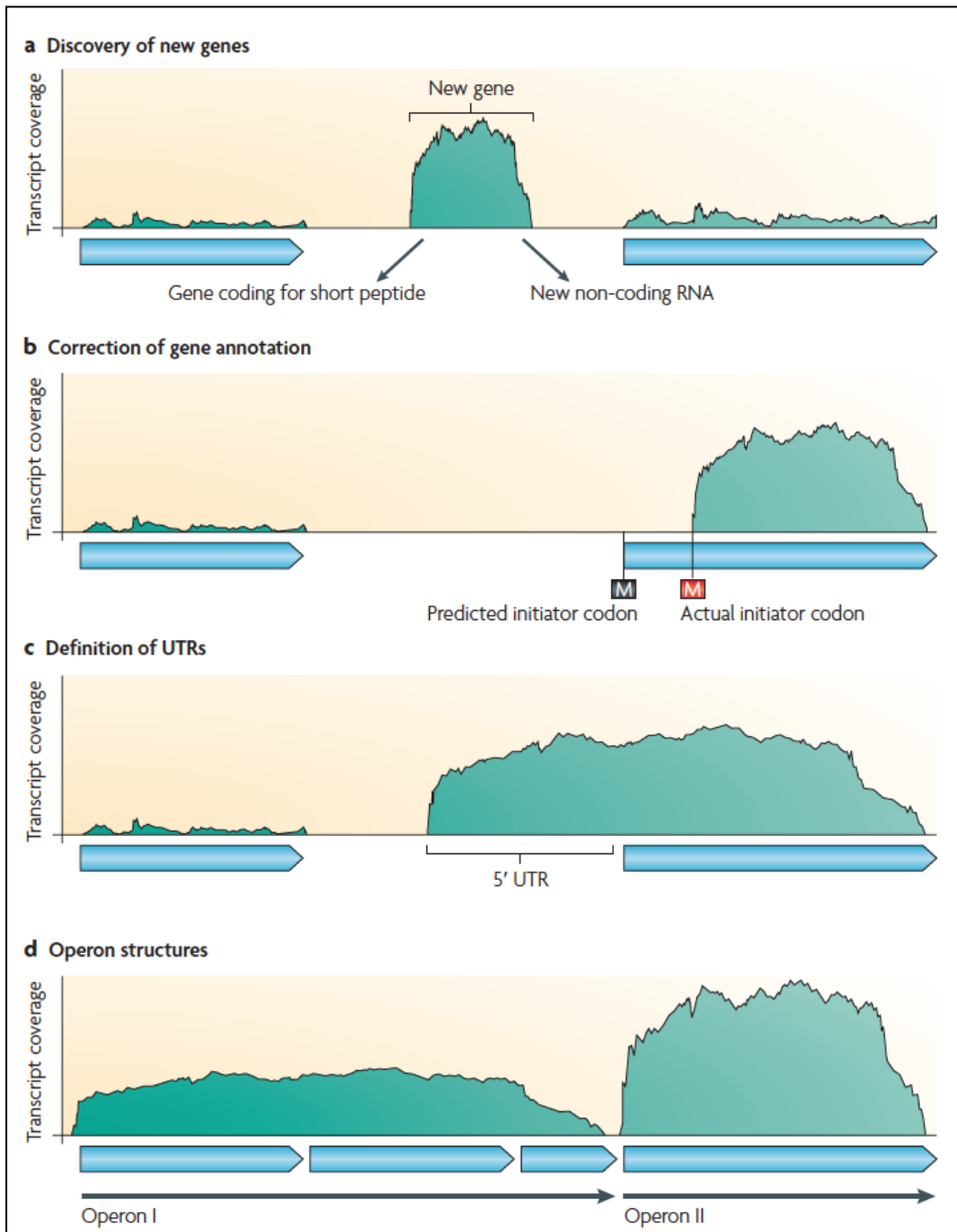


Figure 9: Different applications of RNA-seq (Sorek & Cossart, 2010)

The *x* axis represents a schematic genomic region and the *y* axis represents transcript coverage as derived from RNA-seq. The light blue arrows depict annotated genes. Transcriptomic information can be used to improve genome annotation by enabling: the discovery of new genes or sRNAs (**a**); the correction of gene structure annotations (**b**); the detection of UTRs and transcription start sites (**c**); and the determination of operon relationships (**d**).

RESULTS

I. Characterization of a *hfq* knock out mutant in *Neisseria meningitidis*

1.9 The *hfq* locus of *N. meningitidis*

In *N. meningitidis*, the *hfq* gene (NMB0748) is predicted to encode a protein of 97 amino acids and shows 65% identity with the Hfq protein from *E. coli*. In the MC58 genome *hfq* is flanked upstream by a 147-bp intergenic region possibly containing its promoter and is followed downstream by a putative transcriptional terminator (Fig. 10A). This is in contrast to *E. coli* and other similar enterobacteria, in which *hfq* appears to be located in a cluster of genes which form an operon, usually transcriptionally linked to the upstream gene *miaA* (Tsui *et al.*, 1994). We mapped the promoter of the *hfq* gene of *N. meningitidis* in the intergenic region directly upstream by performing S1 nuclease protection analysis. Total RNA was isolated from the MC58 strain during *in vitro* growth and then hybridized with a *hfq*-specific probe and digested with S1 nuclease. Figure 10B shows an RNA-protected band which corresponds to the 5' end of the *hfq* mRNA, which maps the transcriptional initiation site (+1) to 49 nucleotides upstream of the ATG start site of the gene. Analysis of the nucleotide sequence upstream revealed -10 (TACAAT) and -35 (TGGATA) hexamers, suggesting that the *hfq* gene is transcribed from a σ^{70} promoter. The intensity of this band does not vary significantly in RNA prepared from various time points in the growth curve, suggesting that the

hfq promoter is transcribed constitutively throughout the various growth phases.

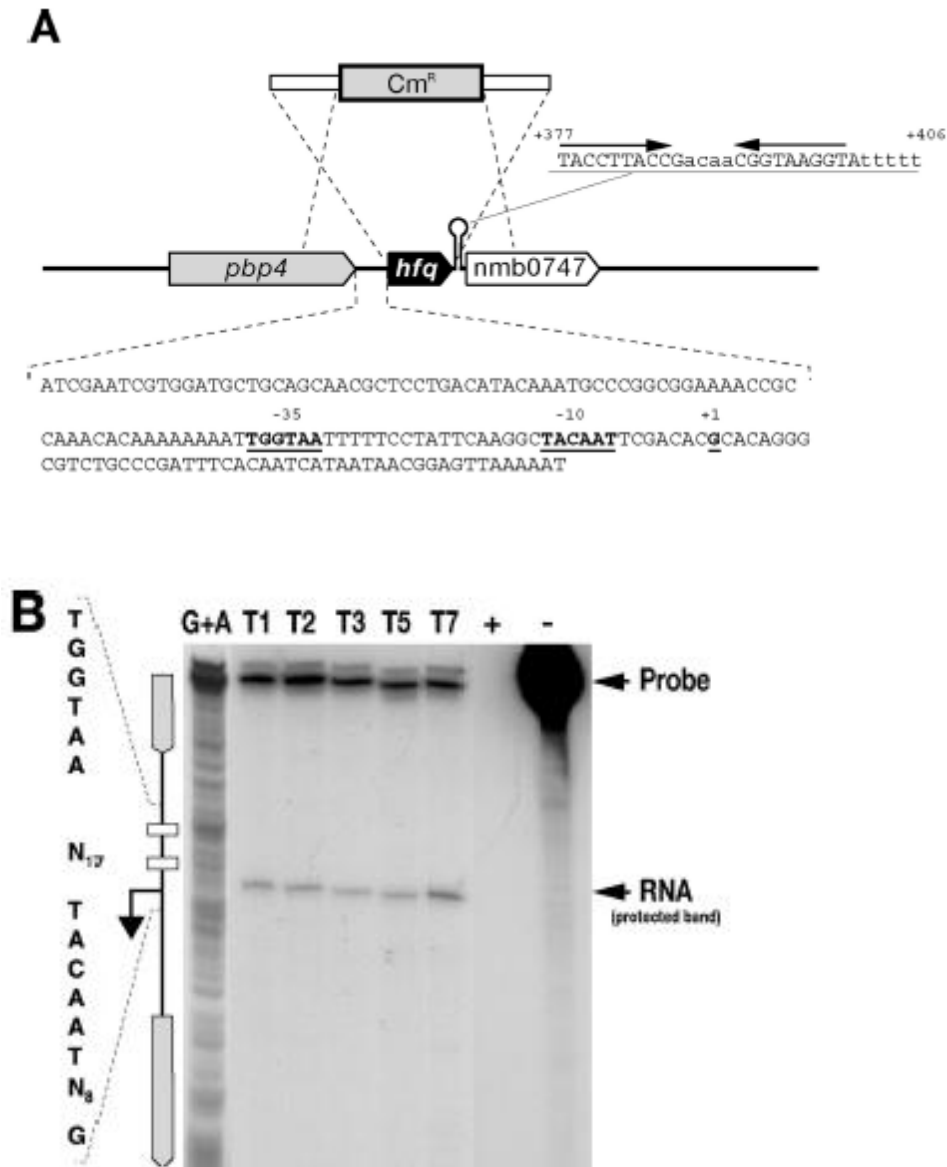


Figure 10: The *hfq* locus of *N. meningitidis*. (A) Diagram of the *hfq* locus in the genome of *N. meningitidis* strain MC58, showing the strategy used to construct the *hfq* null mutant by allelic replacement with a chloramphenicol cassette. The genes flanking the *hfq* gene in meningococcus are an upstream gene encoding a putative D-alanine-endopeptidase and a downstream gene encoding a conserved hypothetical protein with homology to RNA methylases. These genes are different from genes in other Gram-negative and Gram-positive bacteria in which a similar genetic organization has often been observed. In the sequence of the intergenic region upstream of the *hfq* gene underlined bold type indicates -10 and -35 hexamers and the transcriptional start site at position +1, as shown in panel B.

The sequence of the putative rho-independent transcriptional terminator and its position with respect to the initiation of transcription at position +1 are also shown. **(B)** Mapping of the *hfq* promoter by an S1 nuclease protection assay. The DNA probe was radioactively labeled at one end, hybridized to 15 µg of total meningococcal RNA (lanes T1, T2, T3, T5, and T7), and digested with S1 nuclease for mapping of the 5' end of the *hfq* transcript. Total RNA was prepared after 1, 2, 3, 5, and 7 h of growth in GC broth (lanes T1, T2, T3, T5, and T7, respectively). Two control samples with *E. coli* tRNA instead of total RNA were processed in parallel with (lane +) and without (lane -) addition of S1 nuclease. The position of the RNA-specific S1 nuclease-protected band corresponding to the 5' end of the *hfq* transcript is indicated. Lane G+A contained a G-A sequence reaction mixture for the DNA probe used as a size marker. The nucleotide sequence of the coding strand upstream of the transcriptional start site is shown on the left.

1.10 Expression of the meningococcal Hfq protein and generation of an Hfq null mutant

In order to investigate the expression of the Hfq protein in the MC58 strain, we purified the Hfq protein and raised antibodies to Hfq in mice. We cloned the *hfq* gene into an expression vector, expressed it as a recombinant His-tagged protein in *E. coli*, and then purified it by Ni-NTA affinity chromatography. Figure 11A shows the results of an SDS-PAGE analysis of various fractions obtained for the expression and purification steps. The Hfq protein was highly expressed in the soluble fraction (Fig. 11A, lane 3) and gave rise to a highly pure recombinant His-Hfq protein preparation (lanes 6 to 8), and the N-terminal His tag was cleaved and removed after purification, giving rise to an untagged Hfq protein (lane 9). Using *in vitro* cross-linking, we investigated whether this protein oligomerized into its functional hexameric form. As Fig. 11B shows, after treatment for 1 h with the DSS cross-linker, two high-molecular-weight oligomers were visible on the gel. One of the major cross-linked forms migrated at a molecular weight

of approximately 70,000, which is consistent with the hexameric form of the protein, and the other more slowly migrating form may represent two cross-linked hexamers, suggesting that the recombinant Hfq protein forms hexamers in solution. This protein preparation was used to raise antibodies against meningococcal Hfq in mice, and the resulting antiserum was tested in an immunoblot analysis with total protein samples taken from time course cultures of the MC58 strain and an Hfq null mutant strain.

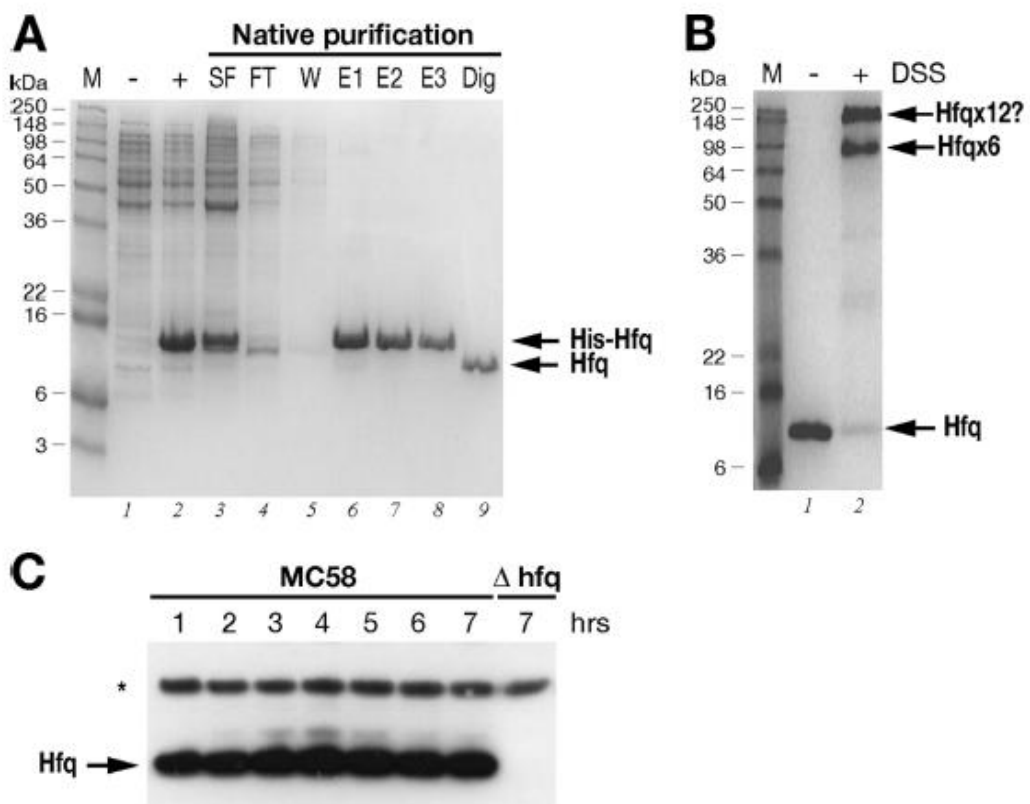


Figure 11 : (A) Expression and purification of the recombinant Hfq protein. SDS-PAGE was performed with protein extracts from uninduced (lane -) and IPTG-induced (lane +) cultures of *E. coli* containing the pET15bHfq expression plasmid, the cleared soluble fraction before (lane SF) and after (lane FT) binding to the Ni-NTA resin, the wash fraction (lane W), elution fractions (lanes E1 to E3), and untagged Hfq protein after thrombin digestion (lane Dig). (B) *In vitro* cross-linking of Hfq reveals hexameric forms in solution. For *in vitro* cross-linking, the untagged protein was not treated (lane -) or treated (lane +) with the cross-linking reagent DSS. The relative positions of the molecular weight markers (lane M) are indicated on the left. The positions of the oligomeric forms of the Hfq protein are indicated on the right. (C) Western blot showing the expression of the Hfq protein in

wild type strain MC58 or the *Δhfq* mutant over time. Total protein samples were taken at the time points shown in Fig. 12A. Five micrograms of total protein was loaded for each time point. Anti-Hfq antiserum recognizes a band at approximately 11 kDa in the wild type strain but not in the Hfq null mutant. Antiserum against NMB2091 was also used to stain the blot as a loading control for total protein, as indicated by the asterisk.

The null mutant of MC58 was generated by replacing the *hfq* gene with a chloramphenicol cassette, as indicated in Fig. 10A. This mutant, when it is grown on solid medium, has an obvious growth phenotype in that it forms small pinpoint colonies after overnight incubation. Furthermore, after approximately 2 to 3 days of growth on solid medium, the centers of the colonies have a concave morphology, and, where there is confluent growth on the plate, the culture appears to be more flat and acquires a silver sheen. We grew the wild type and null mutant in liquid GC medium and took samples every hour over the time course. Consistent with the growth phenotype on plates, the null mutant exhibited a significantly altered growth curve compared with the wild type in liquid medium (Fig. 12A). In particular, it had an increased lag phase and did not reach a cell density equivalent to that of the wild type. Western blot analysis of the expression of Hfq throughout the time course (Fig. 11C) revealed that the anti-Hfq antiserum recognizes a protein band migrating to a position corresponding to approximately 11 kDa in the wild type, which is absent from the null mutant strain. Furthermore, the protein is expressed during all phases of the growth curve, which is consistent with results shown in Fig. 10B, and no significant differences in the level of expression were detected, except possibly for slight accumulation of the protein in late log and stationary phases.

1.11 Complementation of the Hfq mutant.

In order to investigate downstream polar effects due to the *hfq* mutation, we performed RT-PCR analysis of the NMB0747 gene using RNA prepared from the wild type and the Hfq knockout mutant. The results showed that there was a 10-fold reduction in RNA levels for NMB0747, indicating that readthrough of the putative rho-independent terminator occurs and that it is likely that *hfq* is coexpressed with the downstream gene. In order to determine if the phenotypes of the mutant were directly related to the lack of expression of the Hfq protein or possible polar effects, we generated a complemented mutant strain expressing a single copy of the *hfq* gene in *trans* and related this expression to possible restoration of the wild type phenotype. In this strain, Δhfq_C , the expression of the *hfq* gene was inducible by addition of IPTG, as its transcription is under the control of the P_{lac} promoter and the LacI repressor. This strain was grown in liquid cultures in the presence of increasing amounts of IPTG, along with the wild type and mutant strains, and the growth curves are shown in Fig. 12A. Samples were collected at mid-log phase, and total protein extracts of each strain were used to monitor Hfq expression by Western blotting (Fig. 12B). The generation time of the mutant was significantly less (78 ± 10 min) than that of the wild type (48 ± 7 min), while the generation times of the complemented mutant were shorter in cultures with IPTG-induced increases in Hfq expression. It is worth noting that the levels of Hfq expression in the complementing strain at the time of maximal induction were approximately two- to threefold less than the wild type levels, and this may explain the incomplete restoration of the growth phenotype. These results indicate that

the growth defect of the Δhfq mutant can be restored by expression of Hfq in a dose-dependent manner.

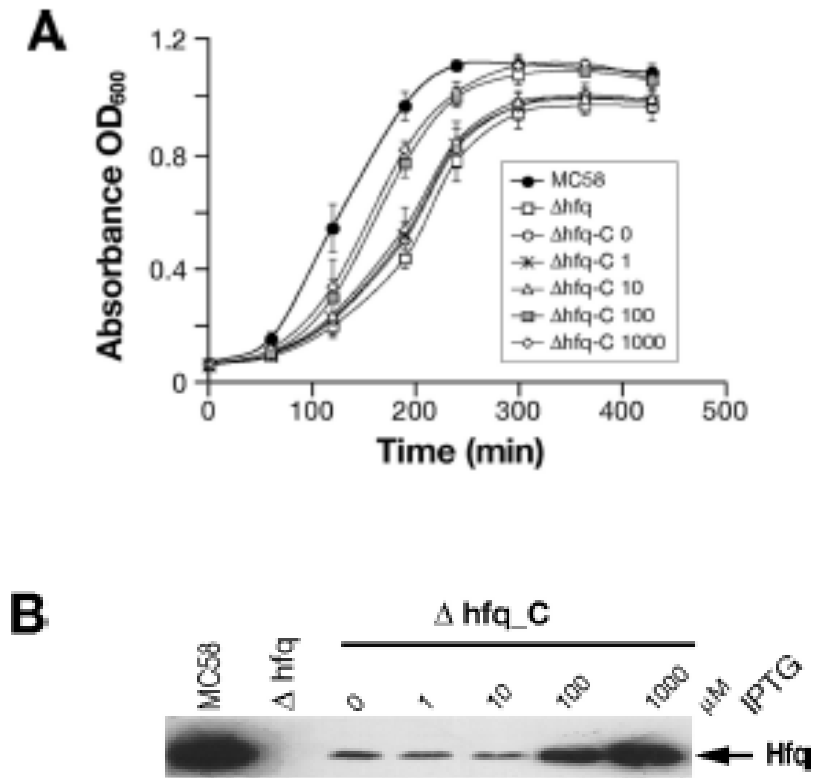


Figure 12 : (A) Growth curves for the wild type, the Δhfq mutant, and the Δhfq_C complemented mutant in GC medium supplemented with different concentrations of IPTG (in μM , as indicated after the mutant designation). Three independent sets of cultures were grown on different days, and the symbols indicate the average of the three cultures for each strain; the error bars show the standard deviations. The calculated generation times of the cultures were as follows: MC58, 48 ± 7 min; Δhfq , 78 ± 10 min; and Δhfq_C with 0, 1, 10, 100, and 1,000 μM IPTG, 80 ± 5 , 80 ± 5 , 70 ± 17 , 55 ± 8 , and 51 ± 10 min, respectively. (B) Western blotting of cell lysates of the MC58 wild type strain, the Δhfq mutant, and the complemented mutant, showing Hfq expression. IPTG was added at the final concentrations indicated to the growth medium for induction of Hfq in the complemented mutant. Cells were grown in GC broth to an OD600 of 0.5, and 10 μg of total protein was added to each lane.

1.12 Hfq plays a major role in stress tolerance in *N. meningitidis*.

As Hfq is reported to be involved in stress tolerance in many pathogens (Christiansen *et al.*, 2004; Robertson & Roop, 1999; Schiano *et al.*, 2010; Meibom *et al.*, 2009) and a large number of proteins are differentially expressed in the Δhfq mutant, we tested the ability of the meningococcal Δhfq mutant to resist several environmental stresses. A series of growth assays and killing assays were performed with the wild type, the Δhfq mutant, and the Δhfq_C complemented mutant strain in the presence of different antimicrobial compounds. The Δhfq mutant was significantly more sensitive than the wild type strain to three membrane-perturbing detergents (the nonionic detergents Triton X-100 and Tween, as well as the anionic detergent SDS), and the results of a representative viability assay are shown in Fig. 13A. Likewise, the lack of expression of the *hfq* gene resulted in increased sensitivity of the null mutant strain to killing by oxidative stress, as investigated using paraquat (which generates superoxide anion radicals inside the cell), xanthine-xanthine oxidase (which generates superoxide and H₂O₂ outside the cell), and H₂O₂ assays (Fig. 14B). We also challenged the strains with 4.5 M NaCl in an osmotic stress assay. Again, the Δhfq mutant was significantly more sensitive than the strains expressing the Hfq protein (Fig. 13C). Finally, we tested whether the meningococcal mutant was more sensitive to antimicrobial peptides, such as polymyxin B or LL-37. Antimicrobial peptides are an important part of the innate immune response, which can attack the outer membrane, forming holes and thereby causing misfolding of the periplasmic proteins and envelope stress. The results

shown in Fig. 13C indicate that Hfq contributes considerably to resistance to antimicrobial peptides in meningococcus. In all assays performed, the complemented mutant exhibited resistance patterns very similar to those of the wild type (Fig. 13A to C), confirming that inactivation of Hfq results in considerable sensitivity of the mutant strain to these antimicrobial compounds. The wild type, the mutant, and the complemented mutant all behaved similarly when they were incubated for the duration of the assay in GC broth, indicating that the differences in survival are not due to intrinsic growth defects (data not shown). Based on all these analyses, the Hfq protein plays an important role in the resistance of meningococcus to a wide range of stresses, many of which may be particularly physiologically relevant to the infectious cycle.

1.13 Hfq contributes to the survival of meningococcus in *ex vivo* and *in vivo* models

To examine how the strains responded to conditions comparable to those in the host, their survival in *ex vivo* whole-blood and serum assays was assessed. The human blood assay was used to assess both cellular and humoral mechanisms of killing (including the action of complement, antibody-mediated serum bactericidal activity, and opsonophagocytosis, as well as killing by neutrophils, macrophages and antimicrobial peptides), while the serum assay was used to assess killing of *N. meningitidis* mediated by the humoral immune response. The Hfq mutant was less able to survive in human blood and exhibited serum sensitivity (Fig. 14A and B). Once the serum was heat inactivated, the sensitivity of the Δhfq mutant was

lost, and the number of CFU did not decrease over the time course of the assay, which implies that the Δhfq mutant is sensitive to a heat-labile component of the complement pathway. For *in vivo* infection studies, an isogenic *hfq* mutant of the adapted 2996 strain was generated for use in the infant rat model. Groups of six mice were inoculated intraperitoneally with either a high (10^5 CFU) or low (10^3 CFU) dose of the wild type or the Δhfq mutant strain. After 18 h, the animals were bled, and bacteria were counted by colony plating. Compared to the counts for the wild type strain, the bacterial counts for the Δhfq mutant were significantly decreased (Fig. 14C). Although we cannot exclude the possibility that the growth phenotype may contribute to the reduced survival in the rat, these results suggest that Hfq plays a role in the pathogenesis of meningococcus in *ex vivo* human models and in the *in vivo* infant rat model.

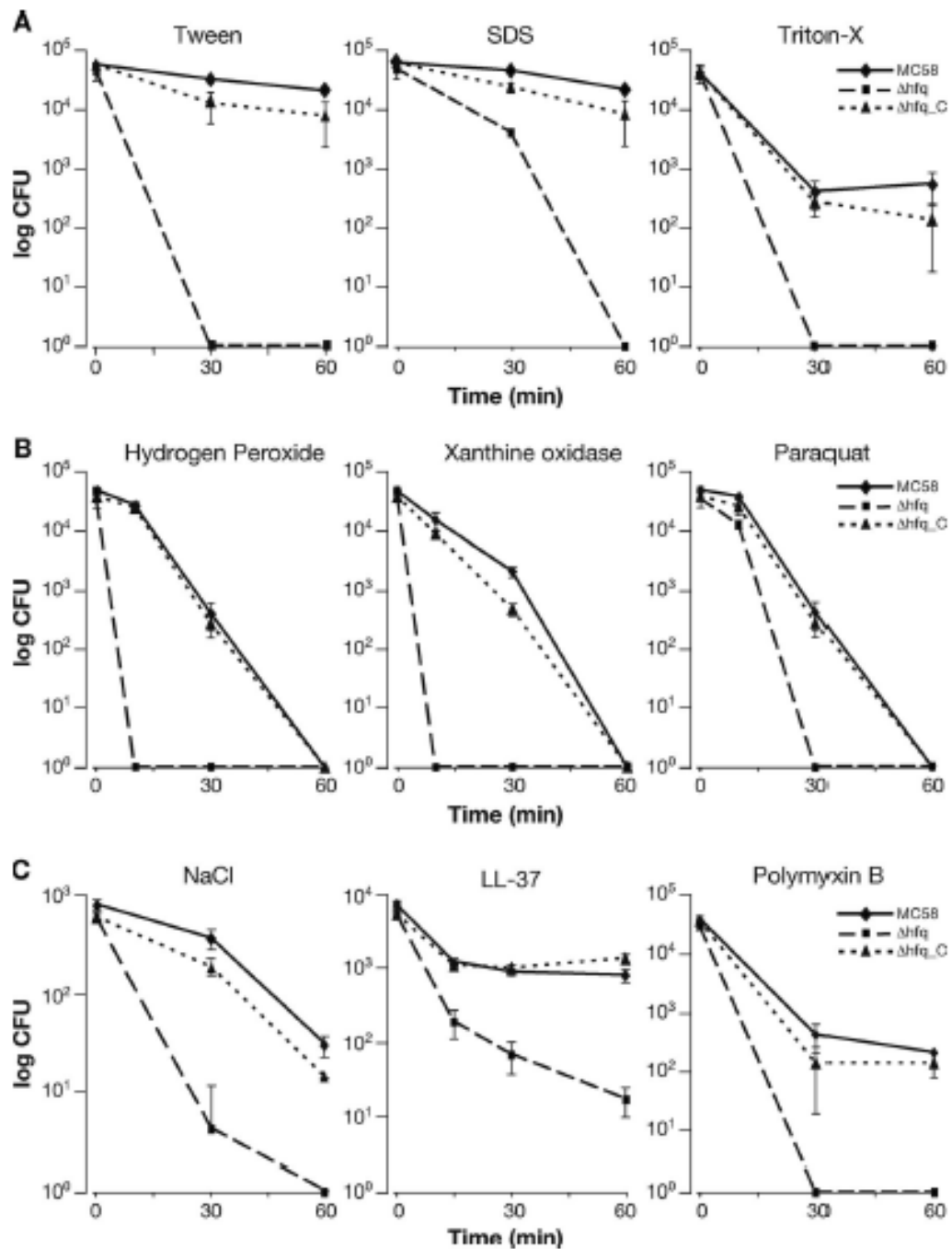


Figure 13: Assays of the viability of wild type strain MC58, the Δhfq mutant, and the Δhfq_C complemented mutant. Cells were grown to an OD600 of 0.5 in GC broth (1 mM IPTG was added for expression of Hfq in the complemented mutant), diluted, and incubated with the antimicrobial compounds indicated. Samples were taken at 15, 30, and/or 60 min, and viable cell counts were determined by plating. The final concentrations of compounds used were as follows: Tween, 0.05%; SDS, 0.01%; Triton X-100, 0.1%; hydrogen peroxide, 5 mM; xanthine oxidase, 4.3 mM xanthine and 300 mU xanthine oxidase; paraquat, 5 mM; NaCl, 4.5 M; LL-37, 2 μ M; and polymyxin B, 10 μ g/ml.

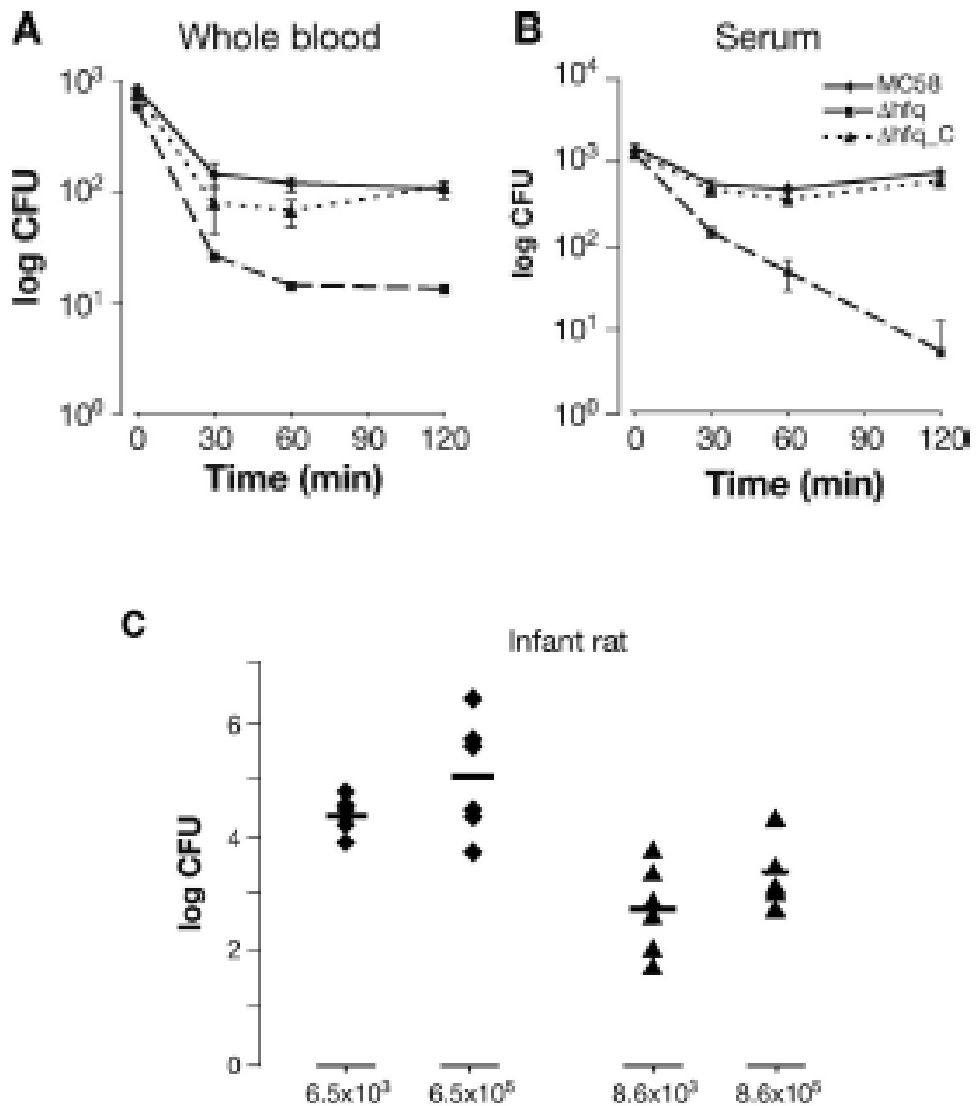


Figure 14: Survival of strain MC58, the Δhfq mutant, and the Δhfq_C complemented mutant in *ex vivo* whole blood (A) and serum (B) assays and an *in vivo* infant rat model (C). There was a reduced level of bacteremia with the Δhfq mutant in an infant rat infection model. Groups of animals were inoculated with two initial doses (approximately 10^3 and 10^5 CFU; specific levels of the initial inoculum were determined in each case and are indicated on the x axis), and bacterial counts for the wild type (diamonds) and the Δhfq mutant (triangles) recovered from the blood of each animal were determined after an 18-h period. The *P* values for comparisons of the levels of the wild type and the Δhfq mutant recovered with initial doses of 10^3 and 10^5 CFU are 0.0007 and 0.0057, respectively

1.14 Identification of proteins differentially expressed in the *Δhfq* mutant

To obtain a preliminary picture of global changes in the expression profiles of proteins altered in the *Δhfq* mutant, we compared the whole-cell protein patterns in SDS-PAGE gels for culture samples obtained at mid-log phase (Fig. 15). The lack of Hfq in the mutant results in global changes in protein expression, and many protein bands are more abundant or less abundant in the Hfq-deficient strain. Furthermore, the expression profile of the mutant is restored to a profile similar to that of the wild type after restoration of Hfq expression in the *Δhfq_C* strain by IPTG addition. In order to identify some of the proteins differentially expressed due to deletion of the Hfq protein, total protein from logarithmically grown cultures of wild type and *Δhfq* mutant cultures were separated by one-dimensional (1D) or 2D electrophoresis. Furthermore, cell cultures were also fractionated to obtain secreted, cytoplasmic, and envelope fractions and separated by 1D SDS-PAGE. Representative gels for triplicate samples are shown in Fig. 15, and the most altered protein spots and bands that were identified by mass spectrometry are shown in Fig. 15B and C, respectively. These spots and bands were excised and digested with trypsin, and the resulting peptides were analyzed by MALDI-TOF mass spectrometry. It is worth noting that a greater number of high-molecular-weight proteins appeared to be released into the supernatants of the *hfq* mutant cultures than into the supernatant of the wild type strain cultures, although many of these proteins could not be identified. Using mass spectrometry analysis following 1D and 2D separation, we were able to identify 27 proteins that showed altered

accumulation in the *Δhfq* mutant, and results of these analyses are shown in Table 1. Twenty of the proteins appear to be upregulated in the *Δhfq* mutant, and seven proteins are downregulated. The functions of the proteins whose abundance is altered can be subdivided into various groups, including energy metabolism, amino acid biosynthesis, oxidative stress responses, and outer membrane proteins (OMPs), many of which are associated with pathogenicity.

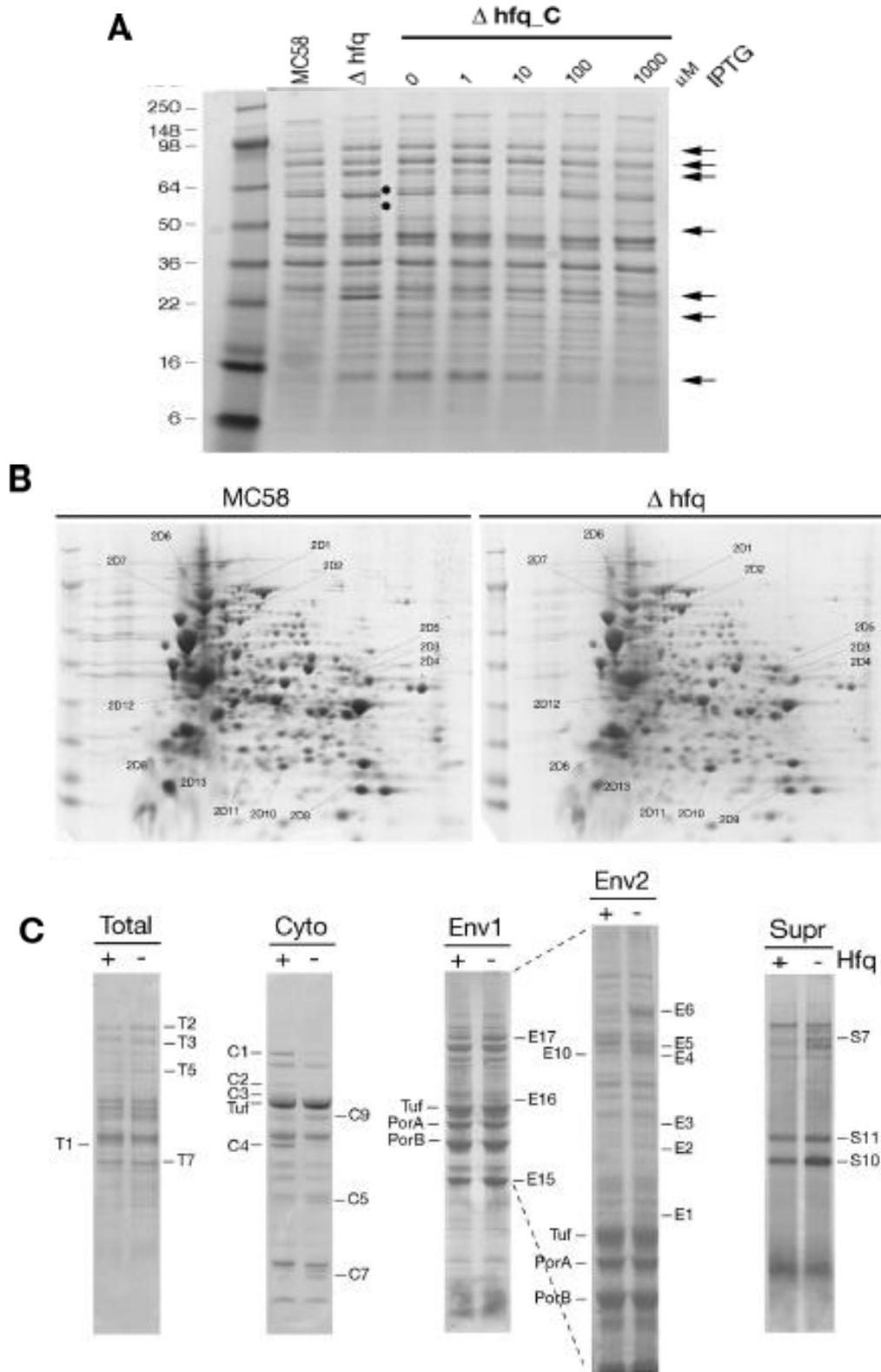


Figure 15 : Identification of differentially abundant proteins in the Δhfq knockout mutant. (A) SDS-PAGE of cell lysates of the MC58 wild type strain, the Δhfq mutant, and the complemented mutant, showing pleiotropic effects of Hfq on protein expression in the Δhfq mutant. The arrows on the right indicate the positions of derepressed protein bands, and the

filled circles indicate downregulated protein bands in the *hfq* null mutant. **(B)** Total proteins of logarithmically grown wild type strain MC58 and the Δhfq mutant were separated by 2D gel electrophoresis. Proteins were first focused on a nonlinear pH 3 to 10 gradient and then separated on a 9 to 16.5% SDS-polyacrylamide gel. Cells were grown to an OD600 of 0.5 in GC broth. **(C)** 1D SDS-PAGE analysis of total proteins (Total) or cytoplasmic (Cyto) or envelope (Env1 and Env2) fractions of cells of the wild type (lane +) and the Hfq mutant (lane -) grown to log phase in GC broth. Both 1D and 2D gels were stained with Coomassie brilliant blue R-250. In addition, wild type and Hfq mutant cultures were grown to an OD600 of 0.2 in Mueller-Hinton medium containing 0.25% glucose, and 22 ml of cell-free supernatant was precipitated and loaded (Supr)

Table 1: Deregulated proteins in *Δhfq* identified by Mass-SPEC

Band/Spot	Designation (gene)	Category or Protein Name	Predicted Function	Molecular weight	Relative change in <i>Δhfq</i> (fold) ^a
Down-regulated proteins					
C1	NMB0758 (<i>pnp</i>)	Polyribonucleotide nucleotidyltransferase	RNA metabolism	76374	-3.0
C2 2D12	NMB1938 (<i>atpA</i>)	ATP synthase F1, alpha subunit	Energy metabolism: ATP-proton motive force interconversion	55257	-2.4
C3	NMB1936 (<i>atpB</i>)	ATP synthase F1 beta subunit	Energy metabolism: ATP-proton motive force interconversion	50360	-2.1
T1 C4	NMB0763 (<i>cysK</i>)	Cysteine synthase	Amino acid biosynthesis: Serine family	32800	-2.4
2D13	NMB0335 (<i>dapD</i>)	2,3,4,5-tetrahydropyridine-2,6-dicarboxylate N-succinyltransferase	Amino acid biosynthesis: Aspartate family	29391	-2.3
2D6	NMB0138 (<i>fusA</i>)	Elongation factor G (EF-G)	Protein synthesis	77408	-1.3
2D7	NMB0618 (<i>ppsA</i>)	Phosphoenolpyruvate synthase	Energy metabolism: Glycolysis/gluconeogenesis Carbohydrate transport and metabolism	87115	-2
Upregulated Proteins^{2.3}					
T2 E6 E17 2D1	NMB1571.42 (<i>acnB</i>)	Aconitase hydratase 2	Energy metabolism: TCA cycle	92657	+2.3
T3 2D2	NMB0920 (<i>icd</i>)	Isocitrate dehydrogenase	Energy metabolism: TCA cycle	80113	+1.4
2D3	NMB0954 (<i>gltA</i>)	Citrate synthase	Energy metabolism: TCA cycle	48587	+2
C9	NMB431 (<i>pprC</i>)	Methylcitrate synthase	Energy metabolism: Propionate metabolism	42792	+2
2D4	NMB0435 (<i>ackA-1</i>)	Acetate kinase	Energy metabolism: Fermentation	43336	+1.3

<i>E2</i>	NMB1388 (<i>pgi-2</i>)	Glucose-6-phosphate isomerase	Energy metabolism: Carbohydrate transport and metabolism	62044	+2.9
2D10 2D11	NMB1796	Conserved hypothetical protein: Oxidoreductase	Energy metabolism: Electron transport	20989	+1.9
2D8	NMB1584	3-hydroxyacid dehydrogenase	Central intermediary metabolism: Other	30359	+3
E1 2D5	NMB1055 (<i>glyA</i>)	Serine hydroxymethyltransferase	Amino acid biosynthesis: Serine family	45243	+1.3
E5	NMB0944 (<i>metH</i>)	5-methyltetrahydropteroyltriglutamate-homocysteine methyltransferase	Amino acid biosynthesis: Aspartate family	85024	+1.4
T7	NMB0946 (<i>prx</i>)	Peroxiredoxin 2 family protein/glutaredoxin	Detoxification: Oxidative stress reponse	26894	+1.4
C5	NMB0884 (<i>sodB</i>)	Superoxide dismutase	Detoxification: Oxidative stress reponse	21879	+1.7
C7	NMB1590	Conserved hypothetical protein: putative peroxidase	Unknown function: Oxidative stress reponse	11526	+1.6
E4, E10	NMB0182 (<i>omp85</i>)	Outer membrane protein Omp85	Outer Membrane lipid biogenesis	88382	+1.2 ^b
E14, E15	NMB1053 (<i>opc</i>)	Class 5 outer membrane protein	Pathogenesis: Adhesion	29973	+1.3
S10	NMB1053 (<i>opc</i>)	Class 5 outer membrane protein	Pathogenesis: Adhesion	29973	+2.3
	NMB1636	Opacity protein		30161	+2.3
S7	NMB1541 (<i>lbpB</i>)	Lactoferrin binding proteinB	Transport of iron cations	81082	+1.8
S11	NMB0634 (<i>fbpA</i>)	Iron ABC transporter, periplasmic binding pr.	Transport of iron cations	35806	+1.5
2D9	NMB0018	Pilin pilE	Pathogenesis: Cell motility and adhesion	18202	+1.6

1.15 Global analysis of gene expression in the Hfq null mutant

In order to investigate, not only protein expression levels, but also global transcription profile differences in *N. meningitidis* expressing or lacking the Hfq RNA chaperone we used custom-made Agilent oligonucleotide microarrays. We identified in this way differentially expressed genes in the transcriptional profiles of the MC58 wild type and Δhfq null mutant strains. Three independent 2-colour microarray experiments were performed comparing pooled RNA from triplicate cultures of each strain grown to mid log phase in GC medium. The results obtained from these three experiments were averaged after slide normalization and differentially expressed genes were identified with a threshold of two-fold transcriptional change and a t-test statistics p-value ≤ 0.05 . Table 6 indicates the average result of the three experiments showing all the genes considered regulated. A total of 152 genes were found to be differently regulated, 112 were up regulated, and 40 were down regulated, in Δhfq , suggesting that Hfq acts more often to repress rather than to activate gene expression in *N. meningitidis*. To validate the microarray results, RT-PCR was performed on 10 selected genes spanning values from the most highly up- to down-regulated and we obtained a good coefficient of correlation (0.9422) between the microarray and RT-PCR results (Fig. 16). The 152 significantly regulated genes can be subdivided into 18 categories based on the function of their products, according to the classification of TIGRfams (Haft *et al.*, 2001) (Table 2).

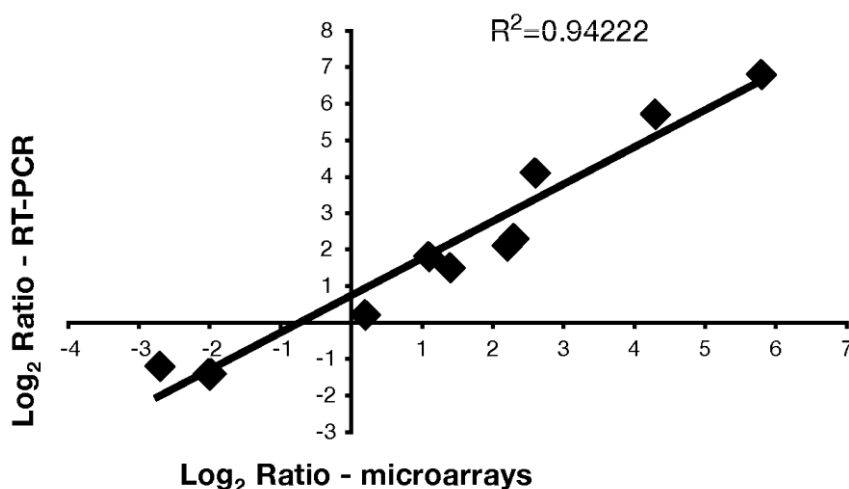


Figure 16 : Quantitative RT-PCR validation of microarray data of the Hfq knock out mutant vs MC58 wild type strain. Values plotted represent the log₂ ratio in transcript level of 10 genes in MC58 vs Δhfq strains. Genes were selected from the most highly up- to down-regulated. The coefficient of correlation obtained is indicated in the graph.

Four functional categories are over-represented within the data: cell envelope, transport and binding proteins, energy metabolism, and hypothetical proteins. These results are in accordance with the proteomic analysis which revealed that the expression of a number of OMPs was altered in the Δhfq mutant (Table 1). Furthermore these findings raise the possibility that membrane composition, particularly outer, may be regulated by sRNAs in meningococcus as reported for other systems (for review see (Vogel & Papenfort, 2006, Valentin-Hansen *et al.*, 2007, Guillier & Gottesman, 2006)).

Many metabolic enzymes involved in glycolysis and/or TCA cycle (*icd*, *acnB*, *acnA*, *gltA*, *pgi2*, *fumC*) are up-regulated. We cannot exclude that this could be an indirect consequence of reduced growth of Δhfq , but interestingly we can notice that *prpC*, *gltA* and *acnB* have been reported in other systems to be under the likely

direct control of sRNAs (Oglesby *et al.*, 2008, Masse & Gottesman, 2002). By contrast, components of electron transfer chains (*fixP*, *fixO*, *fixN*) are downregulated. Since the electron transport chain generates proton motive force across the cytoplasmic membrane, this function may be reduced in Δhfq . Interestingly, some subunits of the ATP synthase (*atpC*, *atpD*, *atpG*.) that use this energy to generate ATP are also down regulated.

These experiments identify genes with differential steady state levels of mRNA transcripts which could be due to transcriptional (initiation) or posttranscriptional (mRNA stability and degradation) effects. While it is still to be determined whether the differential expression is due to direct or indirect effects of Hfq function, with this strategy we are able to reveal Hfq-dependent mRNA regulation in approximately 7.5% of meningococcal genes in log phase, confirming Hfq as a global regulator of gene expression in meningococcus.

Functional group	Down regulated	Up regulated	Total in genome	% regulated genes
Amino acid biosynthesis	1	1	76	3%
Biosynthesis of cofactors, prosthetic groups, and carriers	1	1	83	2%
Cell envelope	3	15	239	8%
Cellular processes	1	5	119	5%
Central intermediary metabolism	1	1	40	5%
Disrupted reading frame	1	0	36	3%
DNA metabolism	0	1	91	1%
Energy metabolism	11	12	151	15%
Fatty acid and phospholipid metabolism	0	0	31	0%
Hypothetical proteins	12	59	664	11%
Mobile and extrachromosomal element functions	0	1	49	2%
Protein fate	2	0	73	3%
Protein synthesis	0	5	129	4%
Purines, pyrimidines, nucleosides, and nucleotides	0	0	43	0%
Regulatory functions	2	1	56	5.4%
Transcription	0	0	38	0%
Transport and binding proteins	5	4	131	7%
Unknown function	0	6	105	6%

Table 2. Numbers of genes deregulated in the Hfq null mutant during *in vitro* logarithmic phase in the different functional groups according to the classification of TIGRfams. The total number of genes in each category and the number of the up or down regulated genes in Δhfq are indicated.

II Identification of AniS: a novel sRNA synthesised under oxygen limitation

1.16 NMB1205 is a small transcript deregulated in the Hfq mutant

NMB1205 is one of the most highly down-regulated genes (4,3 fold change, Table 6) in the Hfq knock out mutant. In the MC58 genome, NMB1205 is annotated as a 147 bp hypothetical gene predicted to encode a protein of 48 amino acids of unknown function, flanked upstream by the bacterioferritin B and A genes and downstream by a transcriptional regulator and a protein-PII uridylyltransferase, all in the same orientation (Fig 17A). NMB1205 is not annotated as a paralogous coding gene in the other *Neisseria* genomes, although there is high nucleotide sequence conservation at the NMB1205 locus in many of the other genome sequences from pathogenic and commensal *Neisseria* spp. (Fig 17A and B), possibly due the absence of a canonical Shine-Dalgarno sequence for the translation initiation upstream of the ATG start codon, or the reduced length of the possible ORFs in the other strains (data not shown). We performed Northern Blot analysis using a radioactively-labeled NMB1205-specific probe on total RNA extracted from MC58 and the Hfq knockout. A single band appeared in RNA from the wild type strain, absent from the Hfq knockout sample, which migrates with an apparent molecular weight of less than 100 nt (Fig 18A). This correlates with the microarray data where transcription of NMB1205 was greatly downregulated in Δhfq . Surprisingly, the size of the transcript was considerably shorter than expected.

We mapped the 5' end of the NMB1205 transcript by primer extension analysis (Fig 18B). The elongated primer resulted in a double band mapping two tandem transcriptional starts at the A (which we nominate +1) and T of the predicted ATG

putative start codon of NMB1205. Analysis of the DNA sequence upstream revealed the presence of a possible -10 (GATAAT) and weakly conserved -35 (AATACC) with respect to the *E. coli* sigma 70 consensus hexamers that are likely to define the P_{aniS} promoter. Interestingly, we found a putative FNR-box (TTGAT-N4-ATCAA) at -41.5 with respect to the transcriptional start (Fig 17B), suggesting the promoter to be FNR-regulated. Furthermore, we found a putative rho-independent terminator of transcription inside the NMB1205 coding region. To assess the ability of this sequence to terminate transcription *in vitro*, we generated two different DNA templates for *in vitro* transcription of the NMB1205 locus consisting of a T7 promoter fused to the +1 transcriptional start site and spanning to either the end of the predicted terminator (+106) or to the end of the predicted ORF (+155). *In vitro* transcription with the T7 RNA polymerase of the shorter template gave rise to a transcript which migrated with an apparent weight of less than 100 nt (lane 1, Fig 18C). The reduced length of the transcript may be due to transcriptional termination at one of the Us upstream of the terminal U of the terminator. Approximately 95% of the transcription reaction from the longer template gave rise to a transcript of similar length (less than 100 nt, lane 2), indicating that the predicted rho-independent terminator works *in vitro* with very high efficiency. Taking together these results, we conclude that the NMB1205 locus gives rise to a short transcript, of approximately 100 nt, that is unlikely to code for a peptide. Comparative analysis of this sequence in the available *Neisserial* genomes from diverse species revealed the likely presence of a sRNA paralogue in all the genomes which was highly conserved over 56 nt at the 3' end (Fig 17B). Interestingly although the 5' of these sequences is variable in length, the presence of conserved regulatory elements of the promoter (FNR-box upstream of a putative -10) and the transcriptional terminator suggests that an FNR-regulated small RNA

is synthesized in each species. Small RNAs in bacteria have been reported to be highly structured RNAs. We used the Mfold program to predict the secondary structure of the novel sRNA (Fig 18D), which shows the presence of a secondary loop and a hairpin structure at the 3' end representing the terminator of transcription.

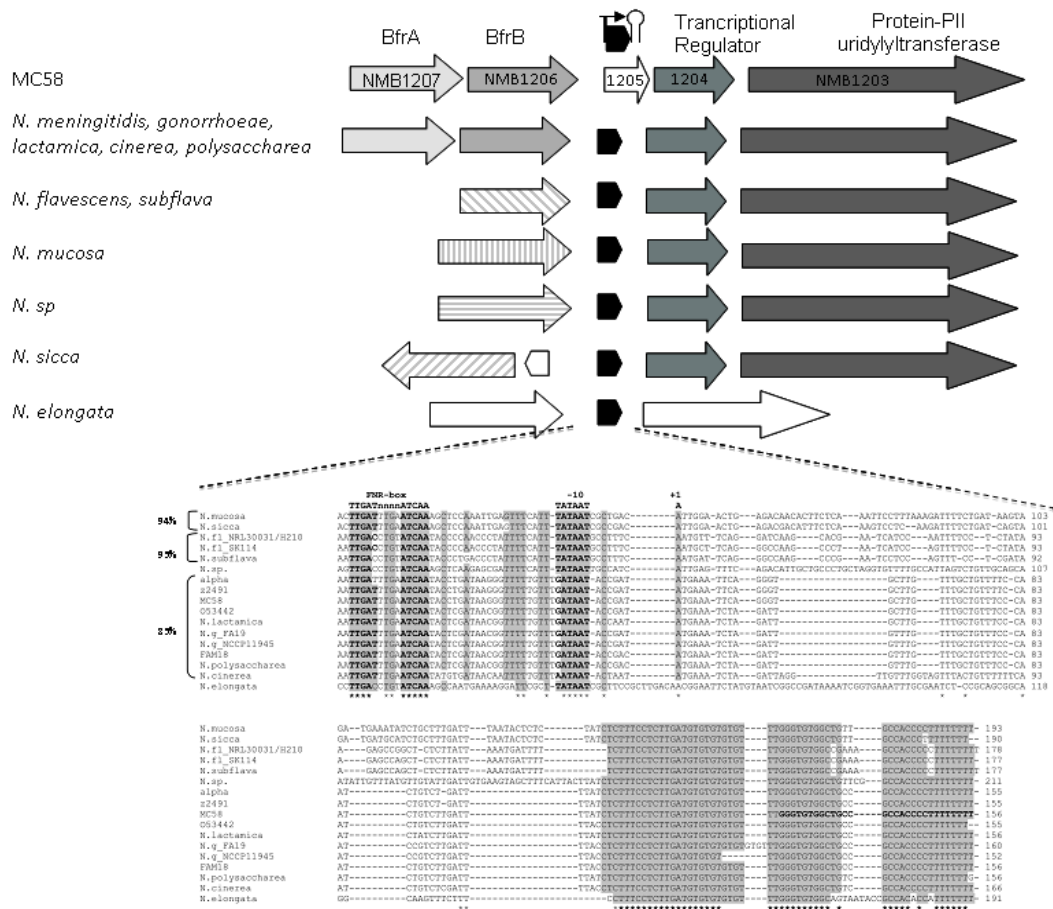


Figure 17 : A sRNA sequence with conserved regulatory elements is present in all *Neisseria* genomes available. And shows conservation in the 3' end of the gene. (A) Diagrammatic representation of the NMB1205 locus in MC58 strain of *Neisseria meningitidis* and other *Neisserial* spp. NMB1205 is annotated in MC58 only as a hypothetical ORF encoding a protein of 48 aminoacids. The orientation of the locus in the other available genomes is indicated. The orientation and size of the annotated genes and the putative sRNA gene are indicated. There is similar organization in other all *N. meningitidis*, *N. gonorrhoea*, *N. lactamica*, *N. cinerea* and *N. polysaccharea* genome sequences. The left flank of the locus appears to be a region of chromosomal rearrangement in the more distance spp.: *N. flavescens* and *N. subflavia* harbour a homologue of the NMB1727; *N. mucosa* a homologue of

NMB0875, *N.* strain F0314 (*N.* sp.) harbours a homologue of NMB1076 and *N. sicca* harbours a homologue of NMB1707, while in *N. elongata* an analogous sequence is present between a *N. elongata*-specific genes. **(B)** Alignment of the nucleotide sequence of the possible *aniS* analogous genes conserved in the available genome sequences of diverse *N.* spp. The regulatory sequences including an FNR-box and the possible -10 hexamer of a sigma 70 promoter, the +1 transcriptional start site as well as a rho-independent transcriptional terminator are conserved in all genomes and are highlighted in bold. The nucleotides conserved in 14 out 17 (80%) sequences are shaded in grey while the absolutely conserved in all sequences are indicated by the asterisk. The sRNA gene sequences vary at the 5' end of the putative RNA sequence cluster in groups and the relative identities exhibited between members of the indicated groups are shown. The alignment was made with the ClustalW software and further edited by hand

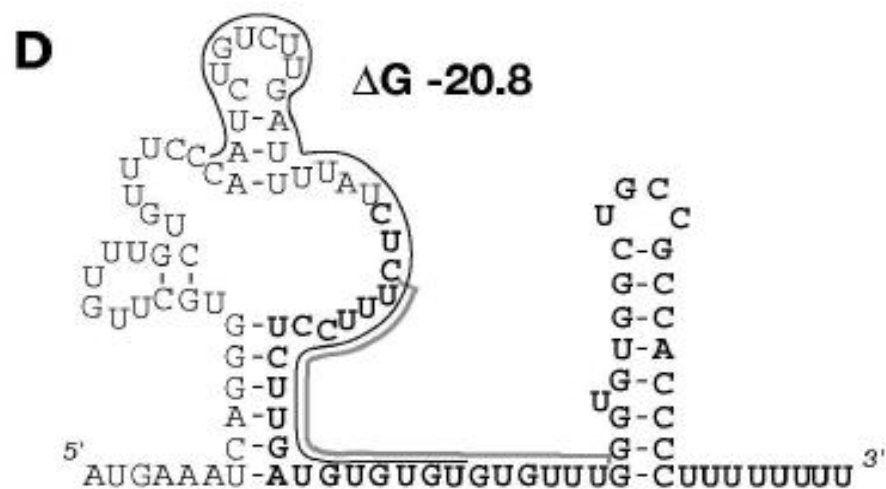
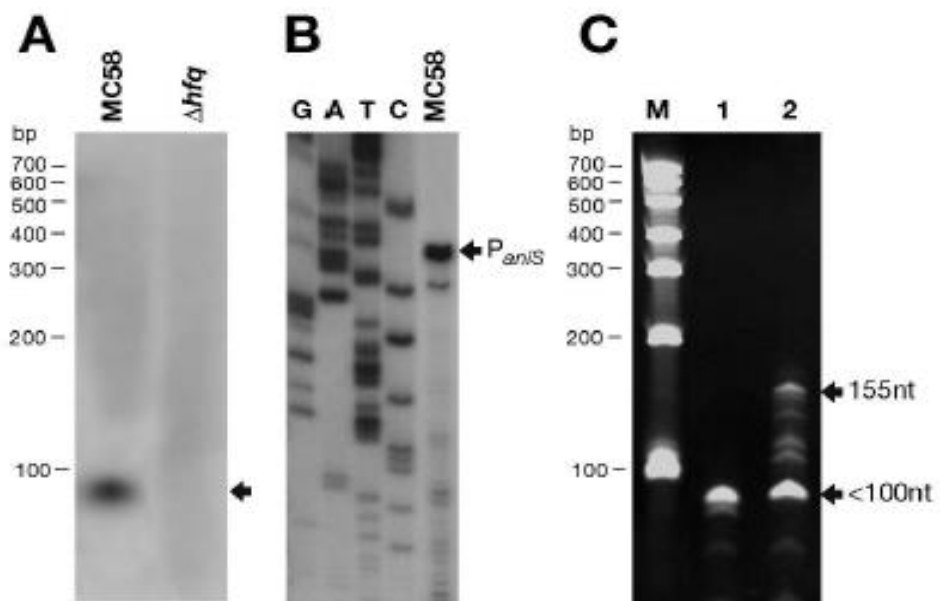


Figure 18: Characterization of the AniS transcript. (A) Northern Blot analysis showing a small transcript (<100nt) detectable in RNA from MC58 strain but not from the Δhfq strain. Total RNA was extracted from MC58 and Δhfq strains grown to log phase, Northern blotted and probed with a radiolabelled PCR product of 304 bp consisting of nucleotides overlapping the NMB1205 locus of the genome. The relative positions of migration of a RNA molecular weight ladder (run on the 6% PAGE 8M Urea gel) are indicated. (B) Mapping of the *PaniS* promoter. Total RNA (20 ug) from *N. meningitidis* MC58 strain was hybridized to the end labeled 1205-3 oligonucleotide (Table 5) and elongated with reverse transcriptase to map 5' end of transcription product synthesized by P_{aniS} promoter. Precise mapping was performed by sequencing the cloned region in plasmid pGem-sR3 with the same primer (lanes G, A, T, C). DNA regions corresponding to promoter elements are indicated in Figure 17. (C) *In vitro* transcripts synthesized with the T7 promoter from templates spanning (1) to the +106 end of the proposed transcriptional terminator and (2) to +155 downstream of the proposed transcriptional terminator. The relative lengths of the main transcript spp. synthesised are indicated. (D) Possible secondary structure of the novel AniS sRNA as predicted by MFOLD resulting in a free energy (ΔG) of -20.8. The nucleotides conserved in other *Neisseria* spp. are indicated in bold and the regions of pairing with NMB1468 and NMB0214 target mRNAs are highlighted in black and grey respectively.

1.17 The synthesis of the novel sRNA is regulated by FNR

The FNR transcription factor regulates gene expression in response to oxygen deprivation in many bacteria by binding target sequences, called FNR-boxes located in promoters and usually activating but also repressing transcription. In order to investigate if the sRNA synthesis is under the control of the transcriptional regulator FNR we investigated transcript levels in cells of the wild type strain or a knock out mutant of FNR (Δfnr) incubated with or without oxygen. RNA was extracted from the wild strain and from the Δfnr mutant grown to mid log phase and then exposed or not to 30 minutes of oxygen limitation. Northern blot analysis revealed that, while the sRNA is weakly detectable in the wild type strain grown under aerobic conditions (Fig 19A, lane 1), levels are strongly induced in the wild type after exposure to oxygen limitation for 30 min (Fig 19A, lane 2). Furthermore, the absence of any signal in the *fnr* null mutant under either oxygen conditions (Fig

19A, lanes 3-4), indicates that the synthesis of the sRNA is positively regulated by FNR and that FNR activates its transcription in response to anaerobiosis or oxygen-limitation. We therefore renamed the sRNA AniS (anaerobically induced sRNA). In order to investigate if the meningococcal FNR protein interacts directly with the *aniS* promoter region we carried out *in vitro* binding assay with a constitutively active mutant of meningococcal FNR protein, FNRD148A (Oriente *et al.*, 2010), here named FNR_c, which is no longer labile to oxygen. We prepared a probe of the promoter region of *aniS* radioactively labeled at one end only, and incubated it without or with increasing amounts of FNR_c protein and subjected to DNase I footprinting, with the results shown in Fig 19B. A DNase I protected region was observed on addition of the FNR_c protein to the binding reaction which spans from position -30 to -50 with respect to the +1 transcription initiation site. The FNR binding site overlaps the FNR-box identified in the sequence at a correct distance for activation within the *aniS* promoter. This result demonstrates a direct role of FNR as a transcriptional activator of the synthesis of AniS.

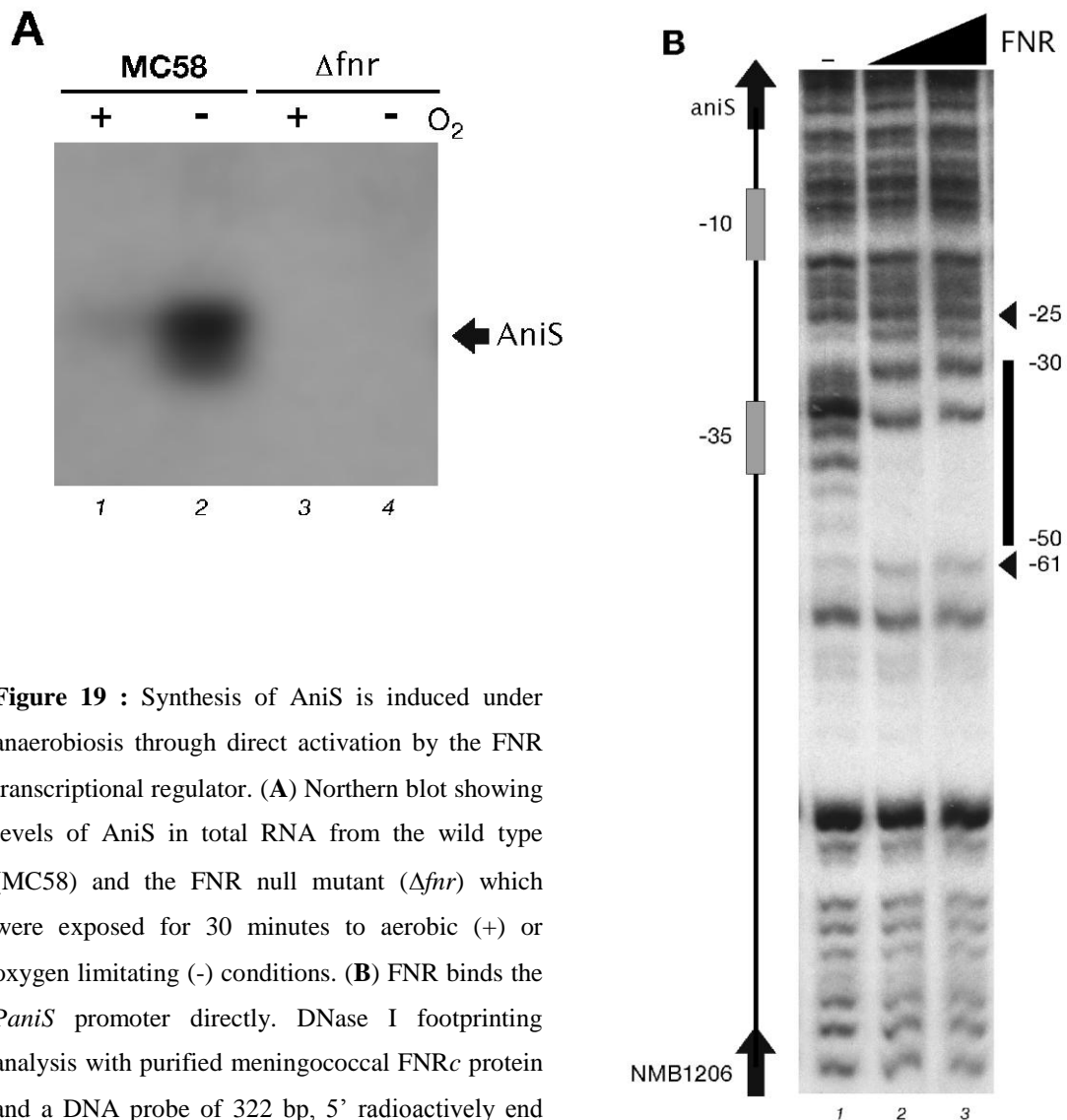


Figure 19 : Synthesis of AniS is induced under anaerobiosis through direct activation by the FNR transcriptional regulator. **(A)** Northern blot showing levels of AniS in total RNA from the wild type (MC58) and the FNR null mutant (Δfnr) which were exposed for 30 minutes to aerobic (+) or oxygen limiting (-) conditions. **(B)** FNR binds the *PaniS* promoter directly. DNase I footprinting analysis with purified meningococcal FNRc protein and a DNA probe of 322 bp, 5' radioactively end labeled at the NcoI site, corresponding to the *PaniS* promoter region. The probe was incubated with increasing concentrations of FNRc protein: lanes 1 to 3 correspond to amounts of 0, 0.12, 0.6 μ g of purified protein. The arrows to the left show the position and direction of the *aniS* and NMB1206 genes. The FNR protected region is indicated to the right as a vertical black bar, and the numbers indicate the boundaries of the binding site with the respect to the +1 transcriptional initiation site

1.18 AniS negatively regulates NMB1468 and NMB0214 genes

In order to find putative targets of the small RNA AniS, we reasoned that genes that are regulated by AniS should be substantially affected when the synthesis of the sRNA is maximal. Therefore, we generated a recombinant strain of MC58 expressing the constitutively active form of FNR, MC_FNR_C, in which the synthesis of AniS should be induced to a maximum level. We reasoned that genes that are regulated by AniS should be also regulated by FNR, therefore we determined the genes regulated in the FNR_C expressing strain with respect to the wild type. In order to identify genes directly regulated by AniS we deleted the *aniS* gene in the MC_FNR_C genetic background generating the strain $\Delta aniS_FNR_C$ and compared the global gene expression profile of these strains by microarray analysis. Total RNA from cultures of MC58, MC_FNR_C and $\Delta aniS_FNR_C$ was prepared for microarray analysis and two independent experiments were performed: 1) MC_FNR_C versus MC58 wild type and 2) $\Delta aniS_FNR_C$ versus MC_FNR_C. By focusing on genes whose expression levels changed at least 2-fold reciprocally between the two experiments we thereby identified possible targets for AniS. Using these criteria, we found only five mRNAs that exhibited down regulation by FNR (MC_FNR_C versus MC58 wild type) together with an upregulation when AniS was deleted in the same background ($\Delta aniS_FNR_C$ versus MC_FNR_C) and only AniS itself exhibited the opposite regulation (Table 3). Four of these possible targets correspond to 2 loci of contiguous putative ORFs, NMB1468 and NMB1469 and NMB0119 and NMB0120, respectively which may represent bicistronic operons. NMB1468 encodes a putative conserved lipoprotein of unknown function and NMB1469 encodes a small hypothetical protein (which is not annotated in the other *Neisserial* genomes) while NMB0119 and NMB0120 are both hypothetical genes.

The fifth putative target for AniS is NMB0214, the oligopeptidase A encoding the *prlC* gene. RT-PCR analysis confirmed significant (over 2-fold) regulation in three of the five targets, NMB0214 and the NMB1468/NMB1469 operon (Table 3).

The down-regulation of these target genes in the strain expressing FNR_C and up-regulation in response to deletion of the AniS sRNA suggests that AniS downregulates these target mRNAs when its synthesis is induced by FNR. To investigate further the role of AniS in regulating the NMB1468 and NMB214 genes we analysed expression of the targets in various recombinant strains with or without AniS, FNR and Hfq and correlated this with levels of AniS synthesis (Fig 20A-C). We extracted total proteins and RNA samples from 5 different strains and we measured AniS levels by quantitative primer extension, and mRNA target levels by RT-PCR to correlate the transcript amount of AniS with mRNA amounts of the targets. We also measured the expression of the NMB1468 protein, for which we had a polyclonal antiserum, to correlate transcript levels to protein expression levels. We found that under aerobic conditions AniS is synthesized at low levels in the wild type strain (Fig 20C, lane 1) and the abrogation of AniS synthesis by deletion of the FNR regulator, Δfnr , had little effect on the targets, either mRNA or NMB1468 protein expression (Fig 20A-C lane 2). However, when AniS synthesis is induced to high levels in the FNR_C strain we observed a significant down regulation of the NMB1468 protein and the mRNA levels of both NMB0214 and NMB1468 targets (Fig 20A-C, lane 3). As seen with the microarray data, this downregulation is dependent on the AniS transcript and deletion of *aniS* in the FNR_C background ($\Delta aniS_{FNRc}$) restores wild type levels of target expression (lane 4). Interestingly, if we remove the Hfq protein (Δhfq_{FNRc} , lane 5) in the FNR_C background we no longer have downregulation of the targets and expression levels are similar to the wild type. This strongly suggests a role for Hfq in

mediating the AniS-dependent regulation. It is worth noting that high levels of AniS are synthesized in the Δhfq_FNR^c strain but the targets are not downregulated suggesting that Hfq is essential in mediating the interaction with the target. Using bioinformatic tools (Fig 20D), we found putative pairings between AniS and the transcript of NMB1468 and NMB0214 which cover the region overlapping the ribosome binding site (RBS), a hallmark of negatively regulating sRNAs (Gottesman, 2004). These results suggest that the AniS transcript, together with the Hfq protein, mediates the downregulation of NMB1468 and NMB0214 target mRNAs and that the role of FNR in negative regulation of NMB1468 is mediated by AniS in a Hfq-dependent manner.

To assay whether the specific accumulation of AniS in the same background had timely and therefore likely direct effects on NMB1468 and NMB0214 mRNA levels we performed a timecourse experiment of the induction of AniS synthesis by IPTG-induction of FNR^c expression and monitored the steady state levels of NMB1468 and NMB0214 mRNA over time. Figure 20E shows that AniS was overproduced after 5 mins of IPTG induction, and NMB1468 and NMB0214 mRNA levels progressively decreased starting at 5 mins after induction. In the absence of the *aniS* gene no reduction in NMB1468 and NMB0214 mRNA was observed on IPTG-induction of FNR^c . Therefore, AniS accumulation results in concomitant decreases of NMB1468 and NMB0214 mRNA steady state levels.

Gene	MC_FNR ^C vs MC58		$\Delta aniS_FNR^C$ vs MC_FNR ^C	
	Microarray fold change	RT-PCR fold change	Microarray fold change	RT-PCR fold change
NMB1468	-3.5	-3.6 ± 0.7	+2.8	3.8 ± 0.7
NMB1469	-3.5	ND	+3.2	-ND
NMB0214	-2.3	-2.2 ± 0.4	+2.5	+3.5 ± 0.4
NMB1205	+4.6	ND	-60	ND
NMB0119	-4.6	-1.4 ± 0.8	+6.5	+2.8 ± 0.6
NMB0120	-6.5	-1.6 ± 0.4	+9.8	+5.5 ± 0.8

Table 3. Putative target genes of AniS. Genes differently regulated in MC_FNR^C strain vs MC58 and in $\Delta aniS_FNR^C$ strain vs MC_FNR^C. Microarray values represent a mean of three independent experiments each performed with a different pool of RNA as described in materials and methods. RT-PCR values represent a mean of two different experiments, each performed in triplicate, with 2 biological replicas of RNA.

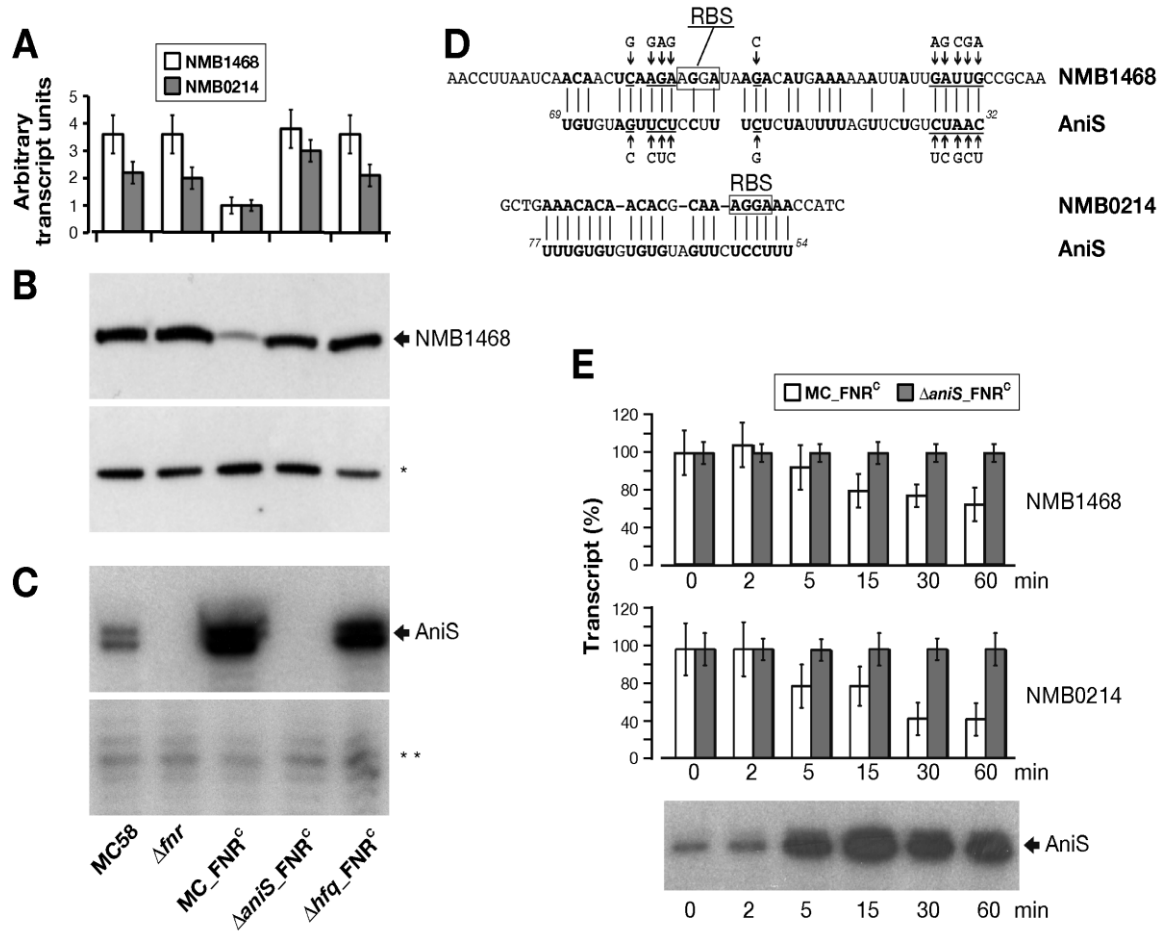


Figure 20 : FNR-induced downregulation of the NMB0214 and NMB1468 targets is mediated by AniS and dependent on Hfq. **(A)** Quantification by real time quantitative PCR of the NMB1468 and NMB0214 target transcripts in various genetic backgrounds. Total RNA was extracted from liquid cultures of following strains: the wild type MC58, the FNR null mutant Δfnr , the constitutively active FNR-expressing strain MC_FNR^c, and its isogenic derivatives (grown in 1 mM IPTG for FNR expression) lacking the *aniS* gene $\Delta aniS_FNR^c$, and Hfq Δhfq_FNR^c respectively. The steady state levels of the NMB0214 and NMB1468 putative target transcripts were quantified by RT-PCR. The log fold changes were calculated with respect to the MC_FNR^c strain and the values represent a mean of two different experiments, each performed in triplicate, with 2 biological replicates of RNA. **(B)** Western blot analysis was performed on total proteins from cultures of the strains indicated and stained with antisera raised against NMB1468 recombinant protein. NMB1869 protein expression was used as a negative control indicated by *. **(C)** Quantitative primer extension showing the levels of synthesis of AniS transcript in indicated strains. The level of *adh* housekeeping gene transcript was also quantified by primer extension using the *adh*-PE1 primer as a negative control in total RNA samples from each of the strains and is indicated by **. **(D)** The predicted target regions of complementarity between the AniS sRNA and its mRNA target genes. The numbers refer to the nucleotide positions with respect to the +1 of transcriptional initiation. **(E)** A timecourse experiment was performed on the MC_FNR^c and $\Delta aniS_FNR^c$ strains grown to mid log in the absence of IPTG and then RNA was prepared before (0 min) or after addition of 1

mM IPTG at indicated timepoints. qRT-PCR was performed on each RNA preparation to assay NMB1468 and NMB0214 mRNA levels with 1468-F/1468-R and 0214-F/0214-R primers respectively and is plotted as a percentage of the level at T0. Quantitative primer extension was performed on the RNA preparations from the MC_FNRc strain using the 1205-3 primer to monitor AniS levels.

1.19 Validation of the direct targeting of NMB1468 by AniS.

To provide further evidence that AniS directly targets NMB1468, we used a GFP-based plasmid system in the heterologous *E. coli* background that is routinely used to validate mRNA targets of heterologous sRNA (Urban & Vogel, 2007, Urban & Vogel, 2009). We cloned the 5' end of the NMB1468 gene including the upstream region into pXG-10 so that the first 10 amino acids were fused to GFP, and cotransformed this plasmid (or a control GFP fusion plasmid, pXG-1) with a compatible plasmid expressing the AniS gene from its own promoter (pGemT-AniS) or the negative control without the AniS gene (pGEMT-). The overall level of GFP expression in the pXG-1 control plasmid was unaltered by the presence of the AniS gene (Figure 21A, lane 1 and 2). However, the expression of the NMB1468-GFP translational fusion when co-transformed with the pGEMT-AniS plasmid resulted in 3-fold less GFP than the strain with the pGEMT- plasmid (Figure 21A, lane 4 vs 3) indicating that AniS down-regulated the NMB1468-GFP translational fusion in *E. coli*. This data provides evidence that AniS targets the 5' end of the NMB1468 gene.

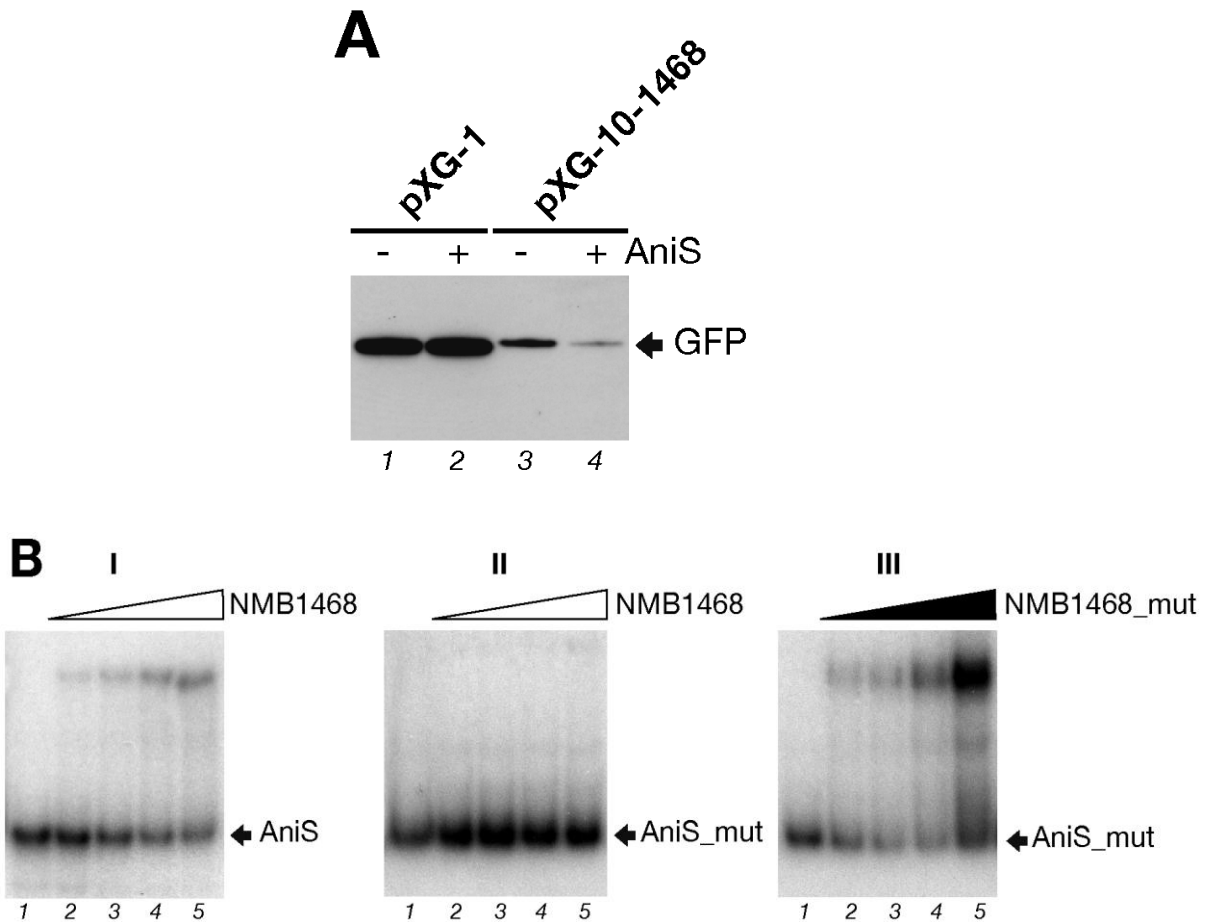


Figure 21 : AniS targets NMB1468 in *E. coli* and *in vitro*. **(A)** DH5- α was co-transformed with either a control plasmid pXG-1 (GFP expressed from the Ptet promoter) or a NMB1468-GFP translation fusion (pXG-10-1468), and the compatible pGEMT-AniS *aniS* containing plasmid (+) or an equivalent plasmid without *aniS* (-), namely pGEMT-. Total protein from plate cultures of the four *E.coli* strains and the amount of GFP expressed in each was quantified by Western blot. **(B)** AniS transcript forms an RNA/RNA duplex with the NMB1468 transcript via the complementary region proposed in Fig 20D. The radiolabeled AniS or mutant AniS (AniS_mut) *in vitro* transcripts (0.5 pmol/reaction or 50 nM final concentration) were incubated with increasing concentrations of cold NMB1468 (1468) or mutant NMB1468 (1468_mut) *in vitro* transcripts (lanes 1 to 5: 0, 0.5, 1, 2, 4 pmols or 0, 25, 50, 100 and 200 nM) in the presence of 1 μ g tRNA from *E. coli* as a nonspecific competitor. The presence of a slower-migrating RNA/RNA duplex is formed on co-incubation of wild type AniS and NMB1468 transcripts or the AniS_mut and 1468_mut transcripts containing compensatory mutations only.

The interaction of AniS with the NMB1468 mRNA was assayed by gel-shift analysis. Radioactively labelled AniS was incubated with *in vitro* generated mRNA corresponding to the first 217 nucleotides of the NMB1468 mRNA and containing the predicted region of base-pairing (Fig 20D) to assay duplex formation. Addition of increasing amounts of NMB1468 transcript resulted in a shift of the AniS probe, confirming that these RNAs can interact (Fig 21B, panel I). To validate the proposed region of interaction, site directed mutagenesis was performed on the AniS transcript (Fig 20D), and the mutant transcript (AniS_mut) did not interact with the wild type 1468 transcript (Fig 21B, panel II) however, the interaction was restored by the introduction of compensatory mutations to the 1468 transcript (1468_mut) (Fig 21B, panel III). These experiments confirm that AniS interacts with NMB1468 mRNA through base-pairing of the proposed region.

1.20 AniS is a small RNA bound by Hfq

In order to determine if Hfq can interact with the AniS transcript we performed *in vitro* gel mobility shift experiments with *in vitro*-synthesized AniS and the meningococcal Hfq recombinant protein. Radioactively labeled AniS transcript was incubated with increasing amounts of purified Hfq protein in the presence of 100 fold excess of tRNA as nonspecific competitor (Fig 22A). The addition of 11 nM Hfq resulted in the complete retardation of the radioactively labeled AniS with the formation of the first stable complex CI (lane 2) and on addition of 100 nM Hfq a second slower migrating complex was formed (CII, lane 4). This suggests that either one or two oligomers of Hfq can bind AniS. It is worth mentioning that Hfq shows affinity for the AniS transcript similar to that of previously reported Hfq-dependent sRNAs (Moller *et al.*, 2002; Metruccio *et al.*, 2009; Papenfort *et al.*, 2006). Most *E. coli* sRNAs are less stable in the absence of Hfq (Moll *et al.*, 2003;

Moller *et al.*, 2002; Sledjeski *et al.*, 2001), presumably because Hfq protects sRNAs from degradation in the absence of base pairing with mRNAs. Since AniS levels are less in the Hfq mutant we decided to measure the stability of AniS in the presence or absence of the Hfq protein *in vivo*. We used the FNR c -expressing strain, as AniS synthesis was maximal in this background, and performed a rifampicin timecourse extracting RNA from the MC-FNR c (Hfq $+$) or Δhfq _FNR c (Hfq $-$) strains at indicated timepoints after rifampicin addition and measured the decay of the AniS transcript (Fig 22B and C). Unexpectedly, the experiment revealed that the AniS transcript was rapidly degraded in the Hfq $+$ background (half life <2 min), whereas the RNA was more stable in the Hfq $-$ background (half life > 10 min) indicating that, Hfq has a negative effect on the stability of AniS. Taken together with previous data, our results suggest that Hfq may be important as a cofactor which facilitates the interaction between AniS and its target mRNAs, and we suggest that this could lead to a more rapid turnover of the sRNA.

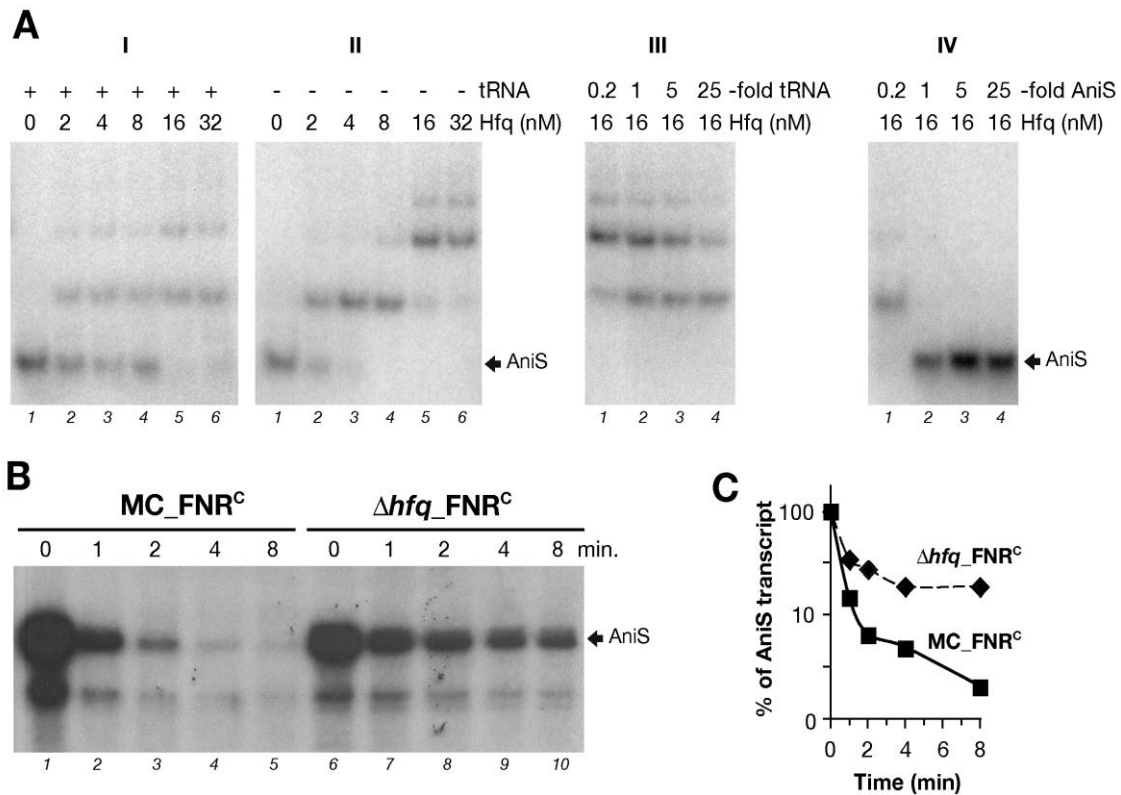


Figure 22: Binding of Hfq to the *in vitro* transcribed AniS sRNA transcript.

(A) Electrophoretic mobility shift assay of radioactively 5'-end labeled AniS transcript (0,5 pmoles/reaction or 50 nM final concentration) with increasing concentrations of the purified Hfq protein [lanes 1 to 4: 0, 11, 33, 100, 300 nM] was performed in the presence (+) or absence (-) (panel I and II) of 31 mM of tRNA per reaction. Specificity of the binding was assayed by co-incubation of AniS and 16 nM Hfq with increasing amounts of indicated tRNA (non-specific competitor, panel III) and cold AniS (specific competitor, panel IV). The free RNA probe (AniS) and the slower-migrating RNA/protein complexes (CI–CIII) are indicated.

(B) Quantification of decay of AniS transcript in Hfq+ and Hfq- backgrounds. The MC_FNR^c (*hfq*+) and the Δ*hfq*_FNR^c (*hfq*-) strains were grown to log phase and, at indicated timepoints, after the addition of 80 ug/ml of rifampicin the cells were added to an equal volume of frozen media to bring immediately to 4°C and RNA was extracted. Primer extension with the 1205-3 end-labelled primer was performed on 15 ug of total RNA from each sample from each timepoint to measure AniS levels. (C) Levels of AniS were quantified in each sample using a phosphoimager and the relative amounts of AniS were plotted and used to estimate the half-life in each background.

III Molecular mechanism of action of the sRNA NrrF

1.21 A bioinformatic approach identified a Fur-regulated sRNA in the *N. meningitidis* MC58 genome

In *N. meningitidis* the majority of iron-responsive gene regulation is mediated by the ferric uptake regulator protein (Fur), a protein classically defined as a transcriptional repressor (see introduction). Recently, however, microarray experiments with the Fur null mutant indicated that Fur positively regulates 43 genes in *N. meningitidis* (Delany *et al.*, 2006), and a subset of these showed no evidence for direct binding of Fur in their promoter regions. Interestingly, Fur has been shown to indirectly activate gene transcription through the repression of small regulatory RNA molecules in other organisms (Wilderman *et al.*, 2004; Masse & Gottesman, 2002; Davis *et al.*, 2005), so we looked for a similar mechanism in meningococcus. We used a bioinformatic approach to screen for the presence of a Fur-regulated sRNA. We generated a weight matrix by aligning sequences from 24 Fur-binding sites identified by footprint analyses (Delany *et al.*, 2006) to screen both strands of the *N. meningitidis* genome sequence. All binding sites mapping upstream of genes that are known to be regulated by Fur and iron, were analysed further for both the proximal presence of a likely rho-independent transcriptional terminator (within 250 bp), and also for conservation across the available neisserial genomes, *meningococcus*, *gonorrhoeae* and *lactamica*. This analysis led us to the identification of a single top candidate for a Fur-regulated sRNA and the locus is schematically represented in Figure 23 and it was called NrrF (neisserial regulatory RNA responsive to iron [Fe]). The *nrrF* gene maps between two predicted

converging genes, NMB2073 and NMB2074 (Fig 23). A putative Furbox sequence overlaps an A/T rich region with strong similarity to sigma 70 promoter sequences, namely a -10 hexamer (TATAAT) and a -35 (TTGATA), suggesting that this region may contain a Fur-regulated promoter, and flanked at a distance of 156 bp with a predicted rho- independent terminator.

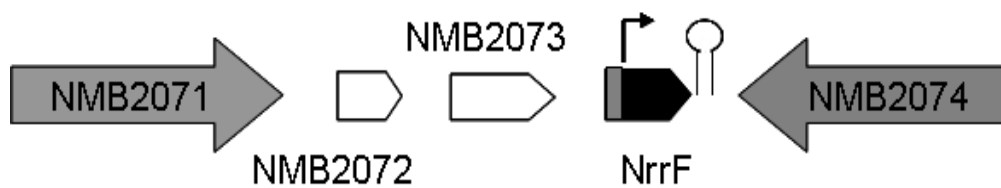


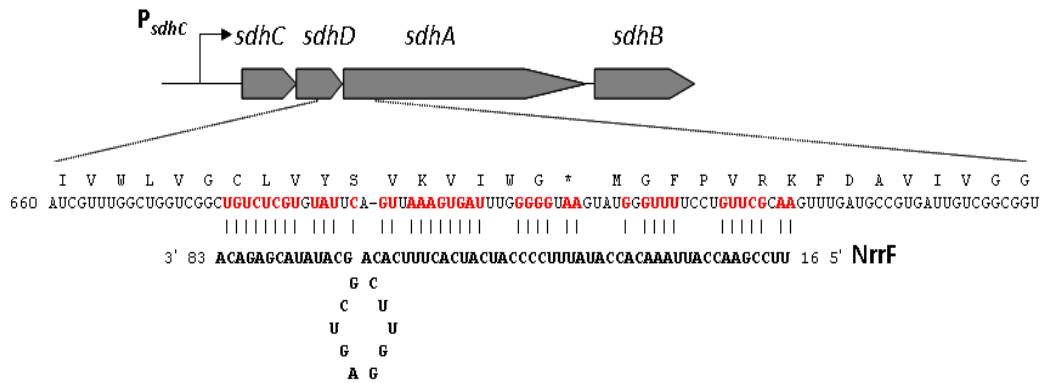
Figure 23: Diagrammatic representation of the locus containing the *nrrF* gene in MC58. The sequence with the regulatory elements verified in this study are indicated. The Fur-box is indicated as a grey rectangle, the transcriptional start of the gene is highlighted with a broken arrow, the rho-independent transcriptional terminator is indicated with a hairpin loop, and the orientation of the sRNA gene is indicated with a black arrow.

1.22 A base pairing mechanism mediated by Hfq is the molecular mechanism of action of NrrF

It was demonstrated (Mellin *et al.*, 2007; Metruccio *et al.*, 2009) that NrrF is a 156 nt sRNA whose transcription is negatively regulated by Fur. Furthermore by microarray analysis it was found that NrrF down-regulates the succinate dehydrogenase operon (Metruccio *et al.*, 2009). In order to understand the molecular mechanism of action of NrrF to regulate the *sdh* operon, we considered that in general small regulatory RNAs act by base-pairing to complementary regions in their mRNA targets. By using the computer program BESTFIT of the GCG Wisconsin package, we analyzed the nucleotide sequence corresponding to the *sdh*

transcript from the 5' untranslated end to beyond the *sdhB* 3' end for the most likely region of interaction between this RNA molecule and the sRNA. An extended region of imperfect base-pairing is shown in Fig. 24A, which overlaps the 3' end of the *sdhD* gene and the 5' end of the *sdhA* gene. As predicted by the Mfold computer program, the NrrF RNA may fold in a secondary structure (Fig. 24B). The proposed interacting region of the sRNA molecule is largely present in the single-stranded loop 28-58, which would be available for base-pairing for the overlapping region of the start of translation of the *sdhA* gene. Interestingly, the predicted structure of the sRNA molecule shows a putative Hfq-binding site, which is an 8- to 12-nt AU-rich region adjacent to stem-loops (Moll *et al.*, 2003), suggesting that the Hfq protein may be involved in binding and mediating NrrF function, as already observed for AniS (see above).

A



B

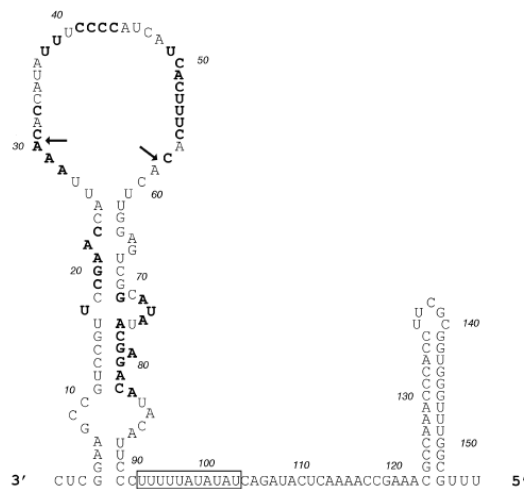


Figure 24: (A) Diagrammatic representation of the *sdhCDAB* locus and the extended region of complementarity found between the NrrF and the *sdhDA* mRNA gene junction. (B) The predicted structure (Mfold) of the NrrF sRNA resulting in a free energy of (ΔG°) -42.2 . The predicted AU-rich Hfq binding site between 94 and 104 nt in the sequence is boxed, and the nucleotides involved in the putative base-pairing with *sdhDA* mRNA are shown in bold. The arrows indicate the positions of the first and last nucleotides of the 18 nt deletion of the loop that was generated for the Nrrf Δ 31-58 mutant transcript (Fig 25B).

In order to determine whether Hfq interacts with NrrF, we performed *in vitro* gel mobility shift experiments with *in vitro*-synthesized NrrF and the meningococcal Hfq recombinant protein. The NrrF *in vitro* transcript was radioactively end labeled and incubated with increasing amounts of purified Hfq protein, and protein-RNA complex formation was monitored as slower-migrating bands in native

polyacrylamide gels. Figure 25A shows the results of gel shift experiments with the NrrF transcript and increasing amounts of Hfq in the absence (I) or presence (II) of a >100-fold excess of tRNA as a nonspecific competitor. In the presence of nonspecific competitor, the addition of 2.4 nM Hfq resulted in retardation of the radioactively labeled NrrF probe and the formation of the first stable complex, CI (Fig. 25A, panel II, lane 3), and on addition 60 nM Hfq a second slower-migrating complex was formed (CII) (lane 5). This suggests that either one or two oligomers of Hfq can bind to NrrF. Hfq shows high affinity for the NrrF transcript with an apparent K_d of \sim 36 nM. Furthermore, we assessed possible duplex formation of NrrF with two different possible target RNAs. We synthesized *in vitro* the predicted *sdhDA* target transcript region and also the 5'UTR of the *sdh* transcript, initiating at the promoter upstream of *sdhC*, as a likely alternative. We then incubated the radioactively labeled NrrF with increasing amounts of either of the putative target transcripts and assayed duplex formation by gel shift assays. As shown in Fig. 25B (panels I and II), while the addition of the unlabeled *sdhDA* region resulted in the retardation of the NrrF probe and the formation of a weakly resolved slower-migrating band, the 5'UTR-*sdhC* probe had no significant effect on the mobility of NrrF, suggesting that indeed the *sdhDA* predicted region can act as a target for RNA-RNA duplex formation *in vitro*. Furthermore, we generated a mutant NrrF transcript with a deletion from positions +31 to +58 lacking most of the single-stranded loop containing the proposed *sdhDA* interacting region of the sRNA molecule (Fig. 24B). This *in vitro* transcript is predicted to maintain a similar secondary structure with a just a smaller loop; however, addition of unlabeled *sdhDA* did not result in retardation of the shorter probe (Fig. 25B, panel III), suggesting that the loop is indeed important for base-pairing and duplex formation. Finally, we performed binding reactions of NrrF and the *sdhDA* target region with

or without the coincubation of the Hfq protein. Figure 25C shows the results of gel shift analysis in which on coincubation of Hfq with NrrF and *sdhDA* a supershifted band was observed (lanes 6 to 8) with slower migration than the Hfq-NrrF protein complexes (lane 2) or the *sdhDA*-NrrF duplex (lane 5), which likely represents the migration of a ternary complex formed by Hfq, NrrF, and the *sdhDA* target. Furthermore, the addition of Hfq to the binding reactions considerably enhances the efficiency of NrrF-*sdhDA* interaction since the ternary complex is clearly visible even at 22 nM *sdhDA* (lane 6), whereas the duplex is clearly visible only at 90 nM *sdhDA* (lane 5). These experiments suggest that Hfq interacts with NrrF and promotes the direct base-pairing at the predicted complementary *sdhDA* region of the *sdhCDAB* mRNA. We propose that these interactions *in vivo* may result in an Hfq-dependent decay of the *sdhCDAB* mRNA by direct targeting by the Fur-regulated sRNA NrrF.

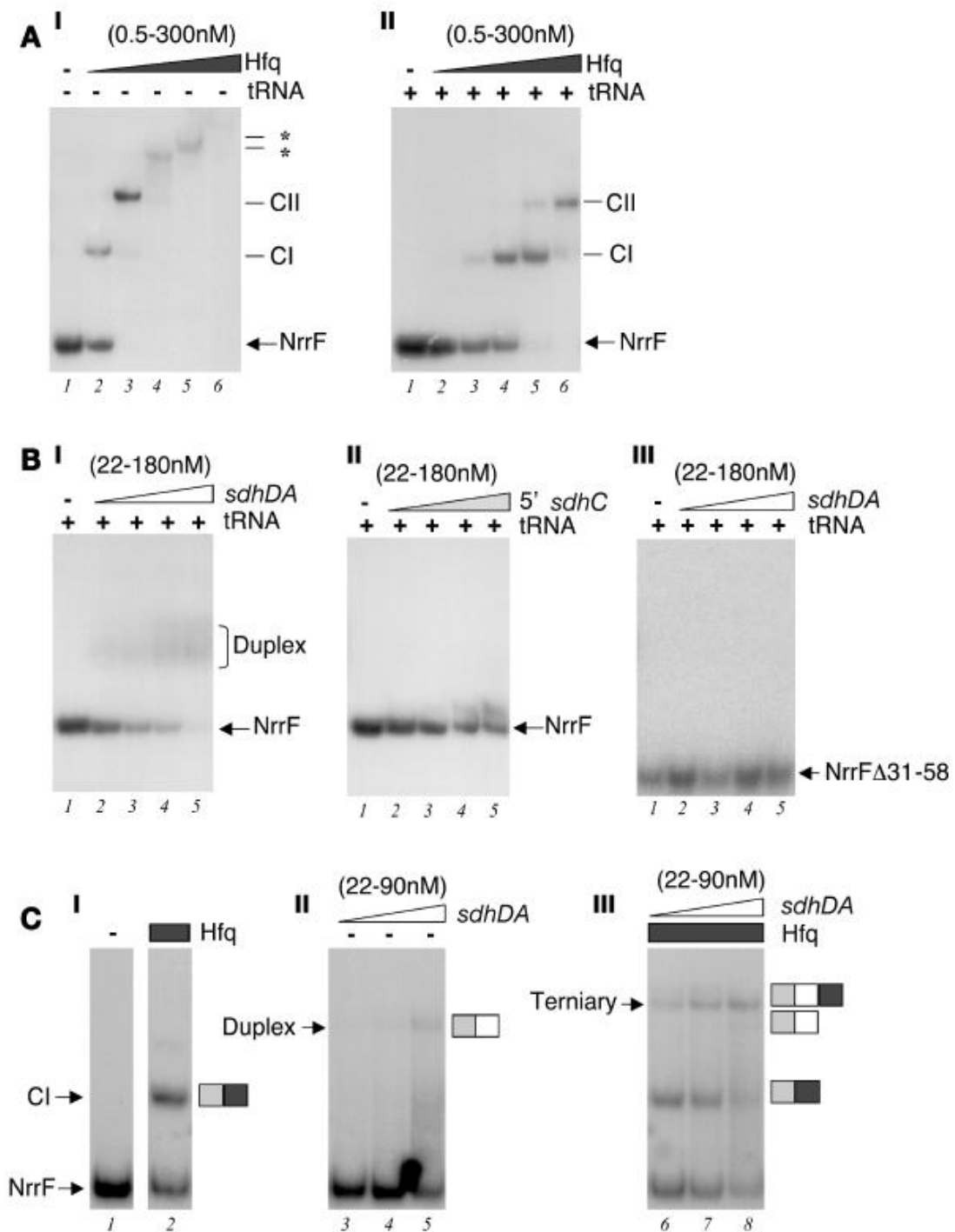


Figure 25: (A) *In vitro* binding of the Hfq protein to the NrrF transcript. Electrophoretic mobility shift assays of radio-actively 5' end-labeled NrrF transcript (0.5 pmoles/reaction or 50 nM final concentration with increasing concentrations of the purified Hfq protein (lanes 1-6: 0, 0.5, 2.4, 12, 60, 300 nM) in (I) the absence (-) or (II) the presence (+) of 10 μ g of tRNA per reaction (i.e. a final concentration of 31 μ M). The free RNA probe (NrrF) and the slower migrating RNA/protein complexes (CI-CII) are indicated to the right of each panel. (B) The NrrF transcript forms an RNA/RNA duplex with the putative complementary region within the *sdhDA* mRNA but not the 5'UTR of *sdhC* *in vitro*. The radio-labeled NrrF probe or mutant probe Nrrf Δ 31-58 (with a deletion from +31 to +58 inclusive) (0.5 pmoles/reaction or 50 nM final concentration) was incubated with

increasing concentrations of cold *sdhDA* (I and III) and *sdhC* (II) *in vitro* transcripts (lanes 1-5: 0, 0.22, 0.45, 0.9, 1.8 pmoles, or 0, 22, 45, 90, and 180 nM final concentration) in the presence of 31 μ M tRNA from *E. coli* as non-specific competitor. The presence of a slower migrating RNA/RNA duplex is formed on addition of the *sdhDA* but not the 5' *sdhC* cold probe to the wild type NrrF probe. (C) Co-incubation of NrrF with Hfq increases the efficiency of target *sdhDA* binding and a higher migrating ternary complex is observed. The radio-labeled NrrF probe (0.5 pmoles/reaction or 50 nM final concentration) was incubated with increasing concentrations of cold *sdhDA* transcript (lanes 3-5 and 6-7: 0.22, 0.45, 0.9, 2 pmoles or 22, 45, 90 nM final concentration, respectively) in the absence (lanes 1, 3-5) or presence (lanes 2, 6-8) of 12 nM of purified Hfq protein.

1.23 Fumarate hydratase and superoxide dismutase are regulated by at least a novel Hfq-dependent sRNA

In vitro experiments showed that Hfq has a role in stabilizing the base pairing between NrrF and *sdhA* mRNA target (Fig 25) and microarray analysis showed that NrrF has a role in down-regulating the RNA steady state level of *sdh* (Metrucchio *et al.*, 2009). In order to investigate the effects of NrrF and Hfq also on the SdhA expression we performed Western blot analysis with antiserum raised in mice to the SdhA protein to investigate the levels of protein expression in the MC58 strain and derivatives lacking Fur, NrrF, or the Hfq protein. As shown in Fig. 26A, SdhA protein is highly expressed in the MC58 strain and the Fur-complemented derivative and is downregulated in the Fur mutant, as expected. The deletion of the *nrrF* gene or the *hfq* gene in the MC58 wild type background both result in a slight induction of SdhA levels (lanes 2 and 6, respectively) with respect to the wild type levels. Furthermore, the deletion of the *nrrF* gene or the *hfq* gene in the Fur knockout background results in a high level of expression of the SdhA gene even in the absence of the Fur protein (lanes 4 and 7), suggesting that both NrrF and Hfq are involved in downregulation of SdhA expression in meningococci. Moreover, the down-regulation of SdhA in the Fur mutant may be mediated by NrrF and Hfq.

Interestingly analyzing other genes that from previous microarray studies (Delany

et al, 2006) resulted to be Fur positively regulated we found, by Western blot analysis, that FumB (fumarate hydratase) expression in the same strains shows an expected Fur-dependent positive regulation, in that the levels of protein were undetectable in the Fur-null mutant and restored to detectable levels in the complemented strain, as expected (lanes 1, 3, and 5). But, although the downregulation of FumB in the Fur mutant was not altered by the deletion of the *nrrF* gene (lane 4 versus lane 3), the deletion of the Hfq protein either in the wild type or the Fur mutant background significantly upregulated FumB expression (lanes 6 and 7). These data suggest that Fur-mediated positive regulation of *fumB* may be mediated by an Hfq-dependent mechanism, but not by the NrrF sRNA, suggesting another Hfq-dependent sRNA is involved. We also investigated the role of Hfq on the positive iron and Fur regulation of the *sodB* gene by assessing the steady-state levels of *sodB* transcript in the single and double Hfq and Fur mutants. The results of quantitative primer extension in Fig. 26B show that the *sodB* transcript is downregulated under iron-limiting conditions in the wild type MC58 (lane 2 versus lane 1) but remains constitutively high in the Δhfq mutant (lane 4 versus lane 3). Furthermore, the downregulation of *sodB* in the Fur mutant (lanes 5 and 6 versus lane 1) is reverted to constitutive high expression in the Fur- Δhfq mutant on deletion of *hfq* (lanes 7 and 8). These results suggest that Hfq mediates Fur and iron-regulation of *sodB* and strongly suggests that another Hfq-dependent sRNA is involved in Fur-mediated positive regulation of *sodB* in meningococcus. In conclusion, our data suggest that Fur regulation of *sdhCDAB* is mediated by NrrF in an Hfq-dependent manner and that the regulation of *sodB* and *fumB* is due to the Hfq-dependent action, possibly via a second Fur-regulated sRNA that is distinct from NrrF.

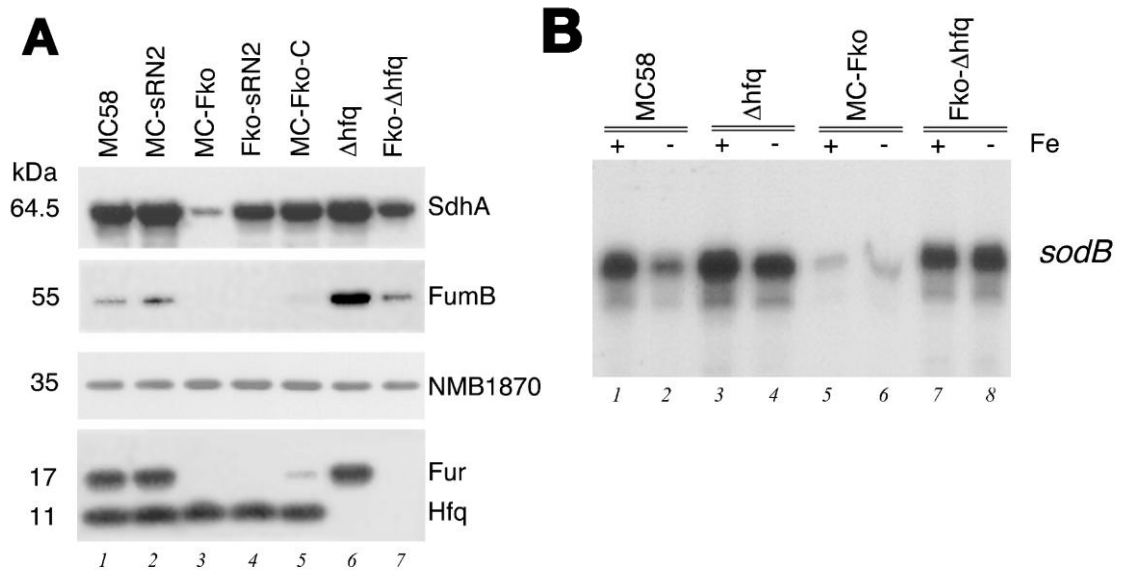


Figure 26: (A) Expression of SdhA and FumB proteins, both regulated positively by Fur, in strains deriving from the MC58 wild type, with or without the *fur* gene, the *nrrF* gene and/or the *hfq* gene. Western Blot analysis was performed on total proteins from overnight plate of the strains indicated and stained with antisera raised against the SdhA and FumB proteins. The expression of the Fur protein (17kDa) and the Hfq protein (11kDa) were verified in the appropriate strains lower panel. NMB1870 protein expression was used as a negative control as it is neither Fur nor iron-1 regulated (Delany *et al.*, 2003). (B) RNA analysis by quantitative primer extension of the levels of the *sodB* transcript in wild type (MC58), Hfq null mutant (Δhfq), the Fur mutant (MC-Fko), and the double Fur-Hfq mutant (Fko-Hfq) grown to mid-log phase under iron replete conditions before (+) and after (-) treatment for 15 min with iron chelator.

IV. Global investigation of sRNAs

1.24 Solexa RNA sequence revealed 19 putative novel sRNAs in meningococcus

The Fur and Hfq dependent regulation of *fumB* and *sodB* genes suggests that other iron-regulated sRNAs are involved in the Fur-mediated positive regulation of these two genes. In order to deeply and globally investigate iron-dependent sRNAs network in *N. meningitidis* we applied Illumina's high throughput sequence technology to analyze the transcriptome of this bacterium. RNA was prepared from 3 independent cultures of *N. meningitidis* MC58 grown to mid log phase in GC broth and then subjected or not to iron chelation (as described in Materials and Methods). The RNA was reverse transcribed to cDNA and sequenced on an Illumina GAI. The resulting 36-base reads were mapped to the *N. meningitidis* MC58 genome. The sequence coverage per base was subsequently plotted and visualised using the genome browser Artemis (Rutherford *et al.*, 2000). It was reported (Perkins *et al.*, 2009) that this method yields RNA transcript reads in a strand-specific manner allowing the identification of antisense transcripts. However, as we observed the same signal both from the antisense and the sense strand in our data set, we did not succeed in obtaining strand-specific signal. In order to facilitate the analysis we summed the signals obtained from the sense and the antisense strand. To find novel sRNA candidates we searched for cDNA peaks that occurred specifically and entirely within intergenic regions in at least 2 of the 3 biological replicates, excluding ribosomal RNAs. For each candidate we calculated the arithmetic mean per base-pair (nt/bp) of mapped sequence reads and we

considered only regions in which nt/bp was ≥ 1 in at least 2 of the 3 biological replicates. In order to discriminate from 5' or 3' UTRs the distance from the upstream and the downstream genes was also calculated and only regions which a distance > 30 nt were considered. Following these steps we were able to identify 23 putative non coding small RNAs (NCRs), 16 of which resulted to be up-regulated under iron limitation, which are listed in Table 4 and some of them represented in Fig 27. Since sRNAs are in general conserved in phylogenetically related species the sequence conservation in other *Neisseria gonorrhoeae* and *lactamica* species was also evaluated (Table 4). 3 of the 23 candidates were derived from tRNA (NCR-) and housekeeping RNAs (NCR-, tmRNA and NCR-, 6S). Interestingly NCR-4 is the previously described sRNA NrrF which demonstrates proof of concept for this analysis (Table 4). This result confirms the efficiency of the Solexa method in identifying non coding small RNAs. Taking together these results strongly suggest the existence of novel sRNAs, some of which could be involved in the post-transcriptional regulation of *sodB* and *fumB* genes (fig 26). Further studies are needed in order to validate the existence of the putative 19 sRNAs and, once confirmed, to characterize their regulatory networks.

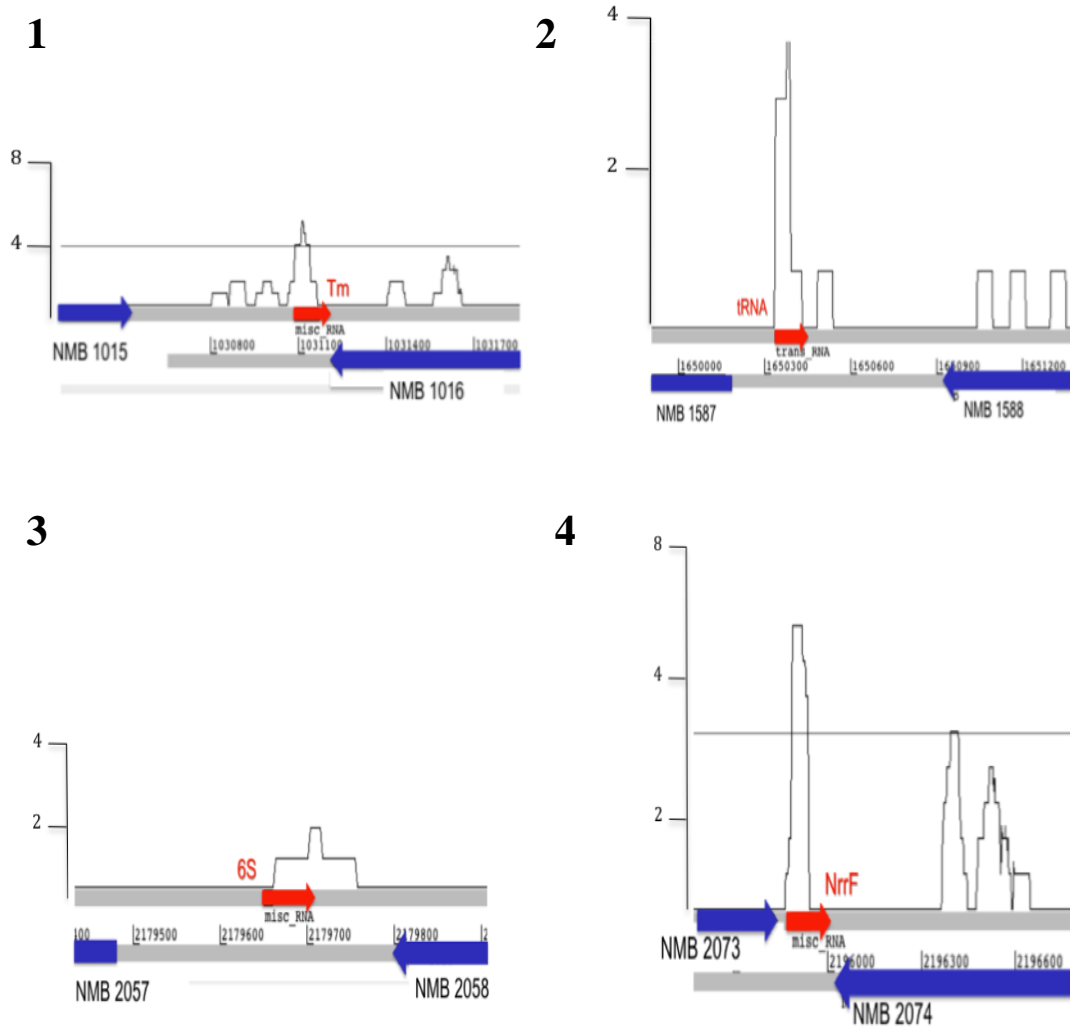


Figure 27: Previously known non-coding RNAs, as listed in Table 4.

RNA-seq data sequence were mapped to the *N. meningitidis* MC58 genome and visualized using Artemis software. Blue and red arrows represent the coding genes and non coding RNAs respectively. The nucleotide coverage (nt/bp) is indicated on the left and represents the mean of the three biological replicates. Numbers on the left are in accordance with Table 4.

Table 4. putative small RNAs identified by RNA-seq

NCR-ID	Upstream ^A	Downstream ^B	Orientation ^C	nt/bp	RNA length	Conservation ^E	nt from upstream	nt from downstream	Regulation in dip.
1	NMB1015	NMB1016	>>	4.3	338	Yes	604	666	Yes
2	NMB1587	NMB1588	<<	3.7	93	Yes	180	523	No
3	NMB2057	NMB2058	<<	3.1	54	Yes	248	61	No
4	NMB2073	NMB2074	>>	7	58	Yes	61	965	Yes
5	NMB0553	NMB0554	<<	2.8	54	No	729	425	Yes
6	NMB0983	NMB0984	>>	2.3	82	Yes	224	307	Yes
7	NMB0992	NMB0993	<<	2.5	52	No	1254	626	Yes
8	NMB0993	NMB0994	<<	3.1	322	Yes	322	39	Yes
9	NMB1391	NMB1391	<<	10.4	95	Yes	151	34	No
10	NMB1451	NMB1452	<>	7.8	55	Yes	459	302	Yes
11	NMB1451	NMB1452	<>	6.6	62	Yes	574	180	Yes
12	NMB1865	NMB1866	<<	4	54	Yes	177	32	Yes
13	NMB1865	NMB1866	<<	3.8	54	Yes	338	162	Yes
14	NMB1921	NMB1922	>>	2.4	101	Yes	93	78	Yes

15	NMB1923	NMB1924	><	5.9	55	Yes	86	77	Yes
16	NMB1982	NMB1983	>>	3.8	85	Yes	87	1174	Yes
17	NMB1982	NMB1983	>>	3.7	71	Yes	187	1088	No
18	NMB0395	NMB0396	>>	4.6	56	No	40	122	No
19	NMB1488	NMB1489	<>	2.2	54	Yes	82	351	No
20	NMB1636	NMB1637	><	11	110	Yes	45	46	No
21	NMB0047	NMB0048	><	2	16	Yes	1263	1296	Yes
22	NMB0195	NMB0196	><	3.2	54	No	176	1068	Yes
23	NMB0400	NMB0401	><	3	54	Yes	552	428	Yes

The respective upstream (A) and downstream (B) genes are indicated as well as their orientation (C) in the genome. The conservation in other Neisserial species was also evaluated (E). Number 1-4 represent already known sRNAs (Fig. 27)

DISCUSSION

It is very well established that sRNAs play critical regulatory roles in many bacteria in response to different stress conditions, and in many pathogens they have been found to have important roles in virulence and host infection (for review see Zhou & Xie, 2011; Papenfort & Vogel, 2010; Toledo-Arana *et al.*, 2007; Gripenland *et al.*, 2010). Although they have such important roles in bacteria many of them have been identified only very recently. This resides in part due to the difficulty in identifying novel sRNAs, since, unlike regulatory proteins, they are not annotated in bacterial genome sequences and their sequence is not conserved between different bacterial species. Nowadays, thanks to the increased availability of novel technologies such as computational predictions of sRNAs, tiling arrays and high-throughput cDNA sequencing (RNA-seq) many novel sRNAs have been discovered in a wide range of bacteria, but in many systems, including *Neisseria* spp., their existence is still largely unexplored. In this thesis we have initiated the characterization of the sRNA network of *N. meningitidis*, demonstrating that a *hfq* knock out mutant displays a pleiotropic phenotype and identifying two novel sRNAs using bioinformatic and microarray-based approaches. Furthermore, using Solexa technology, to sequence the transcriptome of meningococcus, we discovered 19 putative novel sRNAs which will be further investigated.

1.25 Characterization of a *hfq* knock out mutant in *Neisseria meningitidis*

In this section we investigated the role of Hfq in the stress tolerance and virulence of meningococcus. We report that Hfq has a profound effect on the fitness and survival of meningococcus in the presence of a wide range of stresses (Fig 13) and

contributes to virulence in *ex vivo* and *in vivo* models of infection (Fig 14). The stress sensitivity of the *hfq* mutant is consistent with the altered stress responses observed for other bacteria (Christiansen *et al.*, 2004; Robertson & Roop, 1999; Tsui *et al.*, 1994; Meibom *et al.*, 2009; Geng *et al.*, 2009; Sousa *et al.*, 2010) suggesting that Hfq has a conserved function in meningococcus. The ability of meningococci to colonize the hostile environment of the mucosal epithelium and their ability to survive and multiply within human blood are key factors in the development of fulminant meningococcal disease. In the current models of bacteremia, the mutant is considerably attenuated (Fig 14C). The ability of this strain to survive in human blood and serum is not attributed to altered expression of known serum resistance factors of *N. meningitidis*, such as a capsule (Jarvis & Vedros, 1987) or fHbp (Madico *et al.*, 2006), as these factors were not altered by the mutation (data not shown). Hfq was important for survival in the infant rat animal model over an 18-h period. Although we cannot exclude the possibility that the growth phenotype of this strain may partially explain the reduced number of bacteria recovered from the blood, this was certainly not the case in the *ex vivo* assays, where in media or heat-inactivated serum the three strains showed no decreases in cell numbers over the course of the assay (data not shown). Interestingly, in agreement with our findings, signature-tagged mutagenesis screening for attenuated mutants of meningococcus resulted in isolation of an Hfq mutant as 1 of 73 mutants that were attenuated in the infant rat (Sun *et al.*, 2000). Here we performed a proteomic and a whole genome expression analysis of cells lacking Hfq to identify proteins and processes that are directly or indirectly regulated by this protein, thus providing potential target genes for sRNA regulation. Analysing the proteins or genes differently regulated in Δhfq , we found 27 proteins, of which 20 were overproduced in the Hfq mutant, and 152 genes, 112 up regulated

and 40 down regulated in Δhfq . These results suggest that Hfq acts more often to repress rather than to activate gene expression in *N. meningitidis*. Many of these genes are involved in cell energetics and metabolism, amino acid biosynthesis, oxidative stress responses, and pathogenesis (Tables 1 and 6). Considering the pleiotropic effect of Hfq on mRNA stability and translational regulation in other bacteria, it is likely that many of the Hfq-dependent changes in protein expression or mRNA regulation are mediated by altered sRNA circuits. Interestingly we can notice that four genes that we found to be differently regulated in the Hfq knock out were reported to be under probably direct control of sRNAs in other systems, namely *prpC*, *gltA*, *acnB*, and *sodB* (Oglesby *et al.*, 2008; Masse & Gottesman, 2002). Interestingly, we identified a number of OMPs whose accumulation was altered in the Δhfq mutant, although the major expressed OMPs PorA, PorB, and RmpB did not appear to be affected. While regulation could be indirect, the fact that many OMPs are upregulated in the Δhfq mutant raises the possibility that OMP biogenesis and outer membrane composition may be extensively regulated by sRNAs in meningococcus, as has been reported for other systems (Valentin-Hansen *et al.*, 2007; Vogel & Papenfort, 2006).

The phenotypes associated with loss of Hfq in meningococcus may not be completely dependent on its role in directing sRNA posttranscriptional circuits but instead may be related to other Hfq functions or some additional factor or factors that are themselves targets for Hfq regulation. For instance, in *E. coli* Hfq is known to interact with the polynucleotide phosphorylase (PNPase) and poly(A) polymerase I (PAPI) proteins, two components of the degradosome, in an sRNA-independent manner (Mohanty *et al.*, 2004). Here, PNP is identified as one of the proteins that is less abundant in the Δhfq mutant, and it is plausible that the turnover of the protein itself is altered in the absence of Hfq. Alternatively, the binding of an RNA-binding

protein, such as Hfq, directly to mRNA might favor alternative mRNA secondary structures that may either promote or interfere with translational initiation or that may alter the rate of mRNA degradation, as is the case for Hfq-mediated downregulation of OmpA in *E. coli* (Vytvytska *et al.*, 2000). Many of the pleiotropic effects of Hfq mutants in other bacterial systems are related to the requirement of Hfq for efficient translation of the stationary-phase sigma factor (Brown & Elliott, 1996); Tsui *et al.*, 1994) or for downregulation of RpoE and the envelope stress response (Ding *et al.*, 2004; Figueroa-Bossi *et al.*, 2006; Guisbert *et al.*, 2007; Thompson *et al.*, 2007). While *N. meningitidis* does not possess an RpoS-like sigma factor, a protein annotated as an extracellular function sigma factor (NMB2144) with similarity to RpoE is present. However, there are no homologues of the periplasmic protease DegS or the anti-sigma factor RseA, which are responsible for activation of RpoE in response to envelope stress.

A comparison of the initial observations for Hfq phenotypes for meningococcus and other better-studied systems shows many similarities but also some interesting differences. It appears that Hfq plays a pivotal role in virulence and stress adaptation. In the absence of a stationary-phase sigma factor and homologues of the proteins which activate the envelope stress response, the mechanisms by which Hfq could contribute to control global protein expression regulation may differ from the mechanisms in other systems. Nonetheless, due to the pleiotropic nature of the phenotypes of the Hfq mutant, it appears that Hfq plays a fundamental role in coordinating gene regulation in meningococcus, and our findings indicate that there is a large sRNA network in *N. meningitidis* that has yet to be uncovered.

1.26 Identification of AniS: a novel sRNA synthesised under oxygen limitation

The global analysis of transcripts affected in the Hfq knockout, allowed us to identify a small transcript that we show to be a novel regulatory sRNA of meningococcus, which we called AniS. AniS is a Hfq-dependent sRNA of about 100 nucleotides, and in this thesis we describe the signals and regulatory circuits which decide its synthesis as well as candidate target mRNAs that it regulates. AniS is an anaerobically-induced sRNA whose synthesis is strictly dependent on the FNR global anaerobic transcriptional regulator and thus, it can hardly be detected in cells deleted for the *fnr* gene or in cells grown aerobically. FNR binds the *aniS* promoter directly and activates transcription of the sRNA in response to oxygen limitation.

Through transcriptome profiling in appropriate mutants we identified at least 2 possible targets of AniS, NMB1468 and NMB0214. The downregulation of the mRNAs of these genes is mediated by the AniS gene and also by Hfq. The expression of constitutively active FNR, *FNRc*, induces high levels of AniS and concomitant downregulation of these target mRNAs, and AniS and Hfq are necessary for this downregulation. We also showed a direct interaction of Hfq to the AniS sRNA suggesting that Hfq may be directly involved in mediating sRNA base-pairing to its target mRNAs. Both NMB1205 (*aniS*) and NMB1468 were reported to be FNR-regulated in *Neisseria* in independent microarray studies of the FNR deletion mutant and the wild type exposed to oxygen limiting conditions (Bartolini *et al.*, 2006; Whitehead *et al.*, 2007).

The identified regions of complementarity of AniS for NMB1468 and NMB0214 were overlapping the RBS and flanking regions, typical of this class of regulators. Interestingly the same region of AniS is predicted to pair with each target and

contains a pyrimidine-rich region spanning from nt 51 to 62 CUCUUUCCUCU somewhat resembling an anti-Shine-Dalgarno (aSD) sequence. The NMB0214 and NMB1468 gene targets of AniS, respectively encode the PrlC oligopeptidase whose exact function is still unknown although it has been implicated in protein export, degradation and cell cycle regulation in *E. coli* (Trun & Silhavy, 1989, Jain & Chan, 2007; Jiang *et al.*, 1998), and a lipoprotein of unknown function which has been studied as a possible candidate antigen for a meningococcal vaccine (Hsu *et al.*, 2008). Therefore, it is difficult to envisage a logical rationale for their downregulation under oxygen-limitation.

Intriguingly, on analysis of either the similar locus or similar sequences of the *aniS* gene, we were able to find possible homologous sRNAs in all of the other *Neisseria* genomes available. The regulatory sequence of each suggests an anaerobically induced sRNA is synthesised in each species. In fact, the gonococcal AniS equivalent has been reported as a highly FNR-induced transcript in a study of the gonococcal FNR regulon using a Pan-genome array (Whitehead *et al.*, 2007), verifying that AniS is conserved and synthesized in the closely associated pathogen *N. gonorrhoeae*. Interestingly, this study also identified gonococcal mRNAs that were repressed by FNR and had no FNR-box in their promoters, nor were they enriched by FNR Chromatin immunoprecipitations which, we suggest, may represent targets for the gonococcal AniS equivalent (Whitehead *et al.*, 2007). Expanding to less similar spp. the conservation of the 3' end of each sequence including the aSD-like sequence may suggest that these heterologous sequences represent regulatory RNAs that function similarly to AniS and may have some similar targets for instance NMB0214. The variation of the 5' ends of these putative sRNA sequences further suggest that distinct targets may exist which are regulated through partial complementarity of the heterologous sequences. Indeed, different

regions of the FnrS regulator in *E. coli* were shown to control diverse groups of target genes (Durand & Storz, 2010). The conservation during evolution of the regulatory regions (FNR-regulated promoter and terminator) and the divergence of sequence content highlights the potential versatility of this species of molecule: the sRNAs.

Initially, we hypothesized that the level of AniS was less in the Hfq mutant, as the chaperone may play a role in stabilizing the sRNA, as it is known to do with many other sRNAs (reviewed in (Valentin-Hansen *et al.*, 2004, Aiba, 2007). However, our experiments indicated the contrary to be true for the AniS sRNA, i.e. that Hfq enhances the turnover of AniS, since AniS is less stable in Hfq+ background. This is of course a surprising finding, but it is not the only case reported. It was recently demonstrated, in fact, that in *Rhodobacter sphaeroides* the sRNA RSs0019 is stabilized in the absence of Hfq (Berghoff *et al.*, 2009). Based on the literature the contribution of Hfq to sRNA stability is controversial. While it has been shown that the binding of this chaperone, in the absence of base-pairing, stabilizes sRNAs protecting them from RNaseE cleavage (Moll *et al.*, 2003; Masse *et al.*, 2003); it has also been shown that Hfq-mediated pairing of sRNAs to their targets promotes coupled degradation of the interacting RNAs (Masse *et al.*, 2003). Since we showed that Hfq is needed to promote the base-pairing interaction of AniS and its targets, then Hfq may be promoting the turnover of AniS when there are adequate mRNA targets present in the cell. These data suggest that in *Neisseria* either Hfq is involved in the turnover of free AniS, or the turnover of AniS due to base-pairing with the target in the Hfq+ background is more rapid than the turnover of the free AniS. The short half-life of the AniS in the Hfq+ background (<2 min) is quite untypical of many other *E. coli* sRNAs, including DsrS (Sledjeski *et al.*, 2001), RyhB (Moll *et al.*, 2003), OxyS (Basineni *et al.*, 2009, Moller *et al.*, 2002b), Spot

42 (Moller *et al.*, 2002), which exhibit long halflives (>30 min) after rifampicin treatment. However, some *E. coli* sRNA are reported as unstable e.g. GcvB has a halflife of less than 2 minutes, (Vogel *et al.*, 2003) and recently, the other sRNA of meningococcus, NrrF, was reported to have a similar short half-life of 5 min which was unvaried in the Hfq mutant (Mellin *et al.*, 2010).

Since the reduced levels of AniS are not due to increased turnover in the Hfq mutant, the Hfq-dependent down-regulation of AniS must be at the level of transcriptional initiation. In fact, the microarray Hfq data show that known genes of the FNR regulon (namely *aniA*, and *nosR* ; (Bartolini *et al.*, 2006) appear to be downregulated in the Hfq mutant, suggesting that Hfq negatively regulates FNR-mediated transcription, either directly or indirectly, possibly via altered activity of the FNR activator in cells lacking Hfq. It was then serendipity that allowed us to identify a Hfq-dependent sRNA in this way. This highlights the complexity of the effects a Hfq knockout can have on the global transcript profile, suggesting that much of the changes in expression will be due to indirect effects of the loss of function mutation. Indeed up to 25 % of the transcriptome was altered in Hfq mutant in stationary phase (data not shown), and while some direct Hfq/sRNA targets may be present in the deregulated genes, other more direct approaches are needed to detect and identify other sRNA circuits in the meningococcal and other systems for which not a lot is known.

Recently in *E. coli*, two independent groups described a similar FNR-regulated sRNA, nominated FnrS in line with other sRNA nomenclature, that is induced by anaerobiosis and represses the expression of enzymes that are dispensable during growth in low oxygen (Durand & Storz, 2010, Boysen *et al.*, 2010). Since it exhibits neither sequence similarity nor similar genomic localization to our sRNA we have nominated our novel sRNA AniS (anerobically induced sRNA) to

distinguish it. It appears therefore that the same stress regulons (FNR-mediated) have independently evolved to include a riboregulator in evolutionary diverse bacteria. Furthermore, both groups identify numerous targets of FnrS, and demonstrate that FnrS is involved in down-regulating genes with aerobic functions and genes with housekeeping functions in energy metabolism and biosynthesis that are not needed for anaerobic metabolism. While *E. coli* is a facultative anaerobe, which can quite easily adapt its metabolism and grow under complete anaerobiosis; meningococcus fails to grow under strictly anaerobic conditions but instead has a truncated denitrification pathway which allows it to survive anaerobiosis (Anjum *et al.*, 2002, Rock & Moir, 2005). This is an important difference between the 2 systems with respect to the regulatory circuit that they require. The FNR regulon of pathogenic *Neisseria* has been the subject of other studies (Bartolini *et al.*, 2006, Whitehead *et al.*, 2007) and notably it is limited to between 10 and 20 genes, in contrast to *E. coli* where FNR acts as a real global regulator coordinating the switch from aerobic to anaerobic metabolism and altering the expression of greater than 200 operons (Constantinidou *et al.*, 2006, Kang *et al.*, 2005, Salmon *et al.*, 2003). As such the few targets identified here are in line with the limited need for anaerobically induced or repressed genes in meningococcus.

Nonetheless, *N. meningitidis* will encounter anaerobic niches as part of its normal transmission, colonization and infectious cycles within the host. The surface of the upper respiratory tract will have atmospheric oxygen concentration (21kPa). However, it should be noted that human mucous membranes, contain areas of low partial pressure of oxygen, reported as 400 Pa for the buccal folds (Archibald & Duong, 1986) and 300 Pa within a thick mucus layer (Worlitzsch *et al.*, 2002) and FNR is activated by oxygen concentrations below 500 Pa (Sawers, 1999). Importantly, the FNR mutant of meningococcus is attenuated in the rat and mouse

bacteraemia models of infection (Bartolini *et al.*, 2006) highlighting the need for sensing and responding to oxygen limitation for survival *in vivo*. The identification of this novel sRNA underpins the need to rapidly co-ordinate gene expression in response to changing oxygen environments in the host. In *E. coli* the FnrS sRNA plays a major role in the immediate metabolic need of adapting to anaerobic growth (Durand & Storz, 2010, Boysen *et al.*, 2010). The regulation by AniS may have more to do with a coordinated response to an anaerobic environment as a specific niche-relevant signal requiring adaptive physiological changes for meningococcus an exclusively human host-adapted pathogen.

1.27 Molecular mechanism of action of the sRNA NrrF

In this section we have characterized the molecular mechanism of action of the sRNA NrrF in *N. meningitidis*. NrrF was discovered in 2007 ((Mellin *et al.*, 2007)) as an iron regulated sRNA which post-transcriptionally downregulates the succinate dehydrogenase genes (Mellin *et al.*, 2007; Metruccio *et al.*, 2009). In this thesis we have shown that Hfq is able to bind NrrF *in vitro* and increases the efficiency of NrrF duplex formation with the complementary target region within the *sdh* transcript (Fig 25). Numerous *E. coli* sRNAs have been shown to associate with Hfq (Majdalani *et al.*, 2005; Valentin-Hansen *et al.*, 2004) and we showed that in *N. meningitidis* also AniS requires Hfq to down regulate its targets (Fig 20). The complementarity between NrrF and its target sequence lies within an accessible single-stranded loop of the predicted structure of NrrF possibly facilitating initial contact, which Hfq may then enhance or stabilize through its RNA chaperone activity. In fact we showed that removing this loop from the NrrF transcript the interaction with the *sdh* target does not occur anymore (Fig 25B, panel III). It is likely that the formation of the complex between NrrF and *sdh* transcript *in vivo*

results in the rapid degradation of the target mRNA, possibly as a consequence of inhibition of translation. It is clear from *in vitro* binding assays, that NrrF directly targets the *sdh* transcript not in the 5'UTR region, as usual for sRNAs, but overlapping the *sdhDA* gene junction between the second and third gene (Fig. 25B). It was reported that sRNAs can also interact with coding regions (Pfeiffer *et al.*, 2009), regulating their targets by accelerating RNase E-dependent mRNA targets decay. Furthermore in *E. coli* a NrrF analogous sRNA, RyhB, with no sequence identity nor genomic synteny, was reported to down-regulate the succinate dehydrogenase operon through base pairing within a proposed region of complementarity at the junction of the first and second gene in the locus, *sdhCD* (Massè & Gottesmann, 2002). It is intriguing that in two completely different systems the conserved mechanism for regulating these metabolic genes has evolved in two apparently non-homologous but essentially similar mechanistic events. Conceptually, sRNAs are expected to be under appropriate transcriptional control, so that their induction matches requirements for their regulatory activity. Our data are consistent with a model in which high expression and abundance of NrrF in low iron conditions (or in the Fur mutant), results in a Hfq-dependent targeting of the *sdh* transcript, a NrrF-dependent translational inhibition of SdhA, and likely rapid degradation of the mRNA. In this way, the succinate dehydrogenase genes are essentially positively regulated through the repressive action of Fur with iron as a co-repressor.

Furthermore we show that the Fur- and iron- positive regulation of at least two other genes, *sodB* and *fumB* are clearly through a Hfq-dependent mechanism, although the NrrF sRNA is excluded as mediator (Fig 26). The expression of SodB was also found negatively regulated in a Hfq knock out mutant (Table 1). These data implicate at least one other trans-acting sRNA to be involved in the post-

transcriptional down- regulation of *sodB* and *fumB*, and possibly also *sdh*. It is therefore likely that more than one Fur-regulated sRNA is present in the *Neisseria* system and Solexa RNA sequencing data revealed the existence of 16 putative iron regulated sRNAs. It will be interesting to characterize these putative novel sRNAs and to understand if NrrF, along with one or more other sRNAs, control coordinately some of the remaining Fur-positively regulated genes in meningococcus. We also cannot exclude the possibility that other mRNAs are targets for the NrrF regulator. In fact in *N. meningitidis* a subset of genes that are positively regulated by Fur and iron, with no evidence for a direct interaction of Fur in their region, were identified (Delany *et al.*, 2006) and therefore candidate genes for this type of indirect posttranscriptional riboregulation. Many organisms respond to iron deprivation by rearranging their metabolism to bypass iron-dependent enzymes, such as *sodB* and the tricarboxylic acid cycle enzymes such succinate dehydrogenase and fumarase, and to dispense with iron-binding proteins, such as ferritins. In *E. coli* the role of a sRNA, RyhB, in mediating this change in metabolism was the first to be documented (Massè & Gottesmann, 2002). In *Pseudomonas* two tandem small RNAs were found to be responsible for mediating a similar RyhB-like posttranscriptional regulation (Wilderman *et al.*, 2004). Deletion of both of these analogues was necessary for deregulation of a number of iron and Fur induced genes although their findings also demonstrate that the PrrF RNAs do not explain all positive Fur regulation in *Pseudomonas*.

1.28 CONCLUDING REMARKS

The discovery of small noncoding RNAs (sRNAs) as modulators of stress adaptation and virulence gene expression, coordinating complex networks in response to environmental cues, has brought a new insight into regulation of bacterial pathogenesis processes (reviewed in (Toledo-Arana *et al.*, 2007; Papenfort & Vogel, 2010; Gripenland *et al.*, 2010). In the human pathogen *N. meningitidis* we have demonstrated that the Hfq mutant displays a pleiotropic phenotype and identified and characterized 2 novel sRNAs. Furthermore a transcriptome analysis under iron replete or depleted conditions through Solexa RNA sequence revealed 19 intergenic regions actively transcribed in these two conditions.

Taking together these data strongly indicate that there is an extensive circuit of sRNA genes involved in adaptation to stress and pathogenesis in meningococcs as yet largely unexplored.

The identification and characterization of novel sRNAs in this bacterium will help in understanding the mechanisms of pathogenesis of *N. meningitidis* and the finetuning of regulatory and adaptive responses..

MATERIALS AND METHODS

1.29 Bacterial strains and culture conditions

The meningococcal strains used in this study are all derivatives of the *N. meningitidis* MC58 sequenced strain (Tettelin *et al.*, 2001) and 2996 strain. *N. meningitidis* strains were routinely cultured in GC-based (Difco) agar medium supplemented with Kellogg's supplement I (Kellogg *et al.*, 1963) at 37°C in a 5% CO₂-95% air atmosphere with 95% humidity. Stock preparations of strains in 10% skim milk were stored at -80°C. Each bacterial manipulation was started using an overnight culture of a frozen stock. For liquid cultures *N. meningitidis* strains were grown overnight on solid medium, and cells were resuspended in phosphatebuffered saline (PBS) to an optical density at 600 nm (OD₆₀₀) of 1 and inoculated into broth medium at a 1:100 dilution. GC (Difco) broth supplemented with Kellogg's supplement I and 12.5 µM Fe(NO₃)₃ and Mueller-Hinton (Sigma, St.Louis, MO) broth supplemented with 0.2% glucose were used for liquid cultures; when required, erythromycin, chloramphenicol, kanamycin or IPTG were added to final concentrations of 5 µg/ml, 5 µg/ml, 100 µg/ml, and 1mM respectively. For transformation by naturally competent *N. meningitidis*, four to five single colonies of a freshly grown overnight culture were re-suspended in 20 µl of PBS, spotted onto GC plates, and 5–10 µg of linearized plasmid DNA was added, allowed to dry and incubated for 6–8 h at 37°C. Transformants were then selected on plates containing the appropriate antibiotic and single colonies were re-streaked on selective media for further analysis. Transformants were re-suspended in 50 µl of distilled water, placed in a boiling water bath for 5 min and centrifuged in a bench top centrifuge for 5 min at 8000 *g*. One microlitre of the sample was used as

template for PCR analysis for correct insertion by a double homologous recombination event. *E. coli* cultures were grown in Luria-Bertani medium, and, when required, ampicillin was added to a final concentration of 100 µg/ml.

1.30 DNA techniques

DNA manipulations were carried out routinely as described by (Sambrook *et al.*, 1989). Small- and large-scale plasmid DNA preparations were carried out with a QIAprep Spin Mini kit and Plasmid Midi kit (QIAGEN) according to the manufacturer's instructions. DNA fragments or PCR-amplified products were purified from agarose gels with QiaEX DNA purification kit (QIAGEN). PCR was performed in a Perkin-Elmer 2400 thermal cycler with Platinum Taq polymerase (Invitrogen). One microlitre of each reaction mixture contained 10–50 ng of chromosomal DNA or 1 µl bacterial sample (see above), 100 pmols of the required primers and 200 µM concentration of each deoxynucleotide in a volume of 100 µl of 1 x PCR buffer containing MgCl₂ (Invitrogen). After the initial denaturing step at 95°C for 5 min, 30 cycles of denaturing at 95°C, annealing at the appropriate temperatures for the specific primers and elongation at 72°C were carried out. When required, DNA fragments were routinely sequenced according to the dideoxy-chain termination method (Sanger *et al.*, 1977) by using [α -³²P]-dATP (NEN, Perkin Elmer) and a T7 sequencing kit (Pharmacia).

1.31 Construction of plasmids and recombinant strains

In order to knock out the *hfq* gene in the MC58 background, the p Δ hfqko:Cm or p Δ hfqko:Kan plasmids were constructed. Upstream and downstream flanking regions of the *hfq* gene were amplified by PCR with primers Hfq-1 and Hfq-2 and

primers Hfq-3 and Hfq-4 (Table 5), respectively. Then in a second round of PCR the upstream and downstream fragments, which contained regions of overlap due to the design of the primers, were used for self-priming PCR amplification for five cycles, and the united fragment was amplified using external primers Hfq-1 and Hfq-4. The product was cloned into the pGEM-T (Promega) vector, and a chloramphenicol cassette from pDT2548 (Wang & Taylor, 1990) or a kanamycin resistant gene from pill600 (Labigne-Roussel *et al.*, 1988) were inserted into the BamHI site between the flanking regions, generating p Δ hfqko:Cm or p Δ hfqko:Kan, respectively. These plasmids were then linearized and used for transformation. The p Δ hfqko:Kan plasmid was used to transform the MC58 strain to make Δ hfq^{kan} strain, while the p Δ hfqko:Cm plasmid was used to transform MC58 and 2996 strains to make Δ hfq and 2996 Δ hfq mutants, respectively and MC-Fko (Delany *et al.*, 2003) to make a Fur and Hfq double mutant, Fko- Δ hfq. For complementation of the knockout, a plasmid consisting of the ermAM erythromycin resistance genes and the Ptac promoter along with the lacI repressor for isopropyl- β -D-thiogalactopyranoside (IPTG)-inducible expression of the gene of interest, flanked by upstream and downstream regions for allelic replacement, was generated by replacing the 3.4-kb NotI-BamHI fragment carrying the promoterless lacZ gene from pSL-Fla-Ery (Ieva *et al.*, 2005) with a 1.6-kb NotI-BamHI fragment carrying the lacI repressor gene and the Ptac promoter from plasmid pPindCrgA (Ieva *et al.*, 2005), generating pFlaEry-Pind. The hfq coding region was amplified with primers Hfq-F and Hfq-R-Ns and cloned as a 303-bp NdeI-NsiI fragment downstream of the Ptac promoter, generating pFlaPind-Hfq, so that expression of the hfq gene in the complementation construct was induced in an IPTG-inducible manner. This

plasmid was used for transformation of the Δhfq mutant strain, and the resultant complemented mutant was designated Δhfq_C .

In order to knock out the *aniS* gene, by substituting the nucleotides spanning from –45 to +112 with respect to the transcriptional start site with a kanamycin cassette, the p Δ sR3:Kan plasmid was constructed. Upstream and downstream flanking regions of the *aniS* gene were amplified by PCR with the corresponding primers: sR3-1/sR3-2 and sR3-3/sR3-4 (Table 5). Then, the same strategy used for the construction of the p Δ hfqko:Kan plasmid was used, generating p Δ sR3:Kan plasmid. The plasmid was then linearised and used for transformation of the MC58 strain to make a *aniS* knockout mutant, $\Delta aniS$.

To generate recombinant MC58, $\Delta aniS$ and Δhfq_{kan} derivative strains expressing a FNRD148A protein from an integrated copy of the mutant gene, the plasmid pCompInd*fnr*(D148A) (Oriente *et al.*, 2010) which results in integration of a copy of the mutant allele *fnr*(D148A) under the control of the P_{tac} promoter between the NMB1428 and NMB1429 genes, was transformed into MC58, $\Delta aniS$ and Δhfq_{kan} strains, generating MC_FNRc, $\Delta aniS_FNRc$ and Δhfq_FNRc strains respectively.

To knock out the *nrrF* gene plasmid psRN2ko:Erm was generated amplifying upstream and downstream flanking regions of the *nrrF* gene by PCR with the corresponding primers: UsR-F/ UsR-R and DsR-F/ DsR-R (Table 5) and following the same strategy used above to generate plasmids for knockout strains, but using an erythromycin cassette (Trieu-Cuot *et al.*, 1990). The psRN2ko:Erm plasmid was then linearized and used to transform MC58 and MC-Fko (Delany *et al.*, 2003) strains to make respectively a NrrF knockout mutant, MC-sRN2, and a Fur and NrrF double mutant, Fko-sRN2. The Fur complemented strain, Fko_C, was constructed as described in Delany *et al.*, 2003.

In each case case transformants were first isolated by selection for the respective antibiotic resistance and then tested for the double crossover in the flanking regions by PCR.

To study the AniS-mediated regulation of NMB1468 we used the green fluorescent protein (GFP)-based reporter system developed by Urban and Vogel (Urban & Vogel, 2007). The 5' end of the NMB1468 gene, including 213 nt of the upstream region, was amplified by PCR on MC58 genome using primers 1468-pr-F/1468-gfp-R and cloned into pXG-10 as a AatII/NheI fragment, so that the first 10 amino acids were fused to GFP and the P_{LtetO} promoter was removed from pXG-10 and replaced by NMB1468 promoter, generating pXG-10-1468 plasmid. To generate pGemT-AniS plasmid PCR was performed on MC58 genome using primers AniS-pr/AniS-R and the resultant product, containing the *aniS* gene, and 144 nt upstream of the +1 was cloned into pGEMT as a compatible plasmid for co-transformation with pXG-10-1468. pGEMT- plasmid, was also generated as a negative control for AniS , cloning into pGEMT the NMB0375 promoter region amplified by PCR on MC58 genome using primers P375-F/ P375-R. *E. coli* DH5- α cells were co-transformed either with pXG-1 plasmid, as a control for GFP expression, or pXG-10-1468 plasmid and pGemT-AniS or pGEMT-.

1.32 Expression and purification of the Hfq protein.

The *hfq* gene was amplified from the MC58 genome with the Hfq-F/Hfq-R primer pair and cloned as a 302-bp NdeI-XhoI fragment into the pET15b expression plasmid (Invitrogen), generating pET15*hfq*, which was subsequently transformed into *E. coli* strain BL21(DE3) for protein expression. Using an overnight culture of the BL21(DE3)(pET15*hfq*) strain, 200 ml of Luria-Bertani medium was inoculated, the culture was grown until the OD₆₀₀ was 0.5, and expression of the recombinant

Hfq protein containing an N-terminal histidine tag was induced by addition of 1 mM IPTG and further incubation for 3 h. The protein was purified from the harvested cells by Ni-nitrilotriacetic acid (NTA) (Qiagen) affinity chromatography under nondenaturing conditions according to the manufacturer's instructions. The purified protein preparation was then diluted to 1 $\mu\text{g}/\mu\text{l}$ and dialyzed overnight in PBS at 4°C. To remove the His tag, the dialyzed protein was digested with thrombin (10 U/ μg protein; Pharmacia/Amersham) at room temperature for 4 h, and the thrombin was then deactivated by incubation with 1 mM of phenylmethylsulfonyl fluoride at 37°C for 15 min. The digested His tag was removed by dialyzing the protein preparation twice against 1 liter of PBS at 4°C in a 6,000- to 8,000-molecular-weight-cutoff dialysis tube (Membrane Filtration Products, Inc.). The purity of the protein was estimated to be 99% by SDS-PAGE. The concentration of the protein in this preparation was determined by using the Bradford colorimetric assay (Bio-Rad), and the protein was aliquoted and stored at -80°C.

1.33 *In vitro* cross-linking

For *in vitro* cross-linking, the dialyzed Hfq protein was diluted to obtain a concentration of 0.6 $\mu\text{g}/\mu\text{l}$ in PBS. Disuccinimidyl suberate (DSS) was added to 10 μl of the protein solution to a final concentration of 2.5 mM, and this was followed by incubation at room temperature for 1 h. To stop the cross-linking reaction, 20 μl of 1xSDS-PAGE loading buffer (50 mM Tris Cl pH 6.8, 2.5 % SDS, 0.1 % Bromophenol Blue, 10% glycerol, 5% B-mercapto-Ethanol, 50 mM DTT) was added, and the protein was analyzed by SDS-PAGE.

1.34 Generation of anti-Hfq antiserum

To prepare anti-Hfq antiserum, 20 µg of purified protein was used to immunize 6-week-old female CD1 mice (Charles River Laboratories); four mice were used. The protein was given intraperitoneally, together with complete Freund's adjuvant for the first dose and incomplete Freund's adjuvant for the second (day 21) and third (day 35) booster doses. Bleed-out samples were taken on day 49 and used for Western blot analysis.

1.35 Western blot analysis

N. meningitidis colonies from overnight plate cultures were either resuspended in PBS until OD₆₀₀ of 1, or grown to logarithmic phase (OD of 0.5, ca. 2 hours incubation) from a starter inoculum of OD 0.05. Samples of 1-2 ml were harvested and normalised in 1xSDS-PAGE loading buffer to a relative OD of 5. For Western blot analysis, 10 µg of each total protein sample in 1 x SDS-PAGE loading buffer was separated by SDS-PAGE, and transferred onto nitrocellulose membrane using an iBlot Dry Blotting System (Invitrogen). Membranes were blocked overnight at 4°C by agitation in blocking solution (10% skimmed milk, 0.05% Tween-20, in PBS) and incubated for 90 min at 37°C with the appropriate polyclonal sera in blocking solution. After washing, the membranes were incubated in a 1:2000 dilution of peroxidase-conjugated anti-rabbit immunoglobulin (Biorad) or anti-mouse immunoglobulin (Dako), in blocking solution for 1 hour and the resulting signal was detected using the Supersignal West Pico chemiluminescent substrate (Pierce).

For *E. coli* GFP, Western Blots 10 ug of cell extracts from *E. coli* plate cultures were separated by SDS-PAGE and after blotting, filters were stained with 1:1000 dilution of anti-GFP (SantaCruz Biotechnologies,Inc).

1.36 Fractionation of proteins of *N. meningitidis*

Liquid cultures of meningococcus strains were grown to an OD600 of 0.5 and harvested by centrifugation at 8,000 g for 15 min at 4°C. Secreted proteins were precipitated from each spent culture supernatant as follows. The supernatant was filtered through a 0.22- μ m filter to remove bacteria, and to 22 ml of the filtrate 2.5 ml of 100% trichloroacetic acid (Sigma) was added and incubated overnight on ice. The precipitated proteins were then pelleted in a benchtop centrifuge (Beckman) at 13,000 rpm for 30 min at 4°C and washed with 500 μ l of 70% ethanol, and the pellet was then air dried and resuspended in 10 μ l of PBS containing complete protease inhibitor (Roche). For cytoplasmic and envelope fractions, harvested bacteria were resuspended in PBS and inactivated at 56°C for 45 min. The cells were then repelleted by centrifugation at 8,000 g for 15 min at 4°C and resuspended in 20 mM Tris-HCl (pH 7.5) containing complete protease inhibitor. The bacteria were lysed by sonication on ice, and the cell debris was removed by centrifugation at 5,000 g for 20 min. The supernatant was centrifuged at 50,000 g for 75 min (29,000 rpm; Beckman Ti50) to pellet the membrane fraction. The supernatant, containing the soluble cytoplasmic fraction, was then filtered and analyzed by SDS-PAGE. The pellet containing the membrane envelope was washed with 5 ml of 20 mM bis-Tris propane (pH 6.5), 1 M NaCl, 10% glycerol and then pelleted by centrifugation at 50,000 g for 75 min. The membrane fraction was resuspended in PBS and analyzed by SDS-PAGE.

1.37 Separation of total proteins by 2D gel electrophoresis.

N. meningitidis wildtype strain MC58 and the Δhfq mutant were grown at 37°C in GC medium until the OD600 was 0.5 to 0.6. The cells were harvested, washed once in PBS, and heat inactivated for 2 h at 65°C. Bacteria were resuspended in reswelling buffer containing 7M urea, 2M thiourea, 2% 3-[(cholamidopropyl)-dimethylammonio]-1-propanesulfonate (CHAPS), 2% amidosulfobetain 14, 1% dithiothreitol, 2 mM tributylphosphine, 20 mM Tris, and 2% carrier ampholyte (GE Healthcare), and 200 µg of total proteins in 0.125 ml (final volume) was absorbed overnight onto Immobiline DryStrips (7 cm; nonlinear pH 3 to 10 gradient) using an Immobiline DryStrip reswelling tray (GE Healthcare). Proteins were then separated by two-dimensional (2D) electrophoresis. The first dimension was run using an IPGphor isoelectric focusing unit (GE Healthcare) by sequentially applying 150V for 60 min, 500 V for 35 min, 1,000 V for 30 min, 2,600 V for 10 min, 3,500 V for 15 min, 4,200 V for 15 min, and finally 5,000 V until 12,000 V · h was reached. For the second dimension, the strips were equilibrated as described previously (Herbert *et al*, 1998), and proteins were separated on a Nu-Page 4 to 12% bis Tris ZOOM gel (Invitrogen) using 40 mA/gel. An image of each bidimensional gel was acquired with an SI personal densitometer (Molecular Dynamics) at 16 bits and 50 µm per pixel. Images were analyzed with the software Image Master 2D Platinum 6.0 (GE Healthcare).

1.38 In-gel protein digestion and MALDI-TOF mass spectrometry analysis

Protein spots were excised from the gels, washed with 50 mM ammonium bicarbonate-acetonitrile (50/50, vol/vol), and air dried. Dried spots were digested

for 2 h at 37°C in 12 µl of 0.012-µg/µl sequencing grade modified trypsin (sequencing grade modified porcine trypsin; Promega, Madison, WI) in 5 mM ammonium bicarbonate. After digestion, 0.6 µl was loaded on a matrix-prespotted Anchorchip (PAC 384 HCCA; Bruker-Daltonics, Bremen, Germany) and air dried. Spots were washed with 0.6 µl of a solution containing 70% ethanol and 0.1% trifluoroacetic acid. Mass spectra were acquired with an ultraflex matrix-assisted laser desorption ionization—time of flight (MALDI-TOF) mass spectrometer (Bruker-Daltonics). Spectra were externally calibrated by using the combination of standards present on the PAC chip (Bruker-Daltonics). Monoisotopic peptide matching and protein searching were performed automatically using a licensed version of the MASCOT software (Matrix Sciences, London, United Kingdom) run on a local database. The MASCOT search parameters used were as follows: (i) allowed number of missed cleavages, 1; (ii) variable posttranslational modification, methionine oxidation; and (iii) peptide tolerance, ±100 ppm. Only significant hits as defined by MASCOT probability analysis were considered.

1.39 *In vitro* antimicrobial stress assays

To investigate the sensitivities of the Δhfq mutant strain to various stresses, a series of growth assays and killing assays were performed using different antimicrobial compounds. Unless otherwise stated, the Δhfq_C complemented mutant was cultured in the presence of 1 mM IPTG for induction of *hfq* gene expression. Membrane integrity was investigated by looking at the susceptibility to osmotic stress (30% sucrose and 5M NaCl) and detergents (0.01 to 0.05% Tween and sodium dodecyl sulfate [SDS]). To investigate the responses of the strains to

oxidative stress, paraquat (5 to 10 mM; Sigma), xanthine-xanthine oxidase (4.3 mM xanthine and 100 to 300 mU/ml xanthine oxidase; Sigma), and H₂O₂ (5 to 10 mM; Riedel-de Haen) killing assays were performed. For killing assays, cells from GC agar plates were harvested into GC media to obtain an OD₆₀₀ of 0.05, grown to mid-log phase (OD₆₀₀, 0.5 to 0.6), and then diluted to obtain a concentration of 10⁵ to 10⁶ CFU/ml. The killing assay was started by addition of the killing sample. Cultures were incubated at 37°C in an atmosphere containing 5% CO₂ with gentle agitation, and at various time points samples were taken, plated onto Mueller-Hinton agar after serial dilution, and incubated at 37°C in an atmosphere containing 5% CO₂ to determine the number of CFU. Experiments were done in triplicate and repeated on several occasions.

1.40 *Ex vivo* human serum assay and *ex vivo* whole-blood model of meningococcal bacteremia.

N. meningitidis strains were grown on GC agar overnight. Cells were harvested into Mueller-Hinton medium containing 0.25% glucose and 0.02 mM cytidine-5'-monophospho-N-acetylneuraminic acid sodium salt to obtain an OD₆₀₀ of 0.05, grown to mid-log phase (OD₆₀₀, 0.5 to 0.6), and then diluted to obtain a concentration of approximately 10³ CFU/ml. The assay was started by addition of 100% whole human blood or human serum (240 µl) to the bacterial suspension (10 µl). Cultures were incubated at 37°C in an atmosphere containing 5% CO₂ with gentle agitation, and at various time points an aliquot was removed and the number of viable bacteria was determined by plating serial dilutions onto Mueller-Hinton agar and incubating the plates overnight at 37°C in an atmosphere containing 5% CO₂. Experiments were done in triplicate and repeated on several occasions. Whole

venous blood, collected from healthy individuals and anticoagulated with heparin (10 U/ml), was used for whole-blood experiments. For preparation of human serum, whole blood was coagulated at 37°C for 30 min and centrifuged at 1,000 g for 10 min at 4°C, and the supernatant was retained. Statistical analyses of the differences between the survival of the wild type strain and the survival of mutant strains were performed using Student's t test.

1.41 *In vivo* animal model.

The infant rat model was used essentially as previously described (Granoff *et al.*, 2001). The 2996 *N. meningitidis* strain was passaged three times in infant rats. On the day of the experiment the bacteria were grown to log phase in Mueller-Hinton medium supplemented with 0.25% glucose, washed, and resuspended at the desired concentration in PBS. Five- to 6-day-old pups from litters of outbred Wistar rats (Charles River) were challenged intraperitoneally with wild type strain 2996 or the isogenic 2996 Δ *hfq* strain. Eighteen hours after the bacterial challenge, blood specimens were obtained by cheek puncture, and aliquots (100 μ l of undiluted sera and 1:10, 1:100, and 1:1,000 dilutions) were plated onto chocolate agar for viable cell counting. The numbers of CFU per milliliter of blood were determined after overnight incubation of the plates at 37°C in an atmosphere containing 5% CO₂. A statistical analysis was performed using Student's t test.

1.42 RNA extraction

N. meningitidis strains were routinely grown in 16 ml tubes in 7 ml of liquid culture to mid-log phase and then added to an equal volume of the same frozen medium to bring the temperature immediately to 4°C and centrifuge at 3000 g for 20 minutes.

RNA was extracted from the pellet using the RNAeasy Mini-kit (Qiagen) or SV RNA isolation kit (Promega) for Illumina sequencing. RNA pools for microarray experiments were prepared from 3 independent cultures of bacteria. Briefly, for each RNA pool, 3 independent cultures of each strain were grown to mid-log phase and total RNA was extracted separately from each bacterial pellet and 15 µg of each preparation were pooled together. Three independent pools were prepared for each strain. For the oxygen limiting conditions, liquid cultures, once grown to mid-log phase, were first diluted to OD 0.1 and split into 7 ml (microaerobic growth, +O₂) or 15 ml (oxygen limiting conditions, -O₂) in 16 ml tubes, re-incubated at 37°C for 30 min, and then added to an equal volume of frozen media and RNA was extracted. For the iron limiting conditions, liquid cultures grown to mid-log phase were split in two and exposed for 15 min treatment with or without 100 µM 2,2'-dipyridyl (specific iron-chelator) (Sigma). After 15 min the cultures were added to an equal volume of equivalent frozen medium and RNA was extracted. For the rifampicin timecourse, a culture of 100 ml was grown in Erlenmeyer flasks under microaerobic conditions until log phase and then 80 µg/ml of rifampicin were added and, at indicated times, 15 ml were removed and added to an equal volume of frozen medium. RNA was extracted by CsCL gradient as previously described (Metruccio *et al.*, 2009).

1.43 Microarray procedures: design, cDNA labelling and hybridization, and data analysis.

DNA microarray analysis was performed using an Agilent custom-designed oligonucleotide array. Design: A 60-mer oligo-microarray was designed to cover all the 2078 predicted open reading frames of *N. meningitidis* MC58 strain. Probe design was performed respecting oligo sequence specificity, structural and

thermodynamic constraints in order to obtain at least two probes for each open reading frame of the genome. For some specific genes we covered the entire open reading frame with head to tail tiling with a 10 nucleotide overlap (fHbp, nadA, NMB2132, NMB1030; NMB2091). Two probes for each of the previous selected genes together with the seven multi locus typing housekeeping genes, *abcZ*, *adk*, *aroE*, *fumC*, *gdh*, *pdhC* and *pgm* were used for the design of 21 and 5 replicas randomly distributed on the surface of the chip to have control spots of the signal uniformity within each sample. cDNA probes were prepared from RNA pools (5 ug) using Superscript II reverse transcriptase (Invitrogen), random primers (Promega), and Cy5 and Cy3 dyes (Amersham Biosciences). Labeled cDNA was purified by using a QIAquick PCR purification kit (Qiagen). The efficiency of incorporation of the Cy5 or Cy3 dyes was measured by NanoDrop analysis. Equal amounts of Cy5- and Cy3 labeled cDNAs were hybridized onto the microarray for 17 h at 65°C according to the Agilent protocol. Three hybridizations were performed using cDNA probes from 3 independent pools, respectively, corresponding to RNA extracted from a total of 9 independent bacterial cultures for each strain. Images were acquired by using an Agilent microarray scanner G2505B at 5 µm of resolution and using the extended dynamic range and were analyzed with Agilent Feature Extraction 9.5.1. Extracted raw data were normalized with the BASE application using an intra-slide median centering after a low intensity spot correction (if the average spot intensity, background subtracted, is less than one standard deviation of the background signal, the spot intensity was corrected to the same value of one standard deviation of the background signal). Differentially expressed genes (exhibiting a fold change of at least 2 with respect to the reference) were assessed by grouping all log₂ ratio of the Cy5 and Cy3 values corresponding

to each gene, within experimental replicas and spot replicas, and comparing them against the zero value by Student's t-test statistics (one tail).

1.44 Primer extension, S1 nuclease mapping, Northern blot and real time PCR

Primer extension was performed as previously reported (Delany *et al.*, 2003). To ensure correct mapping of the promoter sequencing reaction was carried out with a T7 sequencing kit (USB Corporation) using the same primer as in the primer extension reactions and the plasmid consisting of the relevant cloned promoter.

A radioactively labeled DNA probe for S1 mapping of the 5' region of the *hfq* transcript from position +1 was prepared as follows. The probe was amplified from the MC58 chromosome using the Hfq-S1/Hfq-S2 primer pair, the appropriate 363-bp fragment was extracted from an agarose gel, and after purification 2 pmol of the probe was labeled at both extremities with T4 polynucleotide kinase and 4 pmol of [γ -³²P]ATP. One labeled extremity was removed by digestion with EcoRI, a site for which was incorporated into the upstream primer (Hfq-S1), and the resultant 345-bp probe, labeled on the 5' complementary strand, was purified using Chomaspin TE-100 columns (Clontech). Approximately 20 fmol of labeled probe was coprecipitated with 15 μ g of total RNA and resuspended in 20 μ l of hybridization buffer (80% formamide, 60 mM Tris-HCl [pH 7.5], 400 mM NaCl, 0.4 mM EDTA). The mixture was overlaid with 5 μ l of paraffin oil, denatured at 100°C for 3 min, and then incubated at the melting temperature (T_m) calculated for the probe on the basis of the following formula: $T_m = 81.5 + 0.5(G+C \text{ content}) + 16.6(\text{natural log of Na concentration}) - 0.6(\text{formamide concentration expressed as a percentage})$. After 4 to 16 h of hybridization, 180 μ l of ice-cold S1 buffer (33 mM

Na acetate [pH 5.2], 5 mM ZnSO₄, 250 mM NaCl) and 100 U of S1 nuclease (Invitrogen) were added, and S1 nuclease digestion was carried out for 30 min at 37°C. Samples were then extracted once with phenol-chloroform, ethanol precipitated, resuspended in 5 µl sequencing loading buffer (Sambrook *et al*, 1989), and subjected to 6% urea-polyacrylamide gel electrophoresis (PAGE). Quantification of the signals from the digested probes was performed using a Phosphorimager and ImageQuant software (Molecular dynamics). A G-A sequencing reaction (Maxam & Gilbert, 1977) was performed with the probe parallel to the S1 nuclease reactions to provide a molecular weight ladder for mapping the 5' end of the transcript.

Northern blot analysis to identify the AniS transcript was carried out using the NorthernMax kit (Ambion, Inc.) according to the manufacturer's instructions. A total of 5 µg of total RNA from different *N. meningitidis* samples was fractionated on a 1% agarose-formaldehyde gel or denaturing 10% polyacrylamide urea gel (10% TBU gel, Invitrogen) and transferred onto nylon membrane (Hybond+, Inc.) through capillary blotting or electro-blotting (45 min, 150mA,) in a semi-dry blotter (Thermo scientific). Then, 2 pmol of a 304-bp PCR product amplified from the MC58 genome using the primers 1205-F and 1205-R was radioactively end labeled by using T4 polynucleotide kinase (New England Biolabs) and [γ-³²P]ATP (Perkin-Elmer) and was used as probe. Hybridization and high stringency washes steps were performed at 42°C, low stringency washes at room temperature.

For real-time quantitative PCR (RT-PCR), approximately 4 µg of total RNA was treated with RQ1 RNase-free DNase (Promega). RNA was then reverse transcribed using random hexamer primers and Moloney murine leukemia virus reverse transcriptase (Promega) as recommended by the manufacturer. For negative controls, all RNA samples were also incubated without reverse transcriptase. All

RT-PCRs were performed in triplicate using a 25- μ l mixture containing cDNA (5 μ l of a 1/5 dilution), 1x brilliant SYBR green quantitative PCR master mixture (Stratagene), and approximately 5 pmol of each primer (Table 5). Amplification and detection of specific products were performed with an Mx3000 real-time PCR system (Stratagene) using the following procedure: 95°C for 10 min, followed by 40 cycles of 95°C for 30 s, 55°C for 1 min, and 72°C for 30 s and then a dissociation curve analysis. The 16S rRNA gene was used as the endogenous reference control, and relative gene expression was determined using the $2^{-\Delta\Delta Ct}$ relative quantification method.

1.45 cDNA library construction and Illumina sequencing

RNA was extracted using SV RNA isolation kit (Promega) not to lose small RNA transcripts. RNA quality was determined using Bioanalyser (Agilent) and quantified using Nanodrop. Genomic DNA was removed with two digestions using 30 U DNaseI (Roche) at 37°C to below PCR-detectable levels. RNA was reverse transcribed using randomprimers (Invitrogen) and Superscript III (Invitrogen) at 45°C for three hours and heat denatured at 70 C for 15 minutes. Highly transcribed genes *fhbp*, *nhba* and *kat* with a maximum amplicon of 250 bp, were used as targets for a PCR as a positive control for reverse transcription. Sequencing libraries for the Illumina GAI platform were constructed by shearing the enriched cDNA by nebulisation (35psi, 6 min) followed by end-repair with Klenow polymerase, T4 DNA polymerase and T4 polynucleotide kinase (to blunt-end the DNA fragments). A single 39 adenosine moiety was added to the cDNA using Klenow exo- and dATP. The Illumina adapters (containing primer sites for sequencing and flowcell surface annealing) were ligated onto the repaired ends on the cDNA and gel-electrophoresis was used to separate library DNA fragments from unligated

adapters by selecting cDNA fragments between 200–250 bps in size. Fragmentation followed by gelelectrophoresis were used to separate library DNA fragments and size fragments were recovered following gel extraction at room temperature to ensure representation of AT rich sequences. Ligated cDNA fragments were recovered following gel extraction at room temperature to ensure representation of AT rich sequences. Libraries were amplified by 18 cycles of PCR with Phusion polymerase. Sequencing libraries were denatured with sodium hydroxide and diluted to 3.5 pM in hybridisation buffer for loading onto a single lane of an Illumina GA flowcell. Cluster formation, primer hybridisation and single-end, 36 cycle sequencing were performed using proprietary reagents according to manufacturers' recommended protocol (<https://icom.illumina.com/>). The efficacy of each stage of library construction was ascertained in a quality control step that involved measuring the adapter-cDNA on a Agilent DNA 1000 chip. A final dilution of 2 nM of the library was loaded onto the sequencing machine.

1.46 Read mapping and visualization

For RNA-seq experiments the computational pipeline developed at the WellcomeTrust Sanger Institute, (<http://www.sanger.ac.uk/Projects/Pathogens/Transcriptome/>) was used to process the raw data. All reads to the MC58 genome using MAQ and discarded all reads that did not align uniquely to the genome. The quality parameter (2q) used in MAQ pileup was 30. MAQ pileup prints an array of delimited information formatted as one line per genomic base. Each base is assigned a value for the number of piled sequences and the mapped strand for each read, represented by a “.” (forward) and “,” (reverse). For example, Forward strand: all_bases, 7887, G, 45, @.....;

Reverse strand: all_bases, 914, G, 6, @,,,,,; Overlapping Strands: all_bases, 7690, G, 38, @,,,,,..... These data were then mapped strand specifically using the perl script maqpileup2depth.pl returning a plot file with two columns which can be read into Artemis as a graph by using commands “Graph, Add User Plot”.

1.47 DNase I footprinting

For footprinting analysis, the promoter region of the *aniS* gene was amplified with the primers 1205-F and 1205-R and cloned into pGEM-T, generating pGem-sR3 plasmid. The pGem-sR3 plasmid was 5'end labeled with [γ -³²P]ATP at its NcoI site and separated from the vector by polyacrylamide gel electrophoresis after digestion with SpeI, producing a probe of the *aniS* promoter region labeled at one extremity only, as previously described (Oriente *et al.*, 2010). A recombinant constitutively active mutant form of meningococcal FNR (FNRD148A, here stated FNR_c) was used in binding studies which has been previously described (Oriente *et al.*, 2010). DNase I footprinting experiments with FNR_c and the radioactively labelled *aniS* promoter probe were carried out as previously described (Oriente *et al.*, 2010).

1.48 Generation of *in vitro* transcripts

DNA templates for *in vitro* transcript generation carrying a T7 polymerase promoter were amplified by PCR using genomic MC58 DNA and the primer pairs are listed in Table 5. To generate an AniS transcript of 106 nucleotides (nt), a 134-bp PCR product was generated with the forward primer T7-sR3-F, which contains the T7 polymerase promoter (28 bp), and the reverse primer T7-sR3-R, overlapping and including the predicted rho-independent terminator sequence of the *aniS* gene.

To test the activity of the rho-independent terminator another PCR product was generated for *in vitro* transcription using the same primer T7-sR3-F and the reverse 1205-R, which overlaps the putative stop codon of the annotated NMB1205 ORF, generating a 183bp that should give rise to a transcript of 155nt. A template for generation of a site-directed mutant of AniS (AniS_mut) was generated by amplification of 2 overlapping PCR fragments, with primers pairs T7-sR3-F/ss-R and ss-F/ T7-sR3-R, which were then using in a self-priming PCR reaction and the product was amplified with the T7-sR3-F/T7-sR3-R primer pair. To generate an *in vitro* NMB1468 transcript corresponding to the first 217 nt of the predicted mRNA, including 104 nt of 5'UTR, (starting from the +1 of the predicted promoter) and 113 nt of the ORF, a template of 244 nt was generated by PCR amplification from MC58 genome, using T7-1468-F and T7-1468-R primers. A template for generation of a site-directed mutant of NMB1468 (1468_mut) was generated by amplification of 2 overlapping PCR fragments, with primers pairs T7-1468-F/1468ss-R and 1468ss-F/ T7-1468-R, which were then using in a self-priming PCR reaction and the product was amplified with the T7-sR3-F/T7-sR3-R primer pair. To generate a NrrF transcript of 156 nt, a 184 bp PCR product was generated with a forward primer T7-sR-F which contains the T7 polymerase promoter (28 bp) and a reverse primer T7-sR-R overlapping and including the predicted rho-independent terminator sequence of the nrrF gene. For mutagenesis of this template the PCR product was cloned in pGemT-easy (Promega) and a deletion spanning from +31 to +58, inclusive, of the nrrf gene was generated using QuikChange site-directed mutagenesis Kit (Stratagene) and del1-f/del1-r the primer pair. The template for the mutant transcript was amplified from the resultant plasmid using the T7-sR-F/ T7-sR-R primers giving rise to a template of 156 bp for generation of the NrrfD31-58 transcript of 128 nt in length. For the 5'UTR region of the sdhC

gene the T7-sC-F/T7sC-R primers were used to amplify a 213 bp PCR fragment including the T7 promoter fused from the +1 of transcription to +185 within the *sdhC* gene. To generate a transcript spanning the region of possible complementarity overlapping the *sdhDA* sequence the T7-sA-F/T7-sA-R primers were used to amplify a 211bp fragment including the T7 promoter fused to a region spanning -96 to +87 with respect to the ATG start site of the *sdhA* gene. In vitro transcription was performed using the MEGAscript High Yield Transcription Kit (Ambion) followed by a clean-up step with the MEGAclean kit (Ambion). The length and integrity of the in vitro transcripts were analyzed on denaturing 6% 1 polyacrylamide urea gels.

1.49 Electrophoretic mobility shift assays of *in vitro* transcription products

To radioactively label AniS, Anis_mut, NrrF and NrrfD31-58 for *in vitro* binding assays with the Hfq protein and/or the possible targets, 20 pmoles of in vitro transcription products were dephosphorylated with Calf intestinal phosphatase (New England Biolabs) at 37°C, purified using MegaClear Kit (Ambion) and 5' end-labeled with 30 μ Ci of (γ -³²P)-ATP (6000 Ci/mmol; NEN) using 10U of T4 polynucleotide kinase (New England Biolabs). The unincorporated radioactive nucleotides were removed using the TE-30 chromaspin columns (Clontech) and the band of the labeled in vitro transcript of appropriate size was extracted after electrophoresis on a denaturing 6% polyacrylamide urea gel and eluted overnight at 4°C in RNA Elution buffer (0.1 M Na Acetate, 0.1% SDS, and 10 mM EDTA). After phenol:chloroform extraction the labeled RNA was precipitated by addition of 2 volumes of ethanol, and resuspended in water. Binding assays were performed with 0.5 pmoles of radioactively labeled probe in 10 μ l reactions in 1x RNA

binding buffer (10 mM Tris-HCl pH 7, 100 mM KCl, 10 mM MgCl₂) with 10 % glycerol final concentration. For use in gel shift assays, the Hfq protein was dialyzed against 1x RNA binding buffer (10 mM Tris [pH 7], 100 mM KCl, 10 mM MgCl₂) containing 10% glycerol and then 1x RNA binding buffer with 50% glycerol and the concentration was calculated for the hexameric form and stored at -20°C. RNA-protein complexes or RNA-RNA duplexes were formed at 37°C for 10 min in the presence or absence of 10 µg of E. coli tRNA (Boehringer Mannheim) as non specific competitor and run on 6% native polyacrilamide gels buffered with 0.5 x TBE at 250 Volts for 40 minutes. Gels were dried and exposed to autoradiographic films at -80°C and radioactivity was quantified using a phosphorimager.

TABLES

Table 5: Oligonucleotides used in this study

Name	Sequence	Site
HFQ-1	AttcagaattcGGTTTCCGTGCGGGTGGTAAGGC	EcoRI
HFQ-2	GCTAAAGGACAAATGTTGCAggatccGCACGAAGCATGACGTGTC	BamHI
HFQ-3	GACACGTGATGCTTCGTGCGgatccTGCAACATTTGTCCTTTAGC	BamHI
HFQ-4	attcagaagcttACGCGAAGCAGGCAGGTCTATGG	HinDIII
Hfq-F	attcagcatATGACAGCTAAAGGACAAATGTTGCAAG	NdeI
Hfq-R	attcagctcgagTTATTCGGCAGGCTGCTGGACGGTTTCC	XhoI
Hfq-R-Nsi	attcagatgcatTTATTCGGCAGGCTGCTGGACGGTTTCC	NsiI
Hfq-S1	CTCAGGAGAACAACGTATTGATCG	
Hfq-S2	GTTACCATCGTATTGCTGAAATCGCCACATC	EcoRI
0747-F	GAAAGTGTGGGCATTCGAC	
0747-R	TTGCTGTAACCTGCTTCCTG	
16S_F	ACGGAGGGTGCAGCGTTAATC	
16S_R	CTGCCTTCGCCTTCGGTATTCTT	
1205-F	attcagaattccacaaacctgccaatacagcagt	EcoRI
1205-R	ggttaaagttaagcatttgctgttacgg	
1205-3	ggcagccacacccaaacac	
T7-sR3-F	gttttttaatacactactataggATGAAATTCAGGGTGCTTGTTG	
T7-sR3-R	AAAAAAAAAGGGGTGGCGGCAG	
Fnr for1	attagcatATGGCTTCGCATAATACTACAC	NdeI

Fnr rev1	attagggatccTCAAATGGCGTGCGAGC	BamHI
D154A-F	GTGAAATCGTGCGCGCCCAAGGTGTTATGCTG	
D154A-R	CAGCATAACACCTTGGGCGCGCACGATTTAC	
sR3-1	attcgatcgatGCTTTGAAGAACTGGGCGAAC	SpeI
sR3-2	TACTTCACATggatccCAATTTAGATTTTATTCGCAAACCG	BamHI
sR3-3	ATCTAAATTGggatccATGTGAAGTAAAATCCGTAACAGC	BamHI
sR3-4	attcggaaattcAGGTTTCCAGTGCTGAAGACAG	EcoRI
Hfq-1	attcagaattcGGTTTCCGTGCGGGTGGTAAGGC	EcoRI
Hfq-4	attcagaagcttACGCGAAGCAGGCAGGTCTATGG	HinDIII
1468-F	GTTAAGGAAGCGGTTCAAGC	
1468-R	GTTACAGCTTCCTCGGCACT	
0920-F	AAGTTCAGCTTGGGTCGTCT	
0920-R	TAGTCGCGCAAGACATTACC	
0431-F	AGCGAATCACACATCAAAGC	
0431-R	TCCGGTAATGCTGGAGTACA	
0577-F	TTTACAAAGGCGATGAGCAG	
0577-R	TCAATCGGTTTGCTCGAATA	
1584-F	CCTCAAAGACCTCAACCTC	
1584-R	CTGCCAGTTTCAGGTAAACG	
1623-F	ATGACCATGGAAGACGGTGT	
1623-R	CACTTCAACCGTATCGCCTT	
1964-F	ACCGACTATGTACGCCCCGAA	
1964-R	TTCGGTGATGTCCAGATTGT	
16s-F	ACGGAGGGTGCGAGCGTTAATC	
16s-R	CTGCCTTCGCCTTCGGTATTCCT	
0214-F	TCCGCAGGCTATTACAGCTA	
0214-R	GACATCGTTCGCTTCTTCAA	
1994-F	GCTGGCACAGCTAATACTGC	

1994-R	TCAGCTTTGTTTCGTAGCGAT	
0435-F	TCGGTATTTCCGAACCTTCC	
0435-R	CCATCGAAGCGATGTATTTG	
1572-F	CTGCCTGATTTGAAAGTGGA	
1572-R	ATCGGCTCTTTGTTGAGCTT	
adk-PE1	CGCGCCTAAAAGTAATGC	
P375-R	GGAGGAGCAGGGTTTTTCATAGCGGGG	
P375-F	CCGCAATGGGTGGAAGCCGCCGC	
1468-pr-F	<u>attcagacgtc</u> TTCGGACATCCCAGGAATATATTTGGG	AatII
1468-gfp-R	attcagctagcCATCATTGCGGCAATCAATAATTTTTTCAT	NheI
AniS-pr	attcaggatccCCACTGCCAAATACAGCAGTCC	BamHI
AniS-R	attcatctagaGCATTTGCTGTTACGGATTTTACTTCAC	XbaI
ss-R	GAGAGGGAAACAGATAAAATCAAGACAAGCGAGGAAACAG	
ss-F	ATTTTATCTGTTTCCCTCTCATGTGTGTGTGTTTGGG	
T7-1468-F	GTTTTTTTTAATACGACTCACTATAGGTAACATAAACGGGAAACCGTTTTTC	
1468ss-F	AGGATAACACATGAAAAAATTATTAGCGACCGCAATGATGGCGGC	
1468ss-R	ATTTTTTCATGTGTTATCCTCTCCTAGTTGTTGATTAAG	
T7-1468-R	ATCGGACTCAACGGCTTGAACCGC	
Sod-pe3	ATGCGTCCAGTTCATAAGGC	
T7-sR-F	GTTTTTTTTAATACGACTCACTATAGGCTCGGAAGCCGTCCGTTCCGAACC	
T7-sR-R	AAACGCCAAACCCACCGCGAAGGTGG	
T7-sC-F	GTTTTTTTTAATACGACTCACTATAGGTGTAACCCAGTGTAGCAATGGG	
T7-sC-R2	CAGGAAAGGCAGCATAATAAACAGC	
T7-sA-F	GTTTTTTTTAATACGACTCACTATAGGCAAACCCCTTCGGCGTGCGTTTG	
T7-sA-R	GGATTTGGATAAATTGGAGGGCTGC	
del1-f	cgttccgaaccattaaaacttgagtcggc	
del1-r	cgttccgaaccattaaaacttgagtcggc	

Capital letters indicate *N. meningitidis* derived sequences, italicised capital letters indicate *E. coli* derived sequences, small letters indicate sequences added for cloning purposes, and underlined letters indicate recognition sites.

Table 6: Deregulated genes in the Hfq null mutant during *in vitro* logarithmic phase. Only genes major than 2 fold regulated in the Hfq mutant and with a p-value ≤ 0.05 are represented and considered regulated. Fold change values represent a mean of 3 independent experiments each performed with a different pool of RNA. The NMB number as well as the orientation in the genome and the function based on the classification of TIGRfams (Haft *et al*, 2001) are indicated for each gene

NMB_ID	ORIENTATION	GENE NAME	GENE SYMBOL	MAIN ROLE	FOLD CHANGE	P VALUE
NMB0431	+	methylcitrate synthase/citrate synthase 2	<i>prpC</i>	Energy metabolism	56.72	8.62E-11
NMB0430	+	putative carboxyphosphoenolpyruvate phosphonmutase		Energy metabolism	28.18	1.31E-10
NMB0435	+	acetate kinase	<i>ackA2</i>	Energy metabolism	18.11	2.37E-07
NMB0429	+	hypothetical protein		Hypothetical proteins	17.20	4.26E-13
NMB0865	-	hypothetical protein		Cell envelope	12.76	6.42E-11
NMB0866	-	hypothetical proteine		Hypothetical proteins	8.88	1.99E-06
NMB0589	-	50s ribosomal protein L19	<i>rplS</i>	Protein synthesis	7.27	1.60E-09
NMB1599	+	hypothetical protein		Hypothetical proteins	6.76	1.86E-07
NMB1584	+	3-hydroxyacid dehydrogenase		Central intermediary metabolism	6.67	4.00E-09
NMB1598	+	hypothetical protein		Cell envelope	5.61	0.00186389
NMB1055	-	serine hydroxymethyltransferase	<i>glyA</i>	Biosynthesis of cofactors	5.43	2.88E-07
NMB0649	+	hypothetical protein,		Hypothetical proteins	5.26	3.86E-10
NMB0325	-	50S ribosomal protein L21	<i>rplU</i>	Protein synthesis	5.20	2.11E-08

NMB0920	-	isocitrate dehydrogenase, NADP-dependent, monomeric type	<i>icd</i>	Energy metabolism	4.95	4.32E-05
NMB0650	+	hypothetical protein		Hypothetical proteins	4.80	4.63E-08
NMB0651	+	hypothetical protein		Hypothetical proteins	4.75	4.01E-10
NMB0754	+	hypothetical protein		Hypothetical proteins	4.68	1.80E-06
NMB0317	-	conserved hypothetical protein		Hypothetical proteins	4.53	5.72E-05
NMB1572	+	aconitate hydratase 2	<i>acnB</i>	Energy metabolism	4.52	4.47E-09
NMB0316	-	conserved hypothetical protein		Hypothetical proteins	4.48	1.50E-06
NMB0954	+	citrate synthase	<i>gltA</i>	Energy metabolism	4.44	1.25E-10
NMB1011	+	hypothetical protein		Hypothetical proteins	4.42	9.42E-10
NMB0755	+	hypothetical protein		Cell envelope	4.05	0.0069228
NMB0177	-	putative sodium/alanine symporter		Transport and binding proteins	4.03	3.69E-08
NMB2136	+	peptide transporter		Transport and binding proteins	3.99	4.95E-10
NMB0432	+	conserved hypothetical protein		Hypothetical proteins	3.89	1.24E-09
NMB1010	+	hypothetical protein		Hypothetical proteins	3.80	3.42E-07
NMB0864	-	hypothetical protein		Cell envelope	3.79	0.0043023
NMB0324	-	50S ribosomal protein L27	<i>rpmA</i>	Protein synthesis	3.74	8.02E-05
NMB0862	-	hypothetical protein		Hypothetical proteins	3.72	2.92E-09
NMB1600	+	hypothetical protein		Hypothetical proteins	3.57	0.000116381
NMB1406	+	hypothetical protein		Hypothetical proteins	3.56	8.31E-05
NMB0952	+	conserved hypothetical protein		Hypothetical proteins	3.53	6.64E-09

NMB0953	+	hypothetical protein		Cell envelope	3.45	2.10E-05
NMB0863	-	hypothetical protein		Cell envelope	3.41	6.07E-05
NMB1796	-	conserved hypothetical protein		Energy metabolism	3.39	3.73E-05
NMB2116	+	hypothetical protein		Hypothetical proteins	3.39	0.0114239
NMB0860	-	hypothetical protein		Hypothetical proteins	3.31	1.69E-05
NMB0176	-	D-amino acid dehydrogenase, small subunit	<i>dadA</i>	Energy metabolism	3.27	9.11E-08
NMB0899	+	hypothetical protein		Hypothetical proteins	3.26	1.03E-06
NMB0660	+	hypothetical protein		Hypothetical proteins	3.18	0.049458999
NMB0229	-	conserved hypothetical protein, authentic frameshift		Hypothetical proteins	3.17	0.00075912
NMB1009	+	conserved hypothetical protein		Hypothetical proteins	3.10	2.07E-05
NMB1088	-	conserved hypothetical protein		Hypothetical proteins	3.05	1.40E-08
NMB1848	-	hypothetical protein		Hypothetical proteins	2.93	0.027465001
NMB2115	+	hypothetical protein		Hypothetical proteins	2.91	0.0044179
NMB1764	-	hypothetical protein		Hypothetical proteins	2.89	4.21E-05
NMB0858	-	hypothetical protein		Hypothetical proteins	2.88	1.85E-05
NMB1306	+	conserved hypothetical protein		Hypothetical proteins	2.83	5.61E-05
NMB0369	-	hypothetical protein		Hypothetical proteins	2.79	0.00145773
NMB0861	-	hypothetical protein		Hypothetical proteins	2.78	0.000122647
NMB0857	-	hypothetical protein		Hypothetical proteins	2.78	2.19E-05
NMB0433	+	aconitate hydratase 1	<i>acnA</i>	Energy metabolism	2.77	0.0154206
NMB0228	-	conserved hypothetical protein		Unknown function	2.73	3.77E-08

NMB0659	+	hypothetical protein		Hypothetical proteins	2.70	0.027744999
NMB1794	-	citrate transporter		Transport and binding proteins	2.68	0.0042221
NMB0859	-	hypothetical protein		Hypothetical proteins	2.67	0.00033661
NMB0235	-	hypothetical protein		Hypothetical proteins	2.66	0.035964999
NMB1388	-	glucose-6-phosphate isomerase	<i>pgi2</i>	Energy metabolism	2.65	7.63E-05
NMB0574	+	glycine cleavage system T protein	<i>gcvT</i>	Energy metabolism	2.63	4.37E-05
NMB1946	-	outer membrane lipoprotein		Cell envelope	2.60	1.31E-06
NMB1225	-	hypothetical protein		Hypothetical proteins	2.57	0.0059564
NMB0094	+	hypothetical protein, putative inner membrane protein		Hypothetical proteins	2.56	1.51E-07
NMB1778	-	hypothetical protein		Hypothetical proteins	2.55	5.43E-09
NMB1777	-	hypothetical protein		Hypothetical proteins	2.50	2.05E-06
NMB0521	+	hypothetical protein		Hypothetical proteins	2.49	0.00047833
NMB2113	+	hypothetical protein		Hypothetical proteins	2.48	0.00020436
NMB0018	-	pilin PilE	<i>pilE</i>	Cell envelope	2.47	7.66E-07
NMB0609	+	30s ribosomal protein S15	<i>rpsO</i>	Protein synthesis	2.46	2.98E-06
NMB1008	+	hypothetical protein		Hypothetical proteins	2.46	8.18E-05
NMB1107	-	hypothetical protein		Hypothetical proteins	2.44	2.13E-05
NMB0791	-	peptidyl-prolyl cis-trans isomerase		Protein fate	2.43	0.000118135
NMB2111	+	MafB-related		Hypothetical proteins	2.41	0.0116247
NMB1292	-	hypothetical protein		Hypothetical proteins	2.39	0.0028034
NMB0226	-	conserved hypothetical protein		Hypothetical proteins	2.39	0.00118358

NMB0227	-	conserved hypothetical protein, inner membrane transport		Cell envelope	2.37	0.0068586
NMB1403	+	FrpA/C-related protein		Unknown function	2.36	0.0198009
NMB1398	+	Cu-Zn-superoxide dismutase	<i>sodC</i>	Cellular processes	2.34	7.05E-07
NMB1370	-	hypothetical protein		Hypothetical proteins	2.34	0.020524001
NMB2124	+	hypothetical protein		Hypothetical proteins	2.34	0.0039806
NMB1590	-	conserved hypothetical protein		Hypothetical proteins	2.33	0.00022209
NMB1763	-	putative toxin-activating protein		Cellular processes	2.31	4.09E-05
NMB1552	+	pilin gene inverting protein	<i>pivNM-1A</i>	Cellular processes	2.30	0.000102026
NMB1458	+	fumarate hydratase, class II	<i>fumC</i>	Energy metabolism	2.29	1.63E-12
NMB1625	-	pilin gene inverting protein		Cellular processes	2.27	0.000140211
NMB1994	+	putative adhesin/invasin	<i>nadA</i>	Cell envelope	2.22	0
NMB2013	-	hypothetical protein		Hypothetical proteins	2.21	5.19E-07
NMB0520	+	hypothetical protein		Cell envelope	2.20	0.0145028
NMB0370	-	hypothetical protein		Transport and binding proteins	2.17	1.66E-05
NMB0083	+	capsule polysaccharide modification protein	<i>lipB</i>	Cell envelope	2.17	1.74E-05
NMB1865	+	hypothetical protein		Hypothetical proteins	2.15	0.044399001
NMB2114	+	MafB-related		Unknown function	2.15	0.0073237
NMB1634	-	conserved hypothetical protein		Hypothetical proteins	2.15	0.0025398
NMB1525	-	VirG-related protein, authentic frameshift		Unknown function	2.15	0.0046596
NMB1985	-	adhesion and penetration protein	<i>hap</i>	Cellular processes	2.13	8.38E-05
NMB1404	+	hypothetical protein		Cell envelope	2.13	0.00114269

NMB1378	+	conserved hypothetical protein	<i>iscR</i>	Regulatory functions	2.11	0.0033604
NMB0491	-	hypothetical protein		Hypothetical proteins	2.11	0.027423
NMB0367	-	hypothetical protein		Hypothetical proteins	2.11	0.00061511
NMB0093	+	hypothetical protein		Hypothetical proteins	2.11	0.0020963
NMB1289	-	putative type II restriction enzyme		DNA metabolism	2.10	0.00035957
NMB0092	+	hypothetical protein		Cell envelope	2.10	0.00103513
NMB1409	+	FrpA/C-related protein		Unknown function	2.09	0.00052141
NMB0603	-	phosphoribosyl-ATP pyrophosphatase	<i>hisE</i>	Amino acid biosynthesis	2.09	0.00033955
NMB1753	+	VapD-related protein		Unknown function	2.06	0.00044239
NMB0095	+	hypothetical protein,		Hypothetical proteins	2.05	1.48E-07
NMB0656	+	hypothetical protein		Hypothetical proteins	2.04	2.06E-06
NMB1397	+	hypothetical protein		Hypothetical proteins	2.03	0.00053515
NMB0722	+	50S ribosomal protein L35	<i>rpmI</i>	Protein synthesis	2.03	7.97E-05
NMB0946	+	peroxiredoxin 2 family protein/glutaredoxin		cell envelope	2.02	3.94E-06
NMB0856	-	hypothetical protein		Hypothetical proteins	2.01	0.0147642
NMB0091	+	hypothetical protein		Hypothetical proteins	2.00	0.0095215
NMB0608	+	protein-export membrane protein SecF	<i>secF</i>	Protein fate	-2.01	0.00038371
NMB2081	-	hypothetical protein		Cell envelope	-2.02	3.18E-06
NMB2071	+	thiG protein	<i>thiG</i>	Biosynthesis of cofactors	-2.02	0.000161736
NMB1938	-	ATP synthase F0, B subunit	<i>atpF</i>	Energy metabolism	-2.02	0.0025764
NMB0258	+	NADH dehydrogenase I, M subunit		Energy metabolism	-2.05	0.00140419

NMB0568	-	Na(+)-translocating NADH-quinone reductase, subunit B	<i>nqrB</i>	Energy metabolism	-2.06	0.00139949
NMB1624	-	hypothetical protein		Hypothetical proteins	-2.07	0.000103593
NMB1344	+	pyruvate dehydrogenase, E3 component, lipoamide dehydrogenase	<i>lpdA</i>	Energy metabolism	-2.11	0.00075886
NMB1617	-	putative tellurite resistance protein		Cellular processes	-2.13	6.92E-07
NMB1494	+	conserved hypothetical protein		Hypothetical proteins	-2.17	0.003384
NMB1975	+	sodium- and chloride-dependent transporter		Transport and binding proteins	-2.17	0.0025352
NMB0178	-	acyl-(acyl-carrier-protein)--UDP-N-acetylglucosamine O-acyltransferase	<i>lpxA</i>	Cell envelope	-2.19	3.51E-05
NMB0881	-	sulfate ABC transporter, permease protein	<i>cysU</i>	Transport and binding proteins	-2.21	0.00131952
NMB1476	-	glutamate dehydrogenase, NAD-specific	<i>gluD</i>	Amino acid biosynthesis	-2.22	3.82E-05
NMB1934	-	ATP synthase F1, beta subunit	<i>atpD</i>	Energy metabolism	-2.24	4.25E-06
NMB0535	+	glucose/galactose transporter	<i>gluP</i>	Transport and binding proteins	-2.24	4.15E-05
NMB1707	+	sodium- and chloride-dependent transporter		Transport and binding proteins	-2.24	0.000140719
NMB1722	-	cytochrome C555		Disrupted reading frame	-2.33	0.0039606
NMB0905	-	hypothetical protein		Hypothetical proteins	-2.34	2.03E-05
NMB0906	-	hypothetical protein		Hypothetical proteins	-2.40	1.69E-05
NMB1935	-	ATP synthase F1, gamma subunit	<i>atpG</i>	Energy metabolism	-2.41	1.58E-06
NMB1723	-	cytochrome c oxidase, subunit III	<i>fixP</i>	Energy metabolism	-2.42	2.63E-06
NMB1933	-	ATP synthase F1, epsilon subunit	<i>atpC</i>	Energy metabolism	-2.43	0.029418999

NMB1493	+	carbon starvation protein A	<i>cstA</i>	Energy metabolism	-2.51	6.50E-05
NMB0904	-	hypothetical protein		Cell envelope	-2.55	0.020461001
NMB0607	+	protein-export membrane protein SecD	<i>secD</i>	Protein fate	-2.60	0.000143422
NMB1724	-	cytochrome c oxidase, subunit II	<i>fixO</i>	Energy metabolism	-2.61	3.74E-05
NMB0907	-	hypothetical protein		Hypothetical proteins	-2.61	0.00022366
NMB0902	-	hypothetical protein		Hypothetical proteins	-2.61	2.30E-05
NMB1725	-	cytochrome c oxidase, subunit I	<i>fixN</i>	Energy metabolism	-2.74	4.13E-05
NMB1365	-	conserved hypothetical protein		Hypothetical proteins	-2.83	0.00057637
NMB0903	-	hypothetical protein		Hypothetical proteins	-2.97	2.14E-05
NMB0543	-	putative L-lactate permease		Transport and binding proteins	-3.45	1.55E-05
NMB1623	-	major anaerobically induced outer membrane protein	<i>panI/aniA</i>	central intermediary metabolism	-3.78	0.00046053
NMB1205	-	hypothetical protein	<i>aniS</i>	Hypothetical proteins	-4.31	0.0022756
NMB0119	-	hypothetical protein		Hypothetical proteins	-5.45	5.02E-08
NMB0747	-	conserved hypothetical protein		Hypothetical proteins	-5.98	0.006558
NMB0577	+	NosR-related protein	<i>nosR</i>	Regulatory functions	-6.00	0.000117817
NMB0120	-	hypothetical protein, putative inner membrane protein		Hypothetical proteins	-7.70	0.003118
NMB0748	-	host factor-I, hfq	<i>hfq</i>	Regulatory functions	-15.98	2.51E-06

REFERENCES

- Aiba, H., (2007) Mechanism of RNA silencing by Hfq-binding small RNAs. *Curr Opin Microbiol* **10**: 134-139.
- Andrews, S. C., A. K. Robinson & F. Rodriguez-Quinones, (2003) Bacterial iron homeostasis. *FEMS Microbiol Rev* **27**: 215-237.
- Anjum, M. F., T. M. Stevanin, R. C. Read & J. W. Moir, (2002) Nitric oxide metabolism in *Neisseria meningitidis*. *J Bacteriol* **184**: 2987-2993.
- Archibald, F. S. & M. N. Duong, (1986) Superoxide dismutase and oxygen toxicity defenses in the genus *Neisseria*. *Infect Immun* **51**: 631-641.
- Arluison, V., S. K. Mutyam, C. Mura, S. Marco & M. V. Sukhodolets, (2007) Sm-like protein Hfq: location of the ATP-binding site and the effect of ATP on Hfq-- RNA complexes. *Protein Sci* **16**: 1830-1841.
- Bartolini, E., E. Frigimelica, S. Giovinazzi, G. Galli, Y. Shaik, C. Genco, J. A. Welsch, D. M. Granoff, G. Grandi & R. Grifantini, (2006) Role of FNR and FNR-regulated, sugar fermentation genes in *Neisseria meningitidis* infection. *Mol Microbiol* **60**: 963-972.
- Basineni, S. R., R. Madhugiri, T. Kolmsee, R. Hengge & G. Klug, (2009) The influence of Hfq and ribonucleases on the stability of the small non-coding RNA OxyS and its target rpoS in *E. coli* is growth phase dependent. *RNA Biol* **6**: 584-594.
- Beisel, C. L. & G. Storz, (2010) Base pairing small RNAs and their roles in global regulatory networks. *FEMS Microbiol Rev* **34**: 866-882.
- Bejerano-Sagie, M. & K. B. Xavier, (2007) The role of small RNAs in quorum sensing. *Curr Opin Microbiol* **10**: 189-198.
- Berghoff, B. A., J. Glaeser, C. M. Sharma, J. Vogel & G. Klug, (2009) Photooxidative stress-induced and abundant small RNAs in *Rhodobacter sphaeroides*. *Mol Microbiol* **74**: 1497-1512.
- Bohn, C., C. Rigoulay & P. Bouloc, (2007) No detectable effect of RNA-binding protein Hfq absence in *Staphylococcus aureus*. *BMC Microbiol* **7**: 10.
- Borg, J., D. Christie, P. G. Coen, R. Booy & R. M. Viner, (2009) Outcomes of meningococcal disease in adolescence: prospective, matched-cohort study. *Pediatrics* **123**: e502-509.
- Boysen, A., J. Moller-Jensen, B. Kallipolitis, P. Valentin-Hansen & M. Overgaard, (2010) Translational regulation of gene expression by an anaerobically induced small non-coding RNA in *Escherichia coli*. *J Biol Chem* **285**: 10690-10702.
- Brandtzaeg, P. & M. van Deuren, (2005) Meningococcal infections at the start of the 21st century. *Adv Pediatr* **52**: 129-162.
- Brennan, R. G. & T. M. Link, (2007) Hfq structure, function and ligand binding. *Curr Opin Microbiol* **10**: 125-133.
- Brescia, C. C., P. J. Mikulecky, A. L. Feig & D. D. Sledjeski, (2003) Identification of the Hfq-binding site on DsrA RNA: Hfq binds without altering DsrA secondary structure. *RNA* **9**: 33-43.
- Brown, L. & T. Elliott, (1996) Efficient translation of the RpoS sigma factor in *Salmonella typhimurium* requires host factor I, an RNA-binding protein encoded by the hfq gene. *J Bacteriol* **178**: 3763-3770.

- Carson, S. D., P. E. Klebba, S. M. Newton & P. F. Sparling, (1999) Ferric enterobactin binding and utilization by *Neisseria gonorrhoeae*. *J Bacteriol* **181**: 2895-2901.
- Cartwright, K. A. & D. A. Ala'Aldeen, (1997) *Neisseria meningitidis*: clinical aspects. *J Infect* **34**: 15-19.
- Caugant, D. A., G. Tzanakaki & P. Kriz, (2007) Lessons from meningococcal carriage studies. *FEMS Microbiol Rev* **31**: 52-63.
- Chao, Y. & J. Vogel, (2010) The role of Hfq in bacterial pathogens. *Curr Opin Microbiol* **13**: 24-33.
- Christiansen, J. K., M. H. Larsen, H. Ingmer, L. Sogaard-Andersen & B. H. Kallipolitis, (2004) The RNA-binding protein Hfq of *Listeria monocytogenes*: role in stress tolerance and virulence. *J Bacteriol* **186**: 3355-3362.
- Claus, H., M. C. Maiden, D. J. Wilson, N. D. McCarthy, K. A. Jolley, R. Urwin, F. Hessler, M. Frosch & U. Vogel, (2005) Genetic analysis of meningococci carried by children and young adults. *J Infect Dis* **191**: 1263-1271.
- Constantinidou, C., J. L. Hobman, L. Griffiths, M. D. Patel, C. W. Penn, J. A. Cole & T. W. Overton, (2006) A reassessment of the FNR regulon and transcriptomic analysis of the effects of nitrate, nitrite, NarXL, and NarQP as *Escherichia coli* K12 adapts from aerobic to anaerobic growth. *J Biol Chem* **281**: 4802-4815.
- Davis, B. M., M. Quinones, J. Pratt, Y. Ding & M. K. Waldor, (2005) Characterization of the small untranslated RNA RyhB and its regulon in *Vibrio cholerae*. *J Bacteriol* **187**: 4005-4014.
- Deghmane, A. E., D. Giorgini, M. Larribe, J. M. Alonso & M. K. Taha, (2002) Down-regulation of pili and capsule of *Neisseria meningitidis* upon contact with epithelial cells is mediated by CrgA regulatory protein. *Molecular microbiology* **43**: 1555-1564.
- Delany, I., R. Grifantini, E. Bartolini, R. Rappuoli & V. Scarlato, (2006) Effect of *Neisseria meningitidis* fur mutations on global control of gene transcription. *J Bacteriol* **188**: 2483-2492.
- Delany, I., R. Ieva, C. Alaimo, R. Rappuoli & V. Scarlato, (2003) The iron-responsive regulator fur is transcriptionally autoregulated and not essential in *Neisseria meningitidis*. *J Bacteriol* **185**: 6032-6041.
- Delany, I., R. Rappuoli & V. Scarlato, (2004) Fur functions as an activator and as a repressor of putative virulence genes in *Neisseria meningitidis*. *Mol Microbiol* **52**: 1081-1090.
- DeVoe, I. W., (1982) The meningococcus and mechanisms of pathogenicity. *Microbiol Rev* **46**: 162-190.
- Dietrich, G., S. Kurz, C. Hubner, C. Aepinus, S. Theiss, M. Guckenberger, U. Panzner, J. Weber & M. Frosch, (2003) Transcriptome analysis of *Neisseria meningitidis* during infection. *J Bacteriol* **185**: 155-164.
- Ding, Y., B. M. Davis & M. K. Waldor, (2004) Hfq is essential for *Vibrio cholerae* virulence and downregulates sigma expression. *Mol Microbiol* **53**: 345-354.
- Durand, S. & G. Storz, (2010) Reprogramming of anaerobic metabolism by the FnrS small RNA. *Mol Microbiol* **75**: 1215-1231.
- Emonts, M., J. A. Hazelzet, R. de Groot & P. W. Hermans, (2003) Host genetic determinants of *Neisseria meningitidis* infections. *Lancet Infect Dis* **3**: 565-577.
- Escolar, L., J. Perez-Martin & V. de Lorenzo, (1999) Opening the iron box: transcriptional metalloregulation by the Fur protein. *J Bacteriol* **181**: 6223-6229.

- Figuroa-Bossi, N., S. Lemire, D. Maloriol, R. Balbontin, J. Casadesus & L. Bossi, (2006) Loss of Hfq activates the sigmaE-dependent envelope stress response in *Salmonella enterica*. *Mol Microbiol* **62**: 838-852.
- Folichon, M., F. Allemand, P. Regnier & E. Hajnsdorf, (2005) Stimulation of poly(A) synthesis by *Escherichia coli* poly(A) polymerase I is correlated with Hfq binding to poly(A) tails. *FEBS J* **272**: 454-463.
- Folichon, M., V. Arluison, O. Pellegrini, E. Huntzinger, P. Regnier & E. Hajnsdorf, (2003) The poly(A) binding protein Hfq protects RNA from RNase E and exoribonucleolytic degradation. *Nucleic Acids Res* **31**: 7302-7310.
- Geissmann, T. A. & D. Touati, (2004) Hfq, a new chaperoning role: binding to messenger RNA determines access for small RNA regulator. *EMBO J* **23**: 396-405.
- Geng, J., Y. Song, L. Yang, Y. Feng, Y. Qiu, G. Li, J. Guo, Y. Bi, Y. Qu, W. Wang, X. Wang, Z. Guo, R. Yang & Y. Han, (2009) Involvement of the post-transcriptional regulator Hfq in *Yersinia pestis* virulence. *PLoS One* **4**: e6213.
- Gottesman, S., (2004) The small RNA regulators of *Escherichia coli*: roles and mechanisms*. *Annu Rev Microbiol* **58**: 303-328.
- Granoff, D. M., G. R. Moe, M. M. Giuliani, J. Adu-Bobie, L. Santini, B. Brunelli, F. Piccinetti, P. Zuno-Mitchell, S. S. Lee, P. Neri, L. Bracci, L. Lozzi & R. Rappuoli, (2001) A novel mimetic antigen eliciting protective antibody to *Neisseria meningitidis*. *J Immunol* **167**: 6487-6496.
- Gripenland, J., S. Netterling, E. Loh, T. Tiensuu, A. Toledo-Arana & J. Johansson, (2010) RNAs: regulators of bacterial virulence. *Nat Rev Microbiol* **8**: 857-866.
- Grundy, F. J. & T. M. Henkin, (2006) From ribosome to riboswitch: control of gene expression in bacteria by RNA structural rearrangements. *Crit Rev Biochem Mol Biol* **41**: 329-338.
- Guell, M., V. van Noort, E. Yus, W. H. Chen, J. Leigh-Bell, K. Michalodimitrakis, T. Yamada, M. Arumugam, T. Doerks, S. Kuhner, M. Rode, M. Suyama, S. Schmidt, A. C. Gavin, P. Bork & L. Serrano, (2009) Transcriptome complexity in a genome-reduced bacterium. *Science* **326**: 1268-1271.
- Guillier, M. & S. Gottesman, (2006) Remodelling of the *Escherichia coli* outer membrane by two small regulatory RNAs. *Mol Microbiol* **59**: 231-247.
- Guisbert, E., V. A. Rhodius, N. Ahuja, E. Witkin & C. A. Gross, (2007) Hfq modulates the sigmaE-mediated envelope stress response and the sigma32-mediated cytoplasmic stress response in *Escherichia coli*. *J Bacteriol* **189**: 1963-1973.
- Haft, D. H., B. J. Loftus, D. L. Richardson, F. Yang, J. A. Eisen, I. T. Paulsen & O. White, (2001) TIGRFAMs: a protein family resource for the functional identification of proteins. *Nucleic Acids Res* **29**: 41-43.
- Hajnsdorf, E. & P. Regnier, (2000) Host factor Hfq of *Escherichia coli* stimulates elongation of poly(A) tails by poly(A) polymerase I. *Proc Natl Acad Sci U S A* **97**: 1501-1505.
- Hammer, B. K. & B. L. Bassler, (2007) Regulatory small RNAs circumvent the conventional quorum sensing pathway in pandemic *Vibrio cholerae*. *Proc Natl Acad Sci U S A* **104**: 11145-11149.
- Hammerschmidt, S., A. Muller, H. Sillmann, M. Muhlenhoff, R. Borrow, A. Fox, J. van Putten, W. D. Zollinger, R. Gerardy-Schahn & M. Frosch, (1996) Capsule phase variation in *Neisseria meningitidis* serogroup B by slipped-strand mispairing in the polysialyltransferase gene (*siaD*): correlation with

- bacterial invasion and the outbreak of meningococcal disease. *Molecular microbiology* **20**: 1211-1220.
- Heckels, J. E., B. Blackett, J. S. Everson & M. E. Ward, (1976) The influence of surface charge on the attachment of *Neisseria gonorrhoeae* to human cells. *J Gen Microbiol* **96**: 359-364.
- Helaine, S., D. H. Dyer, X. Nassif, V. Pelicic & K. T. Forest, (2007) 3D structure/function analysis of PilX reveals how minor pilins can modulate the virulence properties of type IV pili. *Proc Natl Acad Sci U S A* **104**: 15888-15893.
- Hill, D. J., N. J. Griffiths, E. Borodina & M. Virji, (2010) Cellular and molecular biology of *Neisseria meningitidis* colonization and invasive disease. *Clin Sci (Lond)* **118**: 547-564.
- Hsu, C. A., W. R. Lin, J. C. Li, Y. L. Liu, Y. T. Tseng, C. M. Chang, Y. S. Lee & C. Y. Yang, (2008) Immunoproteomic identification of the hypothetical protein NMB1468 as a novel lipoprotein ubiquitous in *Neisseria meningitidis* with vaccine potential. *Proteomics* **8**: 2115-2125.
- Ieva, R., C. Alaimo, I. Delany, G. Spohn, R. Rappuoli & V. Scarlato, (2005) CrgA is an inducible LysR-type regulator of *Neisseria meningitidis*, acting both as a repressor and as an activator of gene transcription. *J Bacteriol* **187**: 3421-3430.
- Jain, R. & M. K. Chan, (2007) Support for a potential role of *E. coli* oligopeptidase A in protein degradation. *Biochem Biophys Res Commun* **359**: 486-490.
- Jarvis, G. A. & N. A. Vedros, (1987) Sialic acid of group B *Neisseria meningitidis* regulates alternative complement pathway activation. *Infect Immun* **55**: 174-180.
- Jiang, X., M. Zhang, Y. Ding, J. Yao, H. Chen, D. Zhu & M. Muramatu, (1998) *Escherichia coli* prlC gene encodes a trypsin-like proteinase regulating the cell cycle. *J Biochem* **124**: 980-985.
- Johansson, J. & P. Cossart, (2003) RNA-mediated control of virulence gene expression in bacterial pathogens. *Trends Microbiol* **11**: 280-285.
- Jousselin, A., L. Metzinger & B. Felden, (2009) On the facultative requirement of the bacterial RNA chaperone, Hfq. *Trends Microbiol* **17**: 399-405.
- Kajitani, M. & A. Ishihama, (1991) Identification and sequence determination of the host factor gene for bacteriophage Q beta. *Nucleic Acids Res* **19**: 1063-1066.
- Kang, Y., K. D. Weber, Y. Qiu, P. J. Kiley & F. R. Blattner, (2005) Genome-wide expression analysis indicates that FNR of *Escherichia coli* K-12 regulates a large number of genes of unknown function. *J Bacteriol* **187**: 1135-1160.
- Kawamoto, H., Y. Koide, T. Morita & H. Aiba, (2006) Base-pairing requirement for RNA silencing by a bacterial small RNA and acceleration of duplex formation by Hfq. *Mol Microbiol* **61**: 1013-1022.
- Kellogg, D. S., Jr., W. L. Peacock, Jr., W. E. Deacon, L. Brown & D. I. Pirkle, (1963) *Neisseria Gonorrhoeae*. I. Virulence Genetically Linked to Clonal Variation. *J Bacteriol* **85**: 1274-1279.
- Kiley, P. J. & H. Beinert, (2003) The role of Fe-S proteins in sensing and regulation in bacteria. *Curr Opin Microbiol* **6**: 181-185.
- Kulesus, R. R., K. Diaz-Perez, E. S. Slechta, D. S. Eto & M. A. Mulvey, (2008) Impact of the RNA chaperone Hfq on the fitness and virulence potential of uropathogenic *Escherichia coli*. *Infect Immun* **76**: 3019-3026.

- Labigne-Roussel, A., P. Courcoux & L. Tompkins, (1988) Gene disruption and replacement as a feasible approach for mutagenesis of *Campylobacter jejuni*. *J Bacteriol* **170**: 1704-1708.
- Link, T. M., P. Valentin-Hansen & R. G. Brennan, (2009) Structure of *Escherichia coli* Hfq bound to polyriboadenylate RNA. *Proc Natl Acad Sci U S A* **106**: 19292-19297.
- Liu, J. M. & A. Camilli, (2010) A broadening world of bacterial small RNAs. *Curr Opin Microbiol* **13**: 18-23.
- Madico, G., J. A. Welsch, L. A. Lewis, A. McNaughton, D. H. Perlman, C. E. Costello, J. Ngampasutadol, U. Vogel, D. M. Granoff & S. Ram, (2006) The meningococcal vaccine candidate GNA1870 binds the complement regulatory protein factor H and enhances serum resistance. *J Immunol* **177**: 501-510.
- Maiden, M. C., (2008) Population genomics: diversity and virulence in the *Neisseria*. *Curr Opin Microbiol* **11**: 467-471.
- Maiden, M. C., J. A. Bygraves, E. Feil, G. Morelli, J. E. Russell, R. Urwin, Q. Zhang, J. Zhou, K. Zurth, D. A. Caugant, I. M. Feavers, M. Achtman & B. G. Spratt, (1998) Multilocus sequence typing: a portable approach to the identification of clones within populations of pathogenic microorganisms. *Proc Natl Acad Sci U S A* **95**: 3140-3145.
- Majdalani, N., C. K. Vanderpool & S. Gottesman, (2005) Bacterial small RNA regulators. *Crit Rev Biochem Mol Biol* **40**: 93-113.
- Marraffini, L. A. & E. J. Sontheimer, (2008) CRISPR interference limits horizontal gene transfer in staphylococci by targeting DNA. *Science* **322**: 1843-1845.
- Masse, E., F. E. Escorcia & S. Gottesman, (2003) Coupled degradation of a small regulatory RNA and its mRNA targets in *Escherichia coli*. *Genes Dev* **17**: 2374-2383.
- Masse, E. & S. Gottesman, (2002) A small RNA regulates the expression of genes involved in iron metabolism in *Escherichia coli*. *Proc Natl Acad Sci U S A* **99**: 4620-4625.
- Masse, E., H. Salvail, G. Desnoyers & M. Arguin, (2007) Small RNAs controlling iron metabolism. *Curr Opin Microbiol* **10**: 140-145.
- Maxam, A. M. & W. Gilbert, (1977) A new method for sequencing DNA. *Proc Natl Acad Sci U S A* **74**: 560-564.
- McGrath, P. T., H. Lee, L. Zhang, A. A. Iniesta, A. K. Hottes, M. H. Tan, N. J. Hillson, P. Hu, L. Shapiro & H. H. McAdams, (2007) High-throughput identification of transcription start sites, conserved promoter motifs and predicted regulons. *Nat Biotechnol* **25**: 584-592.
- McNealy, T. L., V. Forsbach-Birk, C. Shi & R. Marre, (2005) The Hfq homolog in *Legionella pneumophila* demonstrates regulation by LetA and RpoS and interacts with the global regulator CsrA. *J Bacteriol* **187**: 1527-1532.
- Meibom, K. L., A. L. Forslund, K. Kuoppa, K. Alkhuder, I. Dubail, M. Dupuis, A. Forsberg & A. Charbit, (2009) Hfq, a novel pleiotropic regulator of virulence-associated genes in *Francisella tularensis*. *Infect Immun* **77**: 1866-1880.
- Mellin, J. R., S. Goswami, S. Grogan, B. Tjaden & C. A. Genco, (2007) A novel fur- and iron-regulated small RNA, NrrF, is required for indirect fur-mediated regulation of the *sdhA* and *sdhC* genes in *Neisseria meningitidis*. *J Bacteriol* **189**: 3686-3694.
- Mellin, J. R., R. McClure, D. Lopez, O. Green, B. Reinhard & C. Genco, (2010) Role of Hfq in iron-dependent and -independent gene regulation in *Neisseria meningitidis*. *Microbiology* **156**: 2316-2326.

- Metruccio, M. M., L. Fantappie, D. Serruto, A. Muzzi, D. Roncarati, C. Donati, V. Scarlato & I. Delany, (2009) The Hfq-dependent small noncoding RNA NrrF directly mediates Fur-dependent positive regulation of succinate dehydrogenase in *Neisseria meningitidis*. *J Bacteriol* **191**: 1330-1342.
- Mikulecky, P. J., M. K. Kaw, C. C. Brescia, J. C. Takach, D. D. Sledjeski & A. L. Feig, (2004) *Escherichia coli* Hfq has distinct interaction surfaces for DsrA, rpoS and poly(A) RNAs. *Nat Struct Mol Biol* **11**: 1206-1214.
- Mohanty, B. K., V. F. Maples & S. R. Kushner, (2004) The Sm-like protein Hfq regulates polyadenylation dependent mRNA decay in *Escherichia coli*. *Mol Microbiol* **54**: 905-920.
- Moll, I., T. Afonyushkin, O. Vytvytska, V. R. Kaberdin & U. Blasi, (2003a) Coincident Hfq binding and RNase E cleavage sites on mRNA and small regulatory RNAs. *RNA* **9**: 1308-1314.
- Moll, I., D. Leitsch, T. Steinhauser & U. Blasi, (2003b) RNA chaperone activity of the Sm-like Hfq protein. *EMBO Rep* **4**: 284-289.
- Moller, T., T. Franch, P. Hojrup, D. R. Keene, H. P. Bachinger, R. G. Brennan & P. Valentin-Hansen, (2002a) Hfq: a bacterial Sm-like protein that mediates RNA-RNA interaction. *Mol Cell* **9**: 23-30.
- Moller, T., T. Franch, C. Udesen, K. Gerdes & P. Valentin-Hansen, (2002b) Spot 42 RNA mediates discoordinate expression of the *E. coli* galactose operon. *Genes Dev* **16**: 1696-1706.
- Morita, T., Y. Mochizuki & H. Aiba, (2006) Translational repression is sufficient for gene silencing by bacterial small noncoding RNAs in the absence of mRNA destruction. *Proc Natl Acad Sci U S A* **103**: 4858-4863.
- Muffler, A., D. D. Traulsen, D. Fischer, R. Lange & R. Hengge-Aronis, (1997) The RNA-binding protein HF-I plays a global regulatory role which is largely, but not exclusively, due to its role in expression of the sigmaS subunit of RNA polymerase in *Escherichia coli*. *J Bacteriol* **179**: 297-300.
- Nassif, X., (1999) Interactions between encapsulated *Neisseria meningitidis* and host cells. *Int Microbiol* **2**: 133-136.
- Nielsen, J. S., L. K. Lei, T. Ebersbach, A. S. Olsen, J. K. Klitgaard, P. Valentin-Hansen & B. H. Kallipolitis, (2010) Defining a role for Hfq in Gram-positive bacteria: evidence for Hfq-dependent antisense regulation in *Listeria monocytogenes*. *Nucleic Acids Res* **38**: 907-919.
- Obana, N., Y. Shirahama, K. Abe & K. Nakamura, (2010) Stabilization of *Clostridium perfringens* collagenase mRNA by VR-RNA-dependent cleavage in 5' leader sequence. *Mol Microbiol* **77**: 1416-1428.
- Oglesby, A. G., J. M. Farrow, 3rd, J. H. Lee, A. P. Tomaras, E. P. Greenberg, E. C. Pesci & M. L. Vasil, (2008) The influence of iron on *Pseudomonas aeruginosa* physiology: a regulatory link between iron and quorum sensing. *J Biol Chem* **283**: 15558-15567.
- Oriente, F., V. Scarlato & I. Delany, (2010) Expression of factor H binding protein of meningococcus responds to oxygen limitation through a dedicated FNR-regulated promoter. *J Bacteriol* **192**: 691-701.
- Pannone, B. K. & S. L. Wolin, (2000) Sm-like proteins wRING the neck of mRNA. *Curr Biol* **10**: R478-481.
- Papenfort, K., V. Pfeiffer, F. Mika, S. Lucchini, J. C. Hinton & J. Vogel, (2006) SigmaE-dependent small RNAs of *Salmonella* respond to membrane stress by accelerating global omp mRNA decay. *Mol Microbiol* **62**: 1674-1688.
- Papenfort, K. & J. Vogel, (2010) Regulatory RNA in bacterial pathogens. *Cell Host Microbe* **8**: 116-127.

- Passalacqua, K. D., A. Varadarajan, B. D. Ondov, D. T. Okou, M. E. Zwick & N. H. Bergman, (2009) Structure and complexity of a bacterial transcriptome. *J Bacteriol* **191**: 3203-3211.
- Perkins, T. T., R. A. Kingsley, M. C. Fookes, P. P. Gardner, K. D. James, L. Yu, S. A. Assefa, M. He, N. J. Croucher, D. J. Pickard, D. J. Maskell, J. Parkhill, J. Choudhary, N. R. Thomson & G. Dougan, (2009) A strand-specific RNA-Seq analysis of the transcriptome of the typhoid bacillus *Salmonella typhi*. *PLoS Genet* **5**: e1000569.
- Perkins-Balding, D., M. Ratliff-Griffin & I. Stojiljkovic, (2004) Iron transport systems in *Neisseria meningitidis*. *Microbiol Mol Biol Rev* **68**: 154-171.
- Pfeiffer, V., K. Papenfort, S. Lucchini, J. C. Hinton & J. Vogel, (2009) Coding sequence targeting by MicC RNA reveals bacterial mRNA silencing downstream of translational initiation. *Nat Struct Mol Biol* **16**: 840-846.
- Pichon, C. & B. Felden, (2005) Small RNA genes expressed from *Staphylococcus aureus* genomic and pathogenicity islands with specific expression among pathogenic strains. *Proc Natl Acad Sci U S A* **102**: 14249-14254.
- Pichon, C. & B. Felden, (2007) Proteins that interact with bacterial small RNA regulators. *FEMS Microbiol Rev* **31**: 614-625.
- Pizza, M., V. Scarlato, V. Masignani, M. M. Giuliani, B. Arico, M. Comanducci, G. T. Jennings, L. Baldi, E. Bartolini, B. Capecchi, C. L. Galeotti, E. Luzzi, R. Manetti, E. Marchetti, M. Mora, S. Nuti, G. Ratti, L. Santini, S. Savino, M. Scarselli, E. Storni, P. Zuo, M. Broecker, E. Hundt, B. Knapp, E. Blair, T. Mason, H. Tettelin, D. W. Hood, A. C. Jeffries, N. J. Saunders, D. M. Granoff, J. C. Venter, E. R. Moxon, G. Grandi & R. Rappuoli, (2000) Identification of vaccine candidates against serogroup B meningococcus by whole-genome sequencing. *Science* **287**: 1816-1820.
- Podkaminski, D. & J. Vogel, (2010) Small RNAs promote mRNA stability to activate the synthesis of virulence factors. *Mol Microbiol* **78**: 1327-1331.
- Prevost, K., H. Salvail, G. Desnoyers, J. F. Jacques, E. Phaneuf & E. Masse, (2007) The small RNA RyhB activates the translation of *shiA* mRNA encoding a permease of shikimate, a compound involved in siderophore synthesis. *Mol Microbiol* **64**: 1260-1273.
- Ramirez-Pena, E., J. Trevino, Z. Liu, N. Perez & P. Sumbly, (2010) The group A *Streptococcus* small regulatory RNA FasX enhances streptokinase activity by increasing the stability of the *ska* mRNA transcript. *Mol Microbiol* **78**: 1332-1347.
- Rasmussen, S., H. B. Nielsen & H. Jarmer, (2009) The transcriptionally active regions in the genome of *Bacillus subtilis*. *Mol Microbiol* **73**: 1043-1057.
- Repoila, F. & F. Darfeuille, (2009) Small regulatory non-coding RNAs in bacteria: physiology and mechanistic aspects. *Biol Cell* **101**: 117-131.
- Repoila, F., N. Majdalani & S. Gottesman, (2003) Small non-coding RNAs, coordinators of adaptation processes in *Escherichia coli*: the RpoS paradigm. *Mol Microbiol* **48**: 855-861.
- Robertson, G. T. & R. M. Roop, Jr., (1999) The *Brucella abortus* host factor I (HF-I) protein contributes to stress resistance during stationary phase and is a major determinant of virulence in mice. *Mol Microbiol* **34**: 690-700.
- Rock, J. D. & J. W. Moir, (2005) Microaerobic denitrification in *Neisseria meningitidis*. *Biochem Soc Trans* **33**: 134-136.
- Romby, P., F. Vandenesch & E. G. Wagner, (2006) The role of RNAs in the regulation of virulence-gene expression. *Curr Opin Microbiol* **9**: 229-236.

- Romero, J. D. & I. M. Outshoorn, (1997) The immune response to the capsular polysaccharide of *Neisseria meningitidis* group B. *Zentralbl Bakteriol* **285**: 331-340.
- Rosenstein, N. E., B. A. Perkins, D. S. Stephens, T. Popovic & J. M. Hughes, (2001) Meningococcal disease. *N Engl J Med* **344**: 1378-1388.
- Rutherford, K., J. Parkhill, J. Crook, T. Horsnell, P. Rice, M. A. Rajandream & B. Barrell, (2000) Artemis: sequence visualization and annotation. *Bioinformatics* **16**: 944-945.
- Salmon, K., S. P. Hung, K. Mekjian, P. Baldi, G. W. Hatfield & R. P. Gunsalus, (2003) Global gene expression profiling in *Escherichia coli* K12. The effects of oxygen availability and FNR. *J Biol Chem* **278**: 29837-29855.
- Sambrook, J., E. F. Fritsch & T. Maniatis, (1989) *Molecular cloning: A laboratory manual*. Cold Spring Harbor, NY: Cold Spring Harbor Laboratory.
- Sanger, F., G. M. Air, B. G. Barrell, N. L. Brown, A. R. Coulson, C. A. Fiddes, C. A. Hutchison, P. M. Slocombe & M. Smith, (1977) Nucleotide sequence of bacteriophage phi X174 DNA. *Nature* **265**: 687-695.
- Sauter, C., J. Basquin & D. Suck, (2003) Sm-like proteins in Eubacteria: the crystal structure of the Hfq protein from *Escherichia coli*. *Nucleic Acids Res* **31**: 4091-4098.
- Sawers, G., (1999) The aerobic/anaerobic interface. *Curr Opin Microbiol* **2**: 181-187.
- Schiano, C. A., L. E. Bellows & W. W. Lathem, (2010) The small RNA chaperone Hfq is required for the virulence of *Yersinia pseudotuberculosis*. *Infect Immun* **78**: 2034-2044.
- Schielke, S., M. Frosch & O. Kurzai, (2010) Virulence determinants involved in differential host niche adaptation of *Neisseria meningitidis* and *Neisseria gonorrhoeae*. *Med Microbiol Immunol* **199**: 185-196.
- Schneider, M. C., R. M. Exley, H. Chan, I. Feavers, Y. H. Kang, R. B. Sim & C. M. Tang, (2006) Functional significance of factor H binding to *Neisseria meningitidis*. *J Immunol* **176**: 7566-7575.
- Schumacher, M. A., R. F. Pearson, T. Moller, P. Valentin-Hansen & R. G. Brennan, (2002) Structures of the pleiotropic translational regulator Hfq and an Hfq-RNA complex: a bacterial Sm-like protein. *EMBO J* **21**: 3546-3556.
- Selinger, D. W., K. J. Cheung, R. Mei, E. M. Johansson, C. S. Richmond, F. R. Blattner, D. J. Lockhart & G. M. Church, (2000) RNA expression analysis using a 30 base pair resolution *Escherichia coli* genome array. *Nat Biotechnol* **18**: 1262-1268.
- Sharma, C. M., F. Darfeuille, T. H. Plantinga & J. Vogel, (2007) A small RNA regulates multiple ABC transporter mRNAs by targeting C/A-rich elements inside and upstream of ribosome-binding sites. *Genes Dev* **21**: 2804-2817.
- Sharma, C. M. & J. Vogel, (2009) Experimental approaches for the discovery and characterization of regulatory small RNA. *Curr Opin Microbiol* **12**: 536-546.
- Sittka, A., S. Lucchini, K. Papenfort, C. M. Sharma, K. Rolle, T. T. Binnewies, J. C. Hinton & J. Vogel, (2008) Deep sequencing analysis of small noncoding RNA and mRNA targets of the global post-transcriptional regulator, Hfq. *PLoS Genet* **4**: e1000163.
- Sittka, A., V. Pfeiffer, K. Tedin & J. Vogel, (2007) The RNA chaperone Hfq is essential for the virulence of *Salmonella typhimurium*. *Mol Microbiol* **63**: 193-217.
- Sittka, A., C. M. Sharma, K. Rolle & J. Vogel, (2009) Deep sequencing of *Salmonella* RNA associated with heterologous Hfq proteins in vivo reveals

- small RNAs as a major target class and identifies RNA processing phenotypes. *RNA Biol* **6**: 266-275.
- Sledjeski, D. D., C. Whitman & A. Zhang, (2001) Hfq is necessary for regulation by the untranslated RNA DsrA. *J Bacteriol* **183**: 1997-2005.
- Sonnleitner, E., S. Hagens, F. Rosenau, S. Wilhelm, A. Habel, K. E. Jager & U. Blasi, (2003) Reduced virulence of a hfq mutant of *Pseudomonas aeruginosa* O1. *Microb Pathog* **35**: 217-228.
- Sonnleitner, E., I. Moll & U. Blasi, (2002) Functional replacement of the *Escherichia coli* hfq gene by the homologue of *Pseudomonas aeruginosa*. *Microbiology* **148**: 883-891.
- Soper, T., P. Mandin, N. Majdalani, S. Gottesman & S. A. Woodson, (2010) Positive regulation by small RNAs and the role of Hfq. *Proc Natl Acad Sci U S A* **107**: 9602-9607.
- Sorek, R. & P. Cossart, (2010) Prokaryotic transcriptomics: a new view on regulation, physiology and pathogenicity. *Nat Rev Genet* **11**: 9-16.
- Sorek, R., V. Kunin & P. Hugenholz, (2008) CRISPR--a widespread system that provides acquired resistance against phages in bacteria and archaea. *Nat Rev Microbiol* **6**: 181-186.
- Sousa, S. A., C. G. Ramos, L. M. Moreira & J. H. Leitao, (2010) The hfq gene is required for stress resistance and full virulence of *Burkholderia cepacia* to the nematode *Caenorhabditis elegans*. *Microbiology* **156**: 896-908.
- Stephens, D. S., (2007) Conquering the meningococcus. *FEMS Microbiol Rev* **31**: 3-14.
- Stephens, D. S., (2009) Biology and pathogenesis of the evolutionarily successful, obligate human bacterium *Neisseria meningitidis*. *Vaccine* **27 Suppl 2**: B71-77.
- Storz, G., J. A. Opdyke & A. Zhang, (2004) Controlling mRNA stability and translation with small, noncoding RNAs. *Curr Opin Microbiol* **7**: 140-144.
- Sun, X. & R. M. Wartell, (2006) *Escherichia coli* Hfq binds A18 and DsrA domain II with similar 2:1 Hfq6/RNA stoichiometry using different surface sites. *Biochemistry* **45**: 4875-4887.
- Sun, X., I. Zhulin & R. M. Wartell, (2002) Predicted structure and phyletic distribution of the RNA-binding protein Hfq. *Nucleic Acids Res* **30**: 3662-3671.
- Sun, Y. H., S. Bakshi, R. Chalmers & C. M. Tang, (2000) Functional genomics of *Neisseria meningitidis* pathogenesis. *Nat Med* **6**: 1269-1273.
- Tettelin, H., K. E. Nelson, I. T. Paulsen, J. A. Eisen, T. D. Read, S. Peterson, J. Heidelberg, R. T. DeBoy, D. H. Haft, R. J. Dodson, A. S. Durkin, M. Gwinn, J. F. Kolonay, W. C. Nelson, J. D. Peterson, L. A. Umayam, O. White, S. L. Salzberg, M. R. Lewis, D. Radune, E. Holtzapple, H. Khouri, A. M. Wolf, T. R. Utterback, C. L. Hansen, L. A. McDonald, T. V. Feldblyum, S. Angiuoli, T. Dickinson, E. K. Hickey, I. E. Holt, B. J. Loftus, F. Yang, H. O. Smith, J. C. Venter, B. A. Dougherty, D. A. Morrison, S. K. Hollingshead & C. M. Fraser, (2001) Complete genome sequence of a virulent isolate of *Streptococcus pneumoniae*. *Science* **293**: 498-506.
- Thompson, K. M., V. A. Rhodius & S. Gottesman, (2007) SigmaE regulates and is regulated by a small RNA in *Escherichia coli*. *J Bacteriol* **189**: 4243-4256.
- Toledo-Arana, A., O. Dussurget, G. Nikitas, N. Sesto, H. Guet-Revillet, D. Balestrino, E. Loh, J. Gripenland, T. Tiensuu, K. Vaitkevicius, M. Barthelemy, M. Vergassola, M. A. Nahori, G. Soubigou, B. Regnault, J. Y. Coppee, M. Lecuit, J. Johansson & P. Cossart, (2009) The *Listeria*

- transcriptional landscape from saprophytism to virulence. *Nature* **459**: 950-956.
- Toledo-Arana, A., F. Repoila & P. Cossart, (2007) Small noncoding RNAs controlling pathogenesis. *Curr Opin Microbiol* **10**: 182-188.
- Trieu-Cuot, P., C. Poyart-Salmeron, C. Carlier & P. Courvalin, (1990) Nucleotide sequence of the erythromycin resistance gene of the conjugative transposon Tn1545. *Nucleic Acids Res* **18**: 3660.
- Trun, N. J. & T. J. Silhavy, (1989) The genetics of protein targeting in Escherichia coli K12. *J Cell Sci Suppl* **11**: 13-28.
- Tsui, H. C., H. C. Leung & M. E. Winkler, (1994) Characterization of broadly pleiotropic phenotypes caused by an hfq insertion mutation in Escherichia coli K-12. *Mol Microbiol* **13**: 35-49.
- Urban, J. H. & J. Vogel, (2007) Translational control and target recognition by Escherichia coli small RNAs in vivo. *Nucleic Acids Res* **35**: 1018-1037.
- Urban, J. H. & J. Vogel, (2008) Two seemingly homologous noncoding RNAs act hierarchically to activate glmS mRNA translation. *PLoS Biol* **6**: e64.
- Urban, J. H. & J. Vogel, (2009) A green fluorescent protein (GFP)-based plasmid system to study post-transcriptional control of gene expression in vivo. *Methods Mol Biol* **540**: 301-319.
- Valentin-Hansen, P., M. Eriksen & C. Udesen, (2004) The bacterial Sm-like protein Hfq: a key player in RNA transactions. *Mol Microbiol* **51**: 1525-1533.
- Valentin-Hansen, P., J. Johansen & A. A. Rasmussen, (2007) Small RNAs controlling outer membrane porins. *Curr Opin Microbiol* **10**: 152-155.
- Vecerek, B., I. Moll & U. Blasi, (2007) Control of Fur synthesis by the non-coding RNA RyhB and iron-responsive decoding. *EMBO J* **26**: 965-975.
- Virji, M., (2009) Pathogenic neisseriae: surface modulation, pathogenesis and infection control. *Nat Rev Microbiol* **7**: 274-286.
- Virji, M., C. Alexandrescu, D. J. Ferguson, J. R. Saunders & E. R. Moxon, (1992) Variations in the expression of pili: the effect on adherence of Neisseria meningitidis to human epithelial and endothelial cells. *Molecular microbiology* **6**: 1271-1279.
- Vogel, J., V. Bartels, T. H. Tang, G. Churakov, J. G. Slagter-Jager, A. Huttenhofer & E. G. Wagner, (2003) RNomics in Escherichia coli detects new sRNA species and indicates parallel transcriptional output in bacteria. *Nucleic Acids Res* **31**: 6435-6443.
- Vogel, J. & K. Papenfort, (2006) Small non-coding RNAs and the bacterial outer membrane. *Curr Opin Microbiol* **9**: 605-611.
- Vogel, U., H. Claus, G. Heinze & M. Frosch, (1997) Functional characterization of an isogenic meningococcal alpha-2,3-sialyltransferase mutant: the role of lipooligosaccharide sialylation for serum resistance in serogroup B meningococci. *Med Microbiol Immunol* **186**: 159-166.
- Vytvytska, O., I. Moll, V. R. Kaberdin, A. von Gabain & U. Blasi, (2000) Hfq (HF1) stimulates ompA mRNA decay by interfering with ribosome binding. *Genes Dev* **14**: 1109-1118.
- Wang, Y. & D. E. Taylor, (1990) Natural transformation in Campylobacter species. *J Bacteriol* **172**: 949-955.
- Wang, Z., M. Gerstein & M. Snyder, (2009) RNA-Seq: a revolutionary tool for transcriptomics. *Nat Rev Genet* **10**: 57-63.
- Wassarman, K. M., (2002) Small RNAs in bacteria: diverse regulators of gene expression in response to environmental changes. *Cell* **109**: 141-144.

- Wassarman, K. M., A. Zhang & G. Storz, (1999) Small RNAs in Escherichia coli. *Trends Microbiol* **7**: 37-45.
- Waters, L. S. & G. Storz, (2009) Regulatory RNAs in bacteria. *Cell* **136**: 615-628.
- Whitehead, R. N., T. W. Overton, L. A. Snyder, S. J. McGowan, H. Smith, J. A. Cole & N. J. Saunders, (2007) The small FNR regulon of Neisseria gonorrhoeae: comparison with the larger Escherichia coli FNR regulon and interaction with the NarQ-NarP regulon. *BMC Genomics* **8**: 35.
- Wilderman, P. J., N. A. Sowa, D. J. FitzGerald, P. C. FitzGerald, S. Gottesman, U. A. Ochsner & M. L. Vasil, (2004) Identification of tandem duplicate regulatory small RNAs in Pseudomonas aeruginosa involved in iron homeostasis. *Proc Natl Acad Sci U S A* **101**: 9792-9797.
- Worlitzsch, D., R. Tarran, M. Ulrich, U. Schwab, A. Cekici, K. C. Meyer, P. Birrer, G. Bellon, J. Berger, T. Weiss, K. Botzenhart, J. R. Yankaskas, S. Randell, R. C. Boucher & G. Doring, (2002) Effects of reduced mucus oxygen concentration in airway Pseudomonas infections of cystic fibrosis patients. *J Clin Invest* **109**: 317-325.
- Wurtzel, O., R. Sapra, F. Chen, Y. Zhu, B. A. Simmons & R. Sorek, (2010) A single-base resolution map of an archaeal transcriptome. *Genome Res* **20**: 133-141.
- Yoder-Himes, D. R., P. S. Chain, Y. Zhu, O. Wurtzel, E. M. Rubin, J. M. Tiedje & R. Sorek, (2009) Mapping the Burkholderia cenocepacia niche response via high-throughput sequencing. *Proc Natl Acad Sci U S A* **106**: 3976-3981.
- Zhang, A., K. M. Wassarman, J. Ortega, A. C. Steven & G. Storz, (2002) The Sm-like Hfq protein increases OxyS RNA interaction with target mRNAs. *Mol Cell* **9**: 11-22.
- Zhang, A., K. M. Wassarman, C. Rosenow, B. C. Tjaden, G. Storz & S. Gottesman, (2003) Global analysis of small RNA and mRNA targets of Hfq. *Mol Microbiol* **50**: 1111-1124.
- Zhou, Y. & J. Xie, (2011) The roles of pathogen small RNAs. *J Cell Physiol* **226**: 968-973.